J Chem Phys Mumma ~1971

Thirty-First Annual
Gaseous Electronics Conference
October 17-20, 1978

CALSPAN ADVANCED TECHNOLOGY CENTER

State University of New York at Buffalo

Program and Abstracts

A Topical Conference of
The American Physical Society

Sponsored by:

Calspan Corporation, Buffalo
State University of New York at Buffalo
American Physical Society
Division of Electron
and Atomic Physics

Assisted by:

Air Force Office of Scientific Research
Department of Energy
National Science Foundation
Office of Naval Research

ACKNOWLEDGEMENTS

We are pleased to acknowledge the generous support of the following Patrons and Subscribers.

Bell Aerospace Textron*, Division of Textron Inc.
Graphic Controls Corporation*
Jarrell-Ash Division†, Fisher Scientific Company
Moog, Inc.*
Republic Steel Corporation*
Spaulding Fibre Company, Inc.*
The Carborundum Company*
Westinghouse Electric Corporation*, Power Circuit Breaker Division, Trafford, Pennsylvania

*Patron
†Subscriber

We are also pleased to acknowledge the many contributions of the members of the Operations Committee:

R.F. Bennett
T.F. Bernecki
C. Bhansali
Y.K. Chien
D. Dettman
Y.O. Kim
C. King
Y.C. Lau
J. Lee
T.Y. Li
D. Manikopoulos
D. Moll
A.S. Nat
M. Rosenfeld
C. Scheffler
N. Shah
J. Sullivan
P.J. Talarico
D. Tricinski
S.P. Wong

Acknowledgement to Niagara Mohawk Power Corporation, Buffalo, N.Y., for color photograph on front cover.

Acknowledgement to Calspan Corporation, Buffalo, N.Y., for coordination and printing under the direction of A.J. Pifer and M.A. Polino.

CONTENTS

page no.

Acknowledgements ii

Tribute to Professor Leonard B. Loeb . . . . . iv,v

Program 1

Session AA: Metal Vapor Molecular Lasers 17

Session AB: Magnetohydrodynamics 23

Session BA: Rare Gas Halide and Nuclear Pumped Lasers 28

Session BB: Transfer Mechanisms in Arcs 34

Session CA: Kinetic Processes in Rare Gas Halide Lasers 38

Session CB: Arcs and Flows I 43

Session DA: XeF Kinetics and Lasers 48

Session DB: Arcs and Flows II 55

Session E: Workshop on Fundamental Processes in Excimer Lasers 59

Session FA: Electrode Effects and Vacuum Arcs 62

Session FB: Electron and Ion Transport 67

Session GA: Ion Interactions and Mobilities I 71

Session FB: (continued) Electron and Ion Transport 77

Session GB: Glow Discharges 80

Session HA: Ion Interactions and Mobilities II 84

Session HB: Diagnostics and Afterglows 89

Session I: Workshop on Dissociative Recombination 94

Session JA: Electron Ionization and Excitation 96

Session JB: Rare Gas Excimers and Group VI Lasers 102

Session KA: Breakdown 107

Session KB: Novel Laser Pumping Techniques 111

Session LA: Electrode Related Discharge Phenomena 114

Session LB: Photon Interactions 119

Session MA: Attachment 124

Session MB: Plasma Chemistry and Infrared Lasers 131

Session NA: Electron Scattering 136

Session NB: Reactions of Excited Species 139

Index to Abstracts 144

LEONARD BENEDICT LOEB
1891-1978
Scientist and Professor

Leonard Loeb was a professor of physics at the University of California at Berkeley for 36 years and professor emeritus for 20 more. He was a scientist par excellence in many fields but most actively in gaseous electronics. Professor Loeb was the author of 12 books and 180 papers, mentor of countless undergraduates and sixty-two doctoral students including

Hooper, William James		1926
Cravath, Austin M.		1928
Mahoney, Jerry Joseph		1928
Marshall, Lauritson C.		1929
Luhr, Overton		1930
Bradbury, Norris Edwin		1932
Sanders, Frederick Henry		1932
Ko, Cheng-Chuan	May	1933
Finney, Gladys Donaldine	Dec.	1934
Varney, Robert Nathan	May	1935
Posin, Daniel Q.	May	1935
Gardner, Milton Eugene	June	1937
Bowls, Noodford Eugene	Nov.	1937
Chapman, Seville	May	1938
Ehrenkranz, Florence Anna	May	1938
Trichel, Gervais William	May	1938
Hershey, Allen Vincent	July	1938
Kip, Arthur Frederic	March	1939
Gorrill, William Sterling	March	1939
Hale, Donald Herbert	Sept.	1939
Weissler, Gerhard Ludwig	May	1942
Geballe, Ronald	Oct.	1942
Fisher, Leon Harold	Sept.	1943
Morton, Paul Lester	Aug.	1943
Debeau, David Edmond	May	1944
McReynolds, Andrew Wetherbee	Feb.	1945
Koller, Ruedi	Feb.	1946
Johnson, Gerald Woodrow	Feb.	1947
English, William Noel	Jan.	1948
Miller, Charles G.	June	1949
Lauer, Eugene John	June	1951
Kunkel, Wulf Bernard	Sept.	1951
Dodd, Edward Elliot	Jan.	1952
Stein, Robert Preston	June	1952
Theobald, Jacob Karl	Jan.	1953
Amin, Mohammad Reza	June	1953
Bradley, Richard Crane	Sept.	1953
Peterson, John Wright	Sept.	1953
Hurlbut, Franklin Charles	Jan.	1954
Parker, James Henry, Jr.	Jan.	1954
Bandel, Herman William	June	1954
Evans, Ralph Aiken	June	1954
Huber, Elsa Louise	June	1954
Maunsell, Charles Dudley	Jan.	1955
Warren, Roger Wright	Jan.	1955
Gardner, Andrew Leroy (with W. Kunkel)	Sept.	1955
Wagner, Peter Ewing	Sept.	1956
Rohatgi, Vijay Kiemar	June	1957
Hudson, Gilbert Glover	Sept.	1957
Westberg, Russel George	Jan.	1958
Waters, Paul McElroy	June	1958
El-Bakkal, Jafar Mehdi	June	1960
Muray, Julius J.	June	1961
Dowell, Jerry Tray	Feb.	1966
MacLennan, Donald Allan	June	1966
Winn, William Paul	June	1966
Burrow, Paul David	Dec.	1966
Hassoun, Abbass Mohd	June	1967
Borst, Walter	March	1968
Breunig, James L.	Sept.	1972
Estrella, Rogelio Moreno	June	1975
Lanzaro, Andre	Dec.	1975

The Gaseous Electronics Conference (which was first chaired by his former student, Leon H. Fisher) became Professor Loeb's adopted Forum and happy meeting ground. He will be missed.

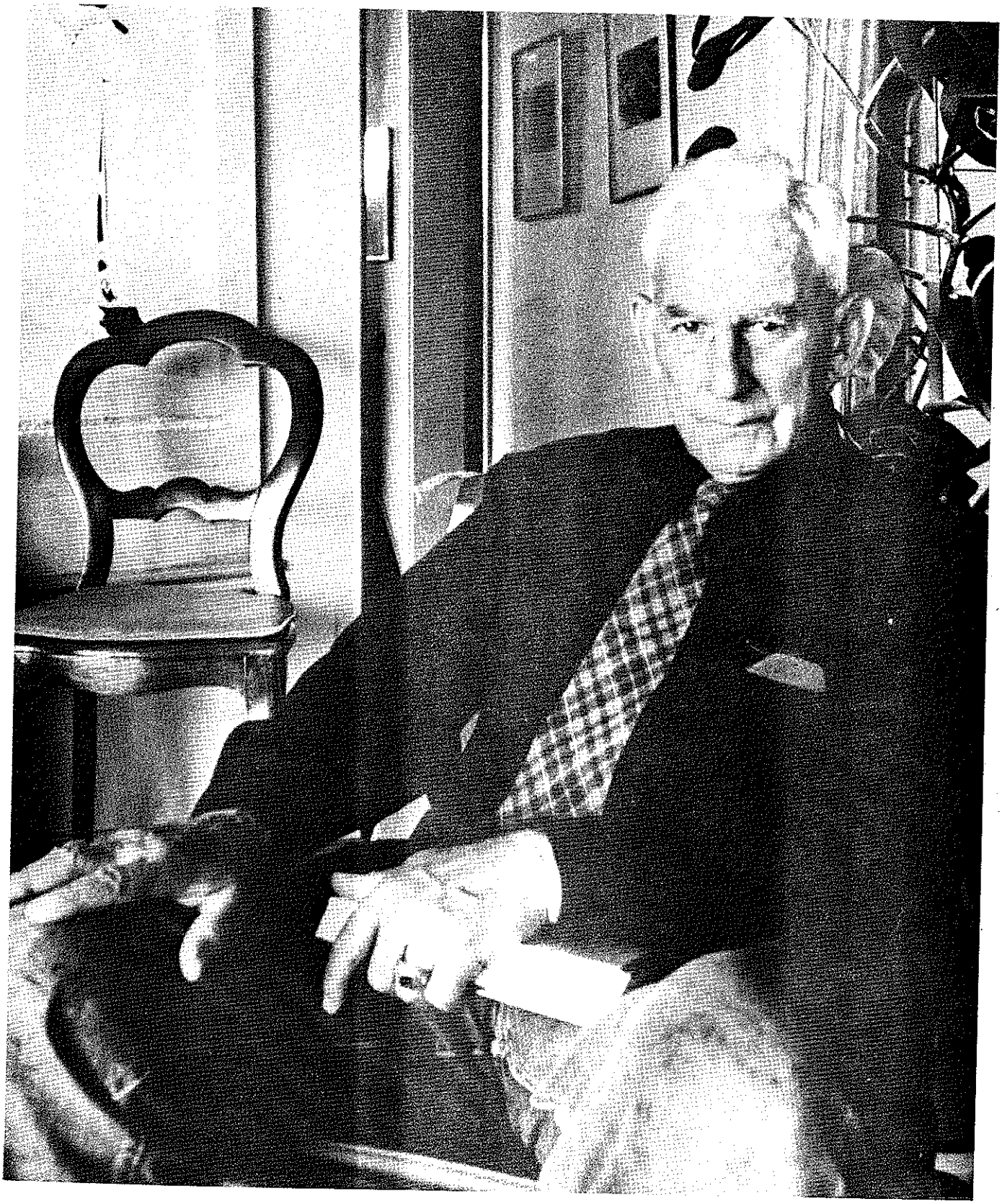

Professor Leonard B. Loeb

31st ANNUAL GASEOUS ELECTRONICS CONFERENCE

PROGRAM

OCTOBER 16, 1978 — **MONDAY EVENING, 7:30-10:00 p.m.**

REGISTRATION AND MIXER (CASH BAR)

Rendezvous Room, Statler Hilton

TUESDAY MORNING, 9:00 a.m.

SESSION AA: METAL VAPOR MOLECULAR LASERS
Chairperson: L.A. Schlie, Air Force Weapons Laboratory — Embassy Room

AA-1 COLLISIONAL QUENCING KINETICS OF HgCℓ * AND HgBr* ($B^2\Sigma$)
A. Mandl and J.H. Parks (7 min)

AA-2 DETERMINATION OF COLLISIONAL RATE CONSTANTS FOR THE HALIDE LASER MOLECULES
R.W. Waynant and J.G. Eden (7 min)

AA-3 CHARACTERIZATION OF ELECTRON-BEAM CONTROLLED HgCℓ DISCHARGES
B.E. Perry, R.M. Hill, M.V. McCusker and D.C. Lorents (7 min)

AA-4 ENERGY TRANSFER IN THE MERCURY-CADMIUM SYSTEM
M.W. McGeoch (7 min)

AA-5 ABSORPTION IN THE 470 nm BAND OF THE CADMIUM-MERCURY EXCIMER
J.B. West, H. Komine and E.A. Stappaerts (7 min)

AA-6 U-V PREIONIZED THALLIUM-MERCURY DISCHARGES
R.A. Hamil, D.L. Drummond, L.A. Schlie and R.P. Benedict (7 min)

AA-7 STRONG Tℓ -Xe EXCIMER BAND EMISSION VIA ELECTRON BEAM INITIATED STABLE GLOW DISCHARGES IN Tℓ I AND Xe MIXTURES
L.A. Schlie, L.E. Jusinski, R.D. Rathge, R.A. Hamil and D.L. Drummond (7 min)

AA-8 MODELS OF HIGH-POWER DISCHARGES IN Na-Xe VAPOR
R.Shuker, A. Gallagher and A.V. Phelps (7 min)

AA-9 OPTICAL STUDIES IN HIGH PRESSURE MERCURY DISCHARGES
R.E. Center and S.E. Moody (7 min)

SESSION AB: MAGNETOHYDRODYNAMICS
Chairperson: M.H. Scott, University of Tennessee Space Institute — Georgian Room

INTRODUCTORY REMARKS
M.H. Scott (12 min)

AB-1 NEAR-ELECTRODE SURFACES EFFECTS INFLUENCING SLAG-COATED ELECTRODES IN A COAL-FIRED MHD GENERATOR
M.H. Scott, M.S. Beaton and J.B. Dicks (7 min)

AB-2 CHARACTERIZATION OF THE DIFFUSE DISCHARGE AT THE ANODE OF AN OPEN-CYCLE MHD GENERATOR
D.S. Dvore, M. Martinez-Sanchez, J.B. Elgin, C.E. Kolb and M.B. Faist (7 min)

AB-3 VOLTAGE-CURRENT CHARACTERISTICS OF FARADAY MHD GENERATORS
D. Trung, H.K. Messerle and J.J. Lowke (7 min)

AB-4 THERMAL INSTABILITY IN MHD CHANNEL
T.-M. Fang (7 min)

AB-5 THE ION FLY-WHEEL EFFECT ON THE ELECTRO-THERMAL INSTABILITY IN NON-EQUILIBRIUM MHD HALL DISC GENERATORS
V. Thiagarajan (7 min)

AB-6 RADIAL DISTRIBUTIONS OF ELECTRICAL CONDUCTIVITY IN A CESIUM SEEDED, H_2-O_2 MHD DUCT
S.Y. Wang (7 min)

AB-7 IDENTIFICATION OF POSITIVE AND NEGATIVE ION SPECIES IN ATMOSPHERIC PRESSURE PULVERIZED COAL/ALKALI COMBUSTION PLASMAS
J.C. Wormhoudt and C.E. Kolb (7 min)

COFFEE BREAK 10:30 - 10:45 A.M.

SESSION BA: RARE GAS HALIDE AND NUCLEAR PUMPED LASERS

Chairperson: L.F. Champagne, Naval Research Laboratory — Embassy Room

BA-1 MULTIATMOSPHERE OPERATION OF A UV-PREIONIZED ELECTRIC DISCHARGE XeCℓ LSER
J.B. Laudenslager, R.V. Svorec and T.J. Pacala (7 min)

BA-2 EFFICIENT EXCITATION OF XeCℓ LASER BY E-BEAM AND DISCHARGE PUMPING
D.E. Rothe and J.B. West (7 min)

BA-3 EFFICIENT ELECTRON BEAM PUMPED XeCℓ LASER
L.F. Champagne (7 min)

BA-4 ENERGY FLOW KINETICS IN A XENON-CHLORIDE LASER
L.J. Palumbo, T.G. Finn and L.F. Champagne (7 min)

BA-5 DRAMATICALLY IMPROVED PERFORMANCE OF THE XeCℓ LASER USING Ar AS DILUENT GAS
R.C. Sze

BA-6 LASER PHOTODISSOCIATION OF $Cℓ_2$ OBSERVED AS A MECHANISM RESPONSIBLE FOR THE LONG STATIC FILL LIFETIME OF THE XeCℓ EXCIPLEX LASER
R.C. Sze and P.B. Scott (12 min)

BA-7 PRODUCTION OF XeF* (B) BY NUCLEAR PUMPING
G.H. Miley, F.P. Boody, S.J.S. Nagalingam and M.A. Prelas (7 min)

BA-8 RECENT RESULTS WITH THE ATOMIC CARBON LASER @ 1.4539 μ
M.A. Prelas, F.P. Boody and G.H. Miley (7 min)

BA-9 AN IMPROVED KINETIC THEORY FOR NUCLEAR-PUMPED LASERS
W.E. Meador and W.R. Weaver (7 min)

SESSION BB: TRANSFER MECHANISMS IN ARCS

Chairperson: R.S. Bergman, General Electric Cleveland — Georgian Room

BB-1 MECHANISM OF COLOR IMPROVEMENT IN THE PULSED HIGH PRESSURE SODIUM ARC
P.D. Johnson and T.H. Rautenberg, Jr. (7 min)

BB-2 NET RADIATION EMISSION OF SF_6, IODINE AND SODIUM FROM ARC MEASUREMENTS
R.J. Zollweg (7 min)

BB-3 THE RADIAL PROFILES OF CURRENT DENSITY AND TEMPERATURE IN A MAGNETICALLY CONFINED HELIUM ARC
T.S. Taylor and G.C. Smith (7 min)

BB-4 TWO TEMPERATURE MODEL OF A NONEQUILIBRIUM DISCHARGE IN ARGON
J.P. Novak, F. Hron and E.S. Krebes (7 min)

BB-5 ADDITIONAL VALIDATION OF THE MTE CONTINUUM RELATION FOR NON-LTE PLASMAS
T.L. Eddy and M.L. Fentress (7 min)

BB-6 HIGH PRESSURE CATAPHORESIS
R.S. Bergman and J.H. Ingold (7 min)

LUNCH 12:10 - 1:30 P.M.

TUESDAY AFTERNOON 1:30 p.m.

SESSION CA: KINETIC PROCESSES IN RARE GAS HALIDE LASERS
Chairperson: J.H. Jacob, Avco Everett Research Laboratory — Embassy Room

CA-1 ION PROCESSES IN RARE-GAS HALIDE LASERS
W.L. Nighan (7 min)

CA-2 POSITIVE IONS IN ATMOSPHERIC PRESSURE HELIUM AND HELIUM-NEON MIXTURES
W.J. Wiegand and R.H. Bullis (7 min)

CA-3 ELECTRONIC STRUCTURE AND PHOTOABSORPTION PROPERTIES OF NOBLE GAS TRIMER IONS
H.H. Michels and R.H. Hobbs (7 min)

CA-4 ULTRAVIOLET LASER EMISSIONS AND FLUORESCENCE ENHANCEMENTS IN AN E-BEAM EXCITED LOW TEMPERATURE AND HIGH DENSITY SUPERSONIC FLOW
B. Fontaine and B. Forestier (20 min)

CA-5 TEMPERATURE EFFECTS ON THE QUENCHING KINETICS OF XeF* IN E-BEAM PUMPED Ne/Xe/F_2 MIXTURES
D.W. Trainor, M. Rokni, J.H. Jacob and J.A. Mangano (7 min)

CA-6 RADIATIVE LIFETIME AND COLLISIONAL KINETICS OF THE XeF (II, 3/2) STATE
C.H. Fisher and R.E. Center (7 min)

CA-7 THEORETICAL STUDY OF FORMATION RATES OF RARE GAS HALIDE TRIMERS
V.H. Shui and C. Duzy (7 min)

CA-8 KINETICS OF KrF* AND Kr_2F* BY PROTON EXCITATION
C.H. Chen, M.G. Payne and J.P. Judish (7 min)

SESSION CB: ARCS AND FLOWS I
Chairperson: G. Frind, General Electric Corporate Research and Development Center — Georgian Room

CB-1 CORRELATED ELECTRICAL AND THERMAL PROPERTIES OF ARCS IN GAS FLOW
G.R. Jones (20 min)

CB-2 ARC INTERRUPTION CAPABILITIES OF GASES AND GAS MIXTURES
A. Lee and L.S. Frost (7 min)

CB-3 THERMAL RECOVERY PERFORMANCE OF BLOWN AC-ARCS IN VARIOUS GASES AND THEIR MIXTURES WITH SF_6
H.O. Noeske (7 min)

CB-4 MEASUREMENT OF CRITICAL POWER LOSS IN GAS BLAST INTERRUPTERS DURING THERMAL RECOVERY
G. Frind, L.E. Prescott and J.H. Van Noy (7 min)

CB-5 MODEL CALCULATIONS FOR POST CURRENT ZERO THERMAL BEHAVIOR IN GAS BLAST INTERRUPTERS
R.E. Kinsinger (7 min)

CB-6 EXPERIMENTAL AND THEORETICAL STUDY OF A D.C. ARC IN AN 8 DEGREE CONICAL NOZZLE FLOW
H.T. Nagamatsu and P.D. Symolon (7 min)

CB-7 ELECTRIC ARCS IN SUPERSONIC FLOW
C.K. Bhansali and D.M. Benenson (7 min)

COFFEE BREAK 3:05 - 3:20 P.M.

TUESDAY AFTERNOON 3:20 p.m.

SESSION DA: XeF KINETICS AND LASERS
Chairperson: D.L. Huestis, SRI International — Embassy Room

DA-1 THEORETICAL STUDY OF XeF VIBRATIONAL EXCITATION AND DISSOCIATION
C. Duzy and V.H. Shui (7 min)

DA-2 XeF GROUND STATE DYNAMICS
S.F. Fulghum, I.P. Herman, M.S. Feld and A. Javan (7 min)

DA-3 LOWER LASER LEVEL REMOVAL IN XeF
K.Y. Tang, R.O. Hunter, Jr. and D.L. Huestis (7 min)

DA-4 THE INFLUENCE OF THE BOUND LOWER LEVEL ON THE XeF* LASER PERFORMANCE
M. Rokni, J.H. Jacob, J.A. Mangano and J.C. Hsia (7 min)

DA-5 IMPROVEMENT IN XeF LASER EFFICIENCY AT ELEVATED TEMPERATURES
J.C. Hsia, J.A. Mangano, J.H. Jacob and M. Rokni (7 min)

DA-6 THE ROLE OF THE BROADBAND EMISSION IN THE XeF LASER
M. Rokni, J.C. Hsia, J.H. Jacob and J.A. Mangano (7 min)

DA-7 KINETIC OPERATION OF THE XeF* WAVEGUIDE LASER EXCITED BY A CAPACITIVELY COUPLED DISCHARGE
L.A. Newman (7 min)

DA-8 SCREENING OF FLUORINE-BEARING GASES FOR SELF-SUSTAINED DISCHARGE PUMPING OF RARE GAS-FLUORIDE LASERS
L.J. Denes, P.J. Chantry, N.T. Melamed and R.J. Spreadbury (7 min)

Session DA continued

DA-9 ENERGY LOADING LIMITATIONS IN 300 ns, SELF-SUSTAINED RARE GAS-HALIDE DISCHARGES
L.J. Denes, J.L. Pack and L.E. Kline (7 min)

DA-10 SELF-SUSTAINED DISCHARGE PUMPED XeF LASER AND DISCHARGE KINETICS
L.E. Kline, L.J. Denes, S.G. Leslie and R.R. Mitchell (7 min)

DA-11 X-RAY PREIONIZATION FOR ELECTRIC DISCHARGE LASERS
J.I. Levatter and S.C. Lin (7 min)

SESSION DB: ARCS AND FLOWS II
Chairperson: A. Lee, Westinghouse Research & Development Center — Georgian Room

DB-1 THEORY OF ARC CLOGGING IN NOZZLES
P. Kovitya, J.J. Lowke and A.D. Stokes (7 min)

DB-2 TEMPERATURE MEASUREMENTS IN TURBULENT ARCS
Y.K. Chien and D.M. Benenson (7 min)

DB-3 FREE CONVECTION IN HORIZONTAL HIGH PRESSURE MERCURY ARCS
D.K. McLain and R.J. Zollweg (7 min)

DB-4 SIMPLE THEORY OF FREE BURNING ARCS
J.J. Lowke (7 min)

DB-5 EMISSION OF A SOUND WAVE FROM A 0.01 TO 80 kA AC ARC
F. Nadeau and M.G. Drouet (7 min)

TUESDAY EVENING 7:30 p.m.

SESSION E: WORKSHOP ON FUNDAMENTAL PROCESSES IN EXCIMER LASERS
Moderator: C.K. Rhodes, University of Illinois at Chicago Circle — Embassy Room

E-1 AB INITIO CALCULATIONS ON HgCℓ AND HgBr: APPLICATION OF THE RELATIVISTIC EFFECTIVE CORE POTENTIAL METHODS
W. R. Wadt

E-2 THE DOMINANT KINETIC PROCESSES IN XeF LASER MEDIA
D.L. Huestis

E-3 APPLICATIONS OF RARE-GAS-HALIDE LASERS TO MULTIQUANTUM SPECTROSCOPY AND NONLINEAR OPTICS
J. Bokor

SESSION FA: ELECTRODE EFFECTS AND VACUUM ARCS
Chairperson: J.V.R. Heberlein, Westinghouse Research & Development Center — Embassy Room

FA-1 MICROWAVE DIAGNOSTICS OF A VACUUM ARC PLASMA
M. Rosenfeld, R. Dollinger and C.N. Manikopoulos

FA-2 NEUTRAL TEMPERATURES AND DENSITIES IN A COPPER VACUUM ARC WITH A RING ANODE
W. Crompton, F.N. Yao, J.L. Lee, R. Dollinger, D.P. Malone and D.M. Benenson
(12 min)

FA-3 CATHODE MATERIAL STUDY WITH A HOLLOW ANODE
P. Schwartz, R. Dollinger, A.S. Gilmour and D.P. Malone (7 min)

FA-4 VOLTAGE FLUCTUATIONS IN LOW CURRENT ATMOSPHERIC D.C. ARCS
M.G. Drouet, R. Haug and M. Goldman (7 min)

FA-5 DYNAMIC MEASUREMENTS OF CATHODIC EMISSION ON OXIDE FILMS
H. Mercure and M.G. Drouet (7 min)

FA-6 CATHODE CURRENT DENSITIES AND CURRENT PER CELL IN A COPPER CATHODE VACUUM ARC
G.P. Smith, D.P. Malone, R. Dollinger and A.S. Gilmour (7 min)

FA-7 POWER FLUX TO THE CATHODE OF A dc MERCURY VACUUM ARC
G. Eckhardt (12 min)

FA-8 A SIMPLE CLASSICAL ANALYSIS FOR PARTICLE-SURFACE ENERGY ACCOMMODATION
L.P. Harris (7 min)

SESSION FB: ELECTRON AND ION TRANSPORT
Chairperson: J.J. Lowke, University of Sydney — Georgian Room

FB-1 THREE-TEMPERATURE THEORY OF GASEOUS ION TRANSPORT
L.A. Viehland, S.L. Lin and E.A. Mason (20 min)

FB-2 DIFFUSION OF IONS IN OXYGEN, NITROGEN, CARBON MONOXIDE AND CARBON DIOXIDE
J.A. Rees and S.R. Alger (7 min)

FB-3 THE DRIFT VELOCITY OF ELECTRONS IN MERCURY VAPOUR
M.T. Elford (7 min)

FB-4 ELECTRON DRIFT AND DIFFUSION IN POLYATOMIC GASES
P. Kleban and H.T. Davis (20 min)

FB-5 MODEL OF DRIFT VELOCITY ENHANCEMENT AND DIFFERENTIAL NEGATIVE CONDUCTIVITY IN MOLECULAR GAS-RARE GAS MIXTURES
M.R. Stamm, W.F. Bailey and A. Garscadden (7 min)

COFFEE BREAK 10:00 - 10:15 A.M.

SESSION GA: ION INTERACTIONS AND MOBILITIES I
Chairperson: P.C. Cosby, SRI International — Embassy Room

GA-1 ION-MOLECULE REACTION STUDIES USING A NEW FLOW-DRIFT TUBE
W. Lindinger, E. Alge, H. Stori and R.N. Varney (20 min)

GA-2 REACTIONS OF EXCITED IONS OF THE RARE GASES
M. Grossl, H. Helm, M. Langenwalter and T.D. Mark (7 min)

GA-3 ION-MOLECULE ASSOCIATION REACTIONS
F.C. Fehsenfeld, T.J. Brown and D.L. Albritton (7 min)

GA-4 ION-MOLECULE REACTIONS OF SINGLY AND MULTIPLY CHARGED ATOMIC AND MOLECULAR IONS IN Kr AND KR + $C\ell_2$ DISCHARGES
F. Howorka, I. Kuen and R.N. Varney (7 min)

GA-5 MEASUREMENTS OF THE REACTION $He^+ + H_2 \rightarrow He + H^+ + H$ AT LOW TEMPERATURES
A.K. Chen, R. Johsen and M.A. Biondi (7 min)

GA-6 THE PRODUCTION OF $NO^+ (a\ ^3\Sigma^+)$ IN THE REACTION OF N^+ WITH O_2
D.L. Albritton, A.A. Viggiano, I. Dotan and F.C. Fehsenfeld (7 min)

GA-7 REACTIONS OF DRIFT-INDUCED VIBRATIONALLY EXCITED IONS
W. Lindinger, D.L. Albritton and F.C. Fehsenfeld (7 min)

GA-8 THE DETERMINATION OF THERMAL ENERGY RATE CONSTANTS USING A MODIFIED VERSION OF THE SELECTED ION FLOW TUBE (SIFT) TECHNIQUE
G.I. Mackay, G. Vlachos, H.I. Schiff and D.K. Bohme (7 min)

GA-9 MOBILITY OF IONS IN METHANE GAS
M. Saporoschenko

GA-10 IONIC POLYMERIZATION IN CH_4
M. Saporoschenko (12 min)

Session FB continued

FB-6 ON THE DIFFUSION APPROXIMATION OF THE BOLTZMANN EQUATION FOR SLOW ELECTRONS
J.H. Jacob, B.N. Srivastava, M. Rokni and J.A. Mangano (7 min)

FB-7 THEORY OF ELECTRON DRIFT AND DIFFUSION IN NEUTRAL GASES IN AN ELECTROSTATIC FIELD
S.L. Lin, R.E. Robson and E.A. Mason (7 min)

FB-8 ANALYTIC SOLUTIONS FOR ELECTRON ENERGY DISTRIBUTIONS IN GAS DISCHARGE LASERS
P.E. Nielsen, T.E. Gist and E.D. Seward (7 min)

10:45 a.m.

SESSION GB: GLOW DISCHARGES
Chairperson: J.T. Verdeyen, University of Illinois — Georgian Room

GB-1 A GENERAL CHARACTERISTIC EQUATION FOR A DIFFUSION-CONTROLLED POSITIVE COLUMN OF ARBITRARY SHAPE WITH ONE-AND TWO-STEP IONIZATION
G.L. Rogoff (12 min)

GB-2 BEHAVIOR OF NEON DISCHARGES
R.M.M. Smits (20 min)

GB-3 MODEL CALCULATIONS ON THE POSITIVE COLUMN OF Hg-NOBLE GAS DISCHARGES
F.A.S. Ligthart (7 min)

GB-4 ELECTRON DENSITY DISTRIBUTIONS IN A LOW-PRESSURE DISCHARGE TUBE CONTAINING AN ARRAY OF DIELECTRIC FIBERS
G.L. Rogoff (7 min)

GB-5 AVERAGE LOSS RATE OF ELECTRON ENERGY IN POSITIVE COLUMN OF OXYGEN GLOW DISCHARGE
K. Nobata, T. Kakishima and M. Kando (7 min)

GB-6 ELECTRON ENERGY RELAXATION IN LOW-PRESSURE GAS DISCHARGES
F.A.S. Ligthart and R.A.J. Keijser (7 min)

LUNCH 12:05 - 1:30 P.M.

SESSION HA: ION INTERACTIONS AND MOBILITIES II

Chairperson: H. Helm, Universität Innsbruck — Embassy Room

HA-1 INELASTIC PROCESSES IN 5-500 eV He^+-Li COLLISIONS
G.D. Myers and J.J. Leventhal (7 min)

HA-2 MOBILITIES OF He^{++}, Ne^{++}, Ar^{++} AND Xe^{++} IN THEIR PARENT GASES
R. Johnsen and M.A. Biondi (7 min)

HA-3 RADIATIVE AND NON-RADIATIVE CHARGE TRANSFER REACTIONS OF DOUBLY CHARGED RARE GAS IONS WITH RARE GASES
R. Johnsen and M.A. Biondi (20 min)

HA-4 INTERACTIONS OF α PARTICLES WITH He ATOMS
J.N. Bardsley, J.S. Cohen and J.M. Wadehra (7 min)

HA-5 POTENTIAL SURFACES GOVERN PROCESSES IN IONIZED GASES
D.G. Hopper (7 min)

HA-6 SWITCHING REACTIONS OF SOLVATED HYDROXYL IONS
J.F. Paulson (7 min)

HA-7 ENERGETICS AND STRUCTURES OF THE EXCITED AND GROUND STATES OF CO_3^-
R.L.C. Wu and T.O. Tiernan (7 min)

HA-8 NEGATIVE ION CHEMISTRY IN AIR-LIKE GAS MIXTURES
V.A. Mohnen and J.A. Kadlecek (7 min)

SESSION HB: DIAGNOSTICS AND AFTERGLOWS

Chairperson: D.P. Malone, State University of New York at Buffalo — Georgian Room

HB-1 NEAR-RESONANT LIGHT SCATTERING FROM GROUND-STATE AND EXCITED Na ATOMS IN A GAS DISCHARGE
L. Vriens and J. de Ruyter (7 min)

HB-2 USE OF COLLISIONAL-RADIATIVE MODEL FOR PLASMA DIAGNOSTIC PURPOSES
A.K. Hui (7 min)

HB-3 INTERACTION BETWEEN VIBRATIONALLY EXCITED MOLECULAR NITROGEN AND ATOMIC CESIUM
R. Chandra, N. Shah, C.H. Lee, C.N. Manikopoulos and D.T. Shaw

HB-4 PULSED DISCHARGE OF CESIUM SEEDED MOLECULAR NITROGEN
N. Hatziprokopiou, F. Radpour, C.N. Manikopoulos and D.T. Shaw (12 min)

HB-5 LASER INITIATED AFTERGLOW IN A HIGH PRESSURE K-Kr MIXTURE
L.K. Lam and L.D. Schearer (7 min)

HB-6 STUDIES OF POPULATION INVERSIONS IN MPD ARC GENERATED HELIUM PLASMAS
T.B. Simpson, T.M. York, W.F. Von Jaskowsky, K.E. Clark and R.G. Jahn (7 min)

HB-7 ELECTRON COLLISION FREQUENCIES IN Ar, He, Ne GASES AND THEIR RELATION TO THE VOLUME RECOMBINATION CONTROLLED PLASMA AFTERFLOW
J.S. Chang, P. Baille, G.L. Ogram, K. Keskinen and R.M. Hobson (7 min)

HB-8 ELECTRONIC RECOMBINATION OF He^+
J.F. Delpech and J. Boulmer (7 min)

COFFEE BREAK 3:05 - 3:20 P.M.

SESSION I: WORKSHOP ON DISSOCIATIVE RECOMBINATION
Moderator: M.A. Biondi, University of Pittsburgh

Embassy Room

Discussion contributors:

A. Experimental Investigations
G.H. Dunn (Stored Ions)
J.W. McGowan (Merged Beams)
A.J. Cunningham (Shock Tubes)
M.A. Biondi (Static Afterglows)
E.C. Zipf (Laser Resonance Fluorescence)

B. Theoretical Investigations
J.N. Bardsley
C.M. Lee
H.H. Michels

C. Ionospheric Inferences
D.G. Torr

Contributed paper:

I-1 ELECTRON AND ION TEMPERATURE DEPENDENCE OF THE DISSOCIATIVE RECOMBINATION COEFFICIENTS OF H_3O^+ AND D_3O^+
G.L. Ogram, J.S. Chang, J.B. Hoye and R.M. Hobson (7 min)

SESSION JA: ELECTRON IONIZATION AND EXCITATION

Chairperson: J. Mazeau, Université Pierre et Marie Curie — Embassy Room

JA-1 ELECTRON IMPACT DOUBLE IONIZATION CROSS SECTIONS OF K^+ IONS
R.K. Feeney and W.E. Sayle, II (7 min)

JA-2 ELECTRON EXCITATION OF THE S AND D STATES OF Li
A. Zajonc and A. Gallagher (7 min)

JA-3 EXCITATION AND PREDISSOCIATION OF TRIPLET STATES IN H_2 AND D_2 MEASURED BY ELECTRON-PHOTON COINCIDENCES
N. Bose (7 min)

JA-4 ELECTRON IMPACT IONIZATION OF RARE GAS DIMERS AND ATOMS
H. Helm, K. Stephan and T.D. Mark (20 min)

JA-5 EXCITATION OF N_2 ($A_3\Sigma^+_u$) BY ELECTRONS
D. Levron and A.V. Phelps (7 min)

JA-6 ELECTRON-IMPACT DISSOCIATION OF O_2: EXCITATION OF THE O^I QUINTET STATES
M.R. Gorman, E.C. Zipf and R.W. McLaughlin (7 min)

JA-7 METASTABLE FRAGMENTATION OF NH_3 INDUCED BY ELECTRON BOMBARDMENT
B.L. Carnahan and E.C. Zipf (7 min)

JA-8 PHOTOABSORPTION SPECTRUM OF CF_3I BY ELECTRON IMPACT
S.K. Srivastava, S. Trajmar and N.W. Winter (7 min)

JA-9 A STUDY OF EXCITED FRAGMENT EMISSION FROM THE ELECTRON IMPACT DISSOCIATION OF VOLATILE MERCURY (II) HALIDES
J. Allison and R.N. Zare (7 min)

SESSION JB: RARE GAS EXCIMERS AND GROUP VI LASERS

Chairperson: H.T. Powell, Lawrence Livermore Laboratory — Georgian Room

JB-1 TIME RESOLVED SPECTROSCOPY OF KRYPTON AND XENON EXCIMERS EXCITED BY SYNCHROTRON RADIATION
T.D. Bonifield, F.H.K. Rambow, G.K. Walters, M.V. McCusker, D.C. Lorents and R.A. Gutcheck (20 min)

JB-2 FLUORESCENCE STUDIES OF Kr_2^* AT 1457 Å
M.J.W. Boness and C. Duzy (7 min)

JB-3 Kr_2^* FLUORESCENCE STUDIES FOR LOW CURRENT, LONG PULSE ELECTRON-BEAM PUMPING
D.J. Eckstrom, H.H. Nakano, D.C. Lorents and J.A. Betts (7 min)

JB-4 ELECTRON DENSITY MEASUREMENTS IN Kr PUMPED BY A LOW CURRENT, LONG PULSE E-BEAM
T. Rothem, H.H. Nakano, D.C. Lorents, D.J. Eckstrom and J.A. Betts (7 min)

JB-5 KINETIC PROCESSES IN SELENIUM ATOM LASERS
M.J. Shaw (20 min)

JB-6 SULFUR ^1S_O - $^1D_2$ LASER BY OCS PHOTODISSOCIATION
H.T. Powell, D. Prosnitz and B.R. Schleicher (7 min)

JB-7 ELECTRON ENERGY DISTRIBUTIONS IN PHOTOLYTICALLY PUMPED LASERS
R.D. Franklin, W.L. Morgan and R.A. Haas (7 min)

COFFEE BREAK 10:15 - 10:30 A.M.

SESSION KA: BREAKDOWN*
Chairperson: L.H. Fisher, California State University at Haywood — Embassy Room

KA-1 THEORY OF LOW PRESSURE SPARK BUILDUP
E.J. Lauer, D.M. Cox and S.S. Yu (7 min)

KA-2 ULTRAVIOLET LASER INDUCED GAS BREAKDOWN
R.R. Butcher and S.H. Gurbaxani (7 min)

KA-3 2-D BREAKDOWN ISOLATORS FOR LASER-FUSION LASERS
R.J. Bjurstrom and C.J. Elliott (7 min)

KA-4 THE RADIAL DISTRIBUTION OF SPACE CHARGE WITHIN A FILAMENTARY DISCHARGE CHANNEL
E. Marode, D. Hilhorst, I. Gallimberti and B. Gallimberti (7 min)

KA-5 CRITERIA FOR MAINTENANCE OF SPATIAL HOMOGENEITY DURING THE FORMATIVE PHASE OF A PULSED AVALANCHE DISCHARGE
S.C. Lin and J.I. Levatter (7 min)

*This session is dedicated to the memory of Leonard B. Loeb.

SESSION KB: NOVEL LASER PUMPING TECHNIQUES
Chairperson: C.B. Collins, University of Texas at Dallas — Georgian Room

KB-1 THE ATOMIC FLUORINE LASER USING A HOLLOW CATHODE DISCHARGE
J.K. Crane and J.T. Verdeyen (7 min)

KB-2 CO_2 LASER-PRODUCED PLASMA-INITIATED RECOMBINATION LASER STUDIES IN Ar, Cℓ, Kr, N, and Xe
W.T. Silfvast, L.H. Szeto and O.R. Wood, II (20 min)

KB-3 ELECTRON COLLISIONAL LASER IN Pb^+ POPULATED BY RECOMBINATION
W.T. Silfvast, L.H. Szeto and O.R. Wood, II (7 min)

KB-4 THE PRODUCTION OF EXCITED METAL ATOMS BY FRAGMENTATION OF METAL CARBONYLS AND OTHER METAL-ENCAPSULATED COMPOUNDS
J. Allison, Z. Karny, R. Naaman and R.N. Zare (7 min)

THURSDAY MORNING

PLENARY SESSION: 11:25 A.M. — **Embassy Room**

"Leonard Loeb: Scientist and Professor Throughout the Twentieth Century Transitions"
R.N. Varney

BUSINESS MEETING: 11:45 - 12:05 P.M. — **Embassy Room**

LUNCH 12:05 - 1:45 P.M.

SESSION LA: ELECTRODE RELATED DISCHARGE PHENOMENA*

Chairperson: W.L. Borst, Southern Illinois University — Embassy Room

LA-1 COMPARISON OF MONTE CARLO AND BOLTZMANN CALCULATIONS OF ELECTRON DIFFUSION TO AN ANODE
G.L. Braglia and J.J. Lowke (7 min)

LA-2 NEGATIVE OXYGEN IONS IN A CYLINDRICAL HOLLOW CATHODE
R.N. Varney, I. Kuen and F. Howorka (7 min)

LA-3 MODEL OF THE HOLLOW CATHODE DISCHARGE USING A TWO-FLUID THEORY
B.E. Warner and K.B. Persson (7 min)

LA-4 POWER DEPOSITION IN THE CATHODE-FALL AND NEGATIVE GLOW REGIONS OF A DISCHARGE
S.B. Hutchison and J.T. Verdeyen (7 min)

LA-5 STEADY-STATE CATHODE FALL MODEL WITH TRANSVERSE GAS FLOW
W.H. Long, Jr. (7 min)

LA-6 OBSERVATIONS OF DENSITY DISTURBANCES IN THE CATHODE REGION OF ELECTRON-BEAM SUSTAINED DISCHARGES
E. Margalith and W.H. Christiansen (7 min)

LA-7 TEA CO_2 LASER PERFORMANCE USING TWO CURRENT EXCITATION PULSES
R. Turner and R.A. Murphy (7 min)

*This session is dedicated to the memory of Leonard B. Loeb.

SESSION LB: PHOTON INTERACTIONS

Chairperson: D.L. Albritton, NOAA — Georgian Room

LB-1 COOLING OF RESONANT ABSORBERS BY PHOTON PRESSURE
R.E. Drullinger, D.J. Wineland and F.L. Walls (20 min)

LB-2 COAXIAL BEAMS PHOTOFRAGMENT SPECTROSCOPY OF O_2^+
P.C. Cosby, J.B. Ozenne, J.T. Moseley and D.L. Albritton (20 min)

LB-3 TWO-PHOTON PHOTODETACHMENT OF C_2^-
P.L. Jones, R.D. Mead and W.C. Lineberger (7 min)

LB-4 PHOTODISSOCIATION AND PHOTODETACHMENT OF IONS IN $O_2/CH_4/H_2O$ FROM 4000 TO 8600 Å
L.C. Lee and G.P. Smith (7 min)

LB-5 PHOTODISSOCIATION CROSS SECTIONS OF ATMOSPHERIC POSITIVE IONS 3500-8600 Å
G.P. Smith and L.C. Lee (7 min)

LB-6 PHOTODESTRUCTION OF IONS FORMED IN $O_2/SO_2/Ar$ GAS MIXTURES
R.V. Hodges and J.A. Vanderhoff (7 min)

LB-7 MULTIPHOTON IONIZATION OF Cs-INSERT GAS EXCIMERS
M.A. Chellehmalzadeh and C.B. Collins

LB-8 MULTIPHOTON IONIZATION OF Cs_2 DIMERS THROUGH DISSOCIATIVE MOLECULAR STATES
J.A. Anderson, C.B. Collins, D. Popescu and I. Popescu

(LB-7, LB-8: 12 min)

OPEN HOUSE: 3:30 P.M.

CALSPAN CORPORATION
OR
LABORATORY FOR POWER AND ENVIRONMENTAL STUDIES AT THE STATE UNIVERSITY OF NEW YORK AT BUFFALO

SOCIAL HOUR: 6:30 P.M.

The Babcock Dining Room, Talbert Hall; Amherst campus, State University of New York at Buffalo.

BANQUET: 7:30 P.M.

The Talbert Banquet Room, Talbert Hall; Amherst campus, State University of New York at Buffalo.

GUEST SPEAKER

Dr. Verner E. Suomi
Professor of Meteorology and
Director, Space Science and Engineering Center
University of Wisconsin-Madison

TOPIC: "Weather and Climate: On the Earth and Other Planets"

SESSION MA: ATTACHMENT
Chairperson: A. Herzenberg, Yale University — Embassy Room

MA-1 H^- NEGATIVE ION BEAM DIRECT EXTRACTION FROM A HYDROGEN MULTIPOLE PLASMA
M. Bacal, A.M. Bruneteau, H.J. Doucet and A.M. Marechal (7 min)

MA-2 DISSOCIATIVE ATTACHMENT FROM VIBRATIONALLY AND ROTATIONALLY EXCITED H_2 BY ELECTRON IMPACT
M. Allan and S.F. Wong (20 min)

MA-3 THE DEPENDENCE OF THE DISSOCIATIVE ATTACHMENT ON THE VIBRATIONAL AND ROTATIONAL STATE IN e-H_2 COLLISIONS
J.M. Wadehra and J.N. Bardsley (7 min)

MA-4 MEASUREMENTS OF ATTACHMENT COEFFICIENTS AND IONIC MOBILITIES IN NF_3-N_2 MIXTURES
V.K. Lakdawala and J.L. Moruzzi (7 min)

MA-5 DISSOCIATIVE ATTACHMENT CROSS SECTION MEASUREMENTS IN F_2 AND NF_3
P.J. Chantry (7 min)

MA-6 ELECTRON ATTACHMENT AND IONIZATION RATES, AND ELECTRON DRIFT VELOCITIES IN RARE GAS - HALIDE GAS MIXTURES
S.R. Hunter, K.J. Nygaard, S.R. Foltyn and H. Brooks (12 min)

MA-7 TEMPERATURE DEPENDENCE OF THE ATTACHMENT REACTION RATE IN I_2-He GAS MIXTURES
H. Brooks, S.R. Hunter and K.J. Nygaard

MA-8 DISSOCIATIVE ATTACHMENT OF ELECTRONS TO F_2
C.A. Brau, A.E. Greene, S.D. Rockwood and B.I. Schneider (7 min)

MA-9 ELECTRON ATTACHMENT RATE CONSTANT FOR $C\ell_2$ AT ROOM TEMPERATURE AND 250°C
M. Rokni, J.H. Jacob and J.A. Mangano (7 min)

MA-10 ELECTRON ATTACHMENT TO CHLOROFLUOROMETHANES
D.L. McCorkle, A.A. Christodoulides and L.G. Christophorou (7 min)

MA-11 NEGATIVE IONS FORMED BY ELECTRON IMPACT ON FLUOROCARBONS
I. Sauers, L.G. Christophorou and J.G. Carter (7 min)

SESSION MB: PLASMA CHEMISTRY AND INFRARED LASERS
Chairperson: J.W. Rich, Calspan Corporation — Georgian Room

MB-1 ANALYSIS OF OZONE GENERATION PROCESSES AT ATMOSPHERIC PRESSURE IN E-BEAM CONTROLLED DISCHARGES
D. Pigache, G. Fournier, G. Gousset and M. Lecuiller (7 min)

MB-2 OZONE PRODUCTION IN FAST PULSED HIGH VOLTAGE DIELECTRIC BARRIER DISCHARGES IN O_2
L.A. Rosocha and W.A. Fitzsimmons (12 min)

MB-3 AN EXPERIMENT TO INVESTIGATE PLASMA CHEMISTRY IN E-BEAM PUMPED CLOSED CYCLE CO_2 LASERS
P. Bletzinger and C.A. DeJoseph (7 min)

MB-4 DISCHARGE CHARACTERISTICS IN CW CO_2 EDLS
D. L. Smith, C.M. Lee, T.W. Meyer and P.D. Tannen (7 min)

MB-5 TRANSVERSE ELECTRODELESS DISCHARGE EXCITATION OF A CO_2 LASER
C.P. Christensen (7 min)

MB-6 THE 16μm CO_2 BENDING MODE LASER
L.H. Taylor and R.B. Feldman (7 min)

MB-7 CO LASER OPERATING ON 1ST OVERTONE INFRARED BAND
R.C. Bergman and J.W. Rich (7 min)

COFFEE BREAK 10:30 - 10:45 A.M.

SESSION NA: ELECTRON SCATTERING
Chairperson: J.N. Bardsley, Los Alamos Scientific Laboratory Embassy Room

NA-1 DECAY OF FESHBACH RESONANCES IN NO: ELECTRONIC AND DYNAMIC COUPLING
J. Mazeau (20 min)

NA-2 TEMPORARY NEGATIVE ION FORMATION IN ALKALI VAPORS
A.R. Johnston and P.D. Burrow (7 min)

NA-3 INELASTIC ELECTRON COLLISIONS AT VERY LOW ENERGIES USING A MAGNETICALLY COLLIMATED ELECTRON BEAM
W.C. Tam and S.F. Wong (7 min)

NA-4 LOW ENERGY ELECTRON SCATTERING IN METHANE AND OTHER SATURATED HYDROCARBONS
P.D. Burrow and J.A. Michejda (7 min)

SESSION NB: REACTIONS OF EXCITED SPECIES
Chairperson: R.E. Drullinger, NBS Boulder Georgian Room

NB-1 MEASUREMENT OF THE RATE COEFFICIENTS FOR THE BIMOLECULAR AND TERMOLECULAR CHARGE TRANSFER REACTIONS OF $He(2^3S)$, $He_2(^3\Sigma_u)$ AND Ar_2^+
C.B. Collins and F.W. Lee (7 min)

NB-2 QUENCHING OF NEON METASTABLE ATOMS IN PURE NEON AFTERGLOWS
R.A. Sierra and A.J. Cunningham (7 min)

NB-3 KINETIC STUDY OF Ar^*-CO_2 TRANSFER. POSSIBILITY OF CO CAMERON LASER
J.P. Gauyacq, F. Collier and P. Cottin (7 min)

NB-4 IONIZATION AND ENERGY POOLING IN LASER EXCITED Na VAPOR
G.H. Bearman and J.J. Leventhal (7 min)

NB-5 EXCITATION OF $O(^3S)$ RESONANCE RADIATION IN INELASTIC COLLISIONS BETWEEN $O(^5S)$ METASTABLES AND O_2 MOLECULES
J. Fricke, H.K. Kiefl and W.L. Borst (7 min)

NB-6 THE EFFECT OF SPIN-ORBIT COUPLING ON QUENCHING OF $O(^1D)$ BY RARE-GAS ATOMS
J.S. Cohen, W.R. Wadt and P.J. Hay (7 min)

NB-7 ANALYSIS OF THE $N_2(C^3\pi_u)$ EXCITATION BY $Ar(^3P_2)$ AND $Ar(^3P_o)$ METASTABLE ATOMS
T.D. Nguyen and N. Sadeghi (7 min)

SESSION AA

9:00 A.M. – 10:30 A.M., Tuesday, October 17

Embassy Room

METAL VAPOR MOLECULAR LASERS

Chairperson: L.A. Schlie,
Air Force Weapons Laboratory

AA-1

Collisional Quenching Kinetics of $HgC\ell^*$ and $HgBr^*(B^2\Sigma)$ - A. MANDL, and J. H. PARKS, Avco Everett Research Laboratory.† --The rates of collisional quenching of $HgC\ell^*$ ($B^2\Sigma^+_{1/2}$) by He, Ar, Xe, N_2, $C\ell_2$, $HC\ell$ and $CC\ell_4$ and $HgBr^*$ ($B^2\Sigma^+_{1/2}$) by He, Ar, Xe, N_2, Br_2, HBr, CF_3Br and $CC\ell_3Br$ have been determined. Steady state measurements were made of $HgC\ell^*$ and $HgBr^*$ fluorescence produced by photolyzing $HgC\ell_2$ and $HgBr_2$, respectively, using Xe_2^* radiation. A background pressure of $[Xe] \geq 100$ Torr was used to ensure that the $HgC\ell^*$ and $HgBr^*$ were vibrationally relaxed. A modified Stern-Volmer analysis together with the measured lifetime of these excimers was used to determine the quenching rates. Both two and three body rates have been observed over the pressure range ($P \leq 4000$ Torr).

†Supported by DARPA/ONR under Contract # N00014-78-C-0334

AA-2

Determination of Collisional Rate Constants for the Halide Laser Molecules† - R.W. WAYNANT AND J.G. EDEN Naval Research Lab., Wash., D.C. 20375--The radiative lifetimes of the HgBr(I) and HgI(B) states have been measured to 23.7 ± 1.5 and 27.3 ± 2.0ns, respectively, by fast photolysis of $HgBr_2$ and HgI_2. The dihalides were photodissociated with UV fluorescence from the ArF (193nm) or KrCl (222nm) molecules, formed by irradiating $Ne/Ar/F_2$ or $Ar/Kr/Cl_2$ gas mixtures with a 3ns beam of 600 KeV electrons. This experimental technique allowed observation of the exponential decay of the desired HgX* (X = Br or I) population from which the HgX(B→X) radiative lifetimes and rate constants for deactivation of the HgX(B) states by HgX_2 were determined. Using a similar approach, the KrF(B→X) radiative lifetime (6.8 ± 0.2ns) and the quenching rate constants for KrF(B) by the rare gases and several halogenated molecules were also measured. The applicability of this technique to the determination of collisional quenching rates for other metal halides (such as SnX* or PbX*) will also be discussed.

†Work supported in part by DARPA.

AA-3

Characterization of Electron-Beam Controlled HgCl Discharges.* B.E. PERRY, R.M. HILL, M.V. McCUSKER† and D.C. LORENTS, Molecular Physics Laboratory, SRI International.--Fluorescence efficiency and stability of electron-beam-controlled discharges have been studied in flowing Ar/Hg/Cl_2 mixtures with several electrode configurations (typical conditions: 1500/10/10 torr, respectively, E/N = 10^{-16} Vcm^2, gas residence time = 2 sec). Stable discharges were obtained under conditions of high discharge power enhancement ($P_{dis}/P_{e-b} > 5$). $HgCl^*$ production efficiencies (power into $HgCl^*$/input power) of up to 15% were observed, although the fluorescence efficiency (photon intensity/input power) is lower due to quenching by Cl_2. Variation of the discharge behavior and fluorescence efficiency with the gas residence time was observed and attributed to Cl_2 removal by the wall-catalyzed pre-reaction with Hg. High production efficiency was observed even at low flow rate. The controlling kinetic processes will be discussed.

*Supported by DARPA through the U.S. Army BMDATC.

†Present address: Spectra-Physics, Inc., Mountain View, CA

AA-4

Energy Transfer in the Mercury-Cadmium System- M.W. McGEOCH, SRC, Rutherford Lab.,UK--The mercury-cadmium excimer is of interest as a potential high efficiency discharge-excited laser system at ∿470 nm. We wish to report an experiment in which Hg/Cd vapour mixtures were pumped by 10 nsec optical pulses at 266 nm. As Cd density increased, the continuum radiation from Hg_3^* underwent spectral and temporal changes which indicated the formation of two radiating Hg/Cd species. The first had a decay lifetime of ∿ 3 μsec and a spectrum centred at 470 nm which was narrower than the Hg_3^* spectrum. At still higher Cd densities, a further transfer occurred into a state which decayed in 1.3 μsec, with a similar spectrum. Possible kinetic models for these processes will be discussed. Preliminary evidence suggests that mixed Cd/Hg trimers have been observed.

AA-5

Absorption in the 470 nm Band of the Cadmium-Mercury Excimer*- J. B. WEST, H. KOMINE, and E. A. STAPPAERTS, Northrop Research & Technology Center, Palos Verdes, CA -- Recently, the cadmium-mercury excimer (CdHg*) has attracted attention as a potential laser medium. We report the experimental observation of net absorption throughout the CdHg* 470 nm fluorescence band. In these experiments Cd, Hg, and Ar were contained in a quartz cell heated to 630 C. Typical number densities are $3x10^{17} cm^{-3}$ of Cd, $2x10^{18}$ cm^{-3} of Hg, and $8.5x10^{18}$ cm^{-3} of Ar. CdHg* was excited by optical excitation of $Cd(5^3P_1)$ at 326.1 nm using a tunable laser. Absorption was probed using several argon-ion laser lines. Net absorption on the order of several percent per pass was observed. This absorption vanishes as the 326.1 nm pump laser is detuned from the Cd absorption line. The most likely cause is an excited state absorption in CdHg*. These measurements cast doubt on the possibility of an efficient CdHg* laser.

*Work supported by Office of Naval Research

AA-6

U-V Preionized Thallium-Mercury Discharges. R.A. HAMIL, D.L. DRUMMOND, L.A. SCHLIE and R.P. BENEDICT, AF Weapons Lab. --Stable glow discharges have been demonstrated in thallium-mercury gas mixtures at mercury densities up to 3×10^{19} and temperatures of 500°C to 900°C. Discharge current densities were varied from .2 A/cm^2 to 1 A/cm^2, pulse durations from 100 ns to 16 μs and E/N's from 6×10^{-17} to $5 \times 10^{-16} V \cdot cm^2$. These discharges have shown themselves to be highly efficient in producing excited Tl ($7^2S_{1/2}$) atoms and Tl-Hg $B^2\Sigma_{1/2}$ excimer molecules. Discharge efficiency as high as 30% ± 10% in producing Tl ($7^2S_{1/2}$) and Tl-Hg $B^2\Sigma_{1/2}$ points to the possibility of the creation of a Tl-Hg excimer laser operating at similar efficiencies. These highly efficient discharges are thought to be due to very fast transfer of energy from mercury excimers into Tl-Hg. The transfer cross section from excited molecular mercury to Tl ($7^2S_{1/2}$) and Tl-Hg excimers has beer determined tc be approximately 1.2×10^{-14} cm^2. This transfer cross section is determined by monitoring the increase in decay rate of the mercury excimer population with the addition of excited thallium.

AA-7

Strong Tl-Xe Excimer Band Emission Via Electron Beam Initiated Stable Glow Discharges in TlI and Xe Mixtures. L.A. SCHLIE, L.E. JUSINSKI, R.D. RATHGE, R.A. HAMIL and D.L.DRUMMOND, AF Weapons Lab. --Stable glow discharges have been produced by electron beam initiation (20 nsec pulse) in TlI/Xe mixtures of approximately 1 torr of TlI and .68 to 6.8 amagats of Xe. The electron beam initiated discharges had an active volume of 57 cm^3 and produced a factor of 40 enhancement in the peak Tl-Xe band emission relative to the pure electron beam pumping. Peak power loadings of 10 KW/cm^3 were attained for approximately 1 μsec at 10 A/cm^2 current densities for E/N values up to 1.4×10^{-16} $V \cdot cm^2$. Very strong emission was observed from the Tl atomic lines 5350, 3776, 3519/29, 3230, 2819/29 and 2768 Å and the Tl-Xe bands centered at approximately 6000, 4300 and 3650 Å. Without the discharge, only very weak Tl atomic emission was observed. The atomic and molecular radiation had a transient behavior identical to that of the current pulse. Monitoring the discharge current decay at an $E/N = 3 \times 10^{-17}$ $V \cdot cm^2$ gave a recombination coefficient in Xe of 1.4×10^{-7} $cm^3 \cdot sec^{-1}$ and an attachment rate constant of 1.8×10^{-10} $cm^3 \cdot sec^{-1}$ for TlI.

AA-8

Models of High-Power Discharges in Na-Xe Vapor. II.* R. SHUKER, ALAN GALLAGHER† and A. V. PHELPS,† JILA, Univ. of Colo. and NBS.--Steady-state (several μs) discharges in Na doped Xe have been modeled under conditions appropriate to possible excimer laser use. Typical densities are: 3×10^{16} cm^{-3} for Na, $\sim 10^{20}$ cm^{-3} for Xe, and $10^{15} - 10^{16}$ cm^{-3} for electrons. A previous model[1] used only the first three excited states of Na, while calculating the electron energy distribution without electron-electron collisions. The present model includes Na excited states to $n^* = 15$, thereby accurately accounting for ionization through laddering. We assume that electron-electron collisions result in a Maxwellian electron energy distribution. We investigated the effect of dissociative recombination of electrons with Na_2^+ and with $NaXe^+$ for various final states of Na. The effects of excimer stimulated emission on the discharge and its efficiency have been investigated.

*This work was supported in part by AFWL and ARPA/ONR.
†Staff Member, Quantum Physics Division, NBS.

1. R. Shuker, L. W. Morgan, A. Gallagher and A. V. Phelps, Bull. Am. Phys. Soc. 23, 142 (1978).

AA-9

Optical Studies in High Pressure Mercury Discharges - R.E. CENTER and S.E. MOODY, MSNW*--The 330 nm ultraviolet band of molecular mercury ($\overline{1_u \rightarrow 0_g^+}$) has been suggested as a possible efficient lasing transition with potential application for a high energy storage laser. Conflicting gain/absorption observations have been reported in electrically and optically pumped high pressure mercury. These observations have been made at only 1 or 2 wavelengths near the peak of the 330 nm emission band. Some model calculations of the structure and spectroscopy of molecular mercury[1] have suggested that positive gain is more likely at wavelengths to the red of the emission peak. The present experiment has been set up to measure gain/absorption characteristics across the entire 330 nm band of electrically excited mercury, using a tunable dye laser probe. In our experiments, mercury at densities up to $5 \times 10^{18}/cm^3$ is excited in a UV preionized discharge with an input energy density up to 20 mJ/cm^3. Measurements will be reported of the optical transmission properties from 310 to 350 nm and gas temperatures up to 400 °C.

*Supported by the Department of Energy.

[1]F.H. Mies, W.J. Stevens and M. Krauss, in press J. Chem. Phys.

SESSION AB

9:00 A.M. – 10:30 A.M., Tuesday, October 17

Georgian Room

MAGNETOHYDRODYNAMICS

Chairperson: M.H. Scott,
University of Tennessee Space Institute

AB-1

Near-Electrode Surfaces Effects Influencing Slag-Coated Electrodes in a Coal-Fired MHD Generator - M.H. SCOTT, M.S. BEATON, J.B. DICKS, Univ. of Tenn. Space Institute *-- Basic processes which feature in the performance of electrode/insulator configurations within a coal combustion plasma with MHD effects are discussed. Among these are the presence of the Lorentz force which presents opposite influences at the anode and cathode sides. Likewise, the presence of a slag coating presents additional requirements in characterization of the model for current transport between the plasma and the electrode surface which differs between the anode and cathode surfaces. Conditions under which arc and diffuse modes exist at the electrode are discussed. The effect of the transport mode is shown. Namely, the diffuse mode at the anode is less desirable than the arc mode under conditions that exist in an MHD generator operating with a coal combustion plasma.

* Supported by DOE under Contract No. EX-76-C-01-1760.

AB-2

Characterization of the Diffuse Discharge at the Anode of an Open-Cycle MHD Generator* D.S. DVORE, M. MARTINEZ-SANCHEZ, J.B. ELGIN, C.E. KOLB, M.B. FAIST, Center for Chemical and Environmental Physics, Aerodyne Research, Inc.--The physics and chemistry of the near electrode region in an open-cycle MHD generator is modeled by a set of numerically solved first order nonlinear differential equations. The model includes the dynamics and electrodynamics which govern variations of the electric field and the density, momentum, and temperature of relevant species perpendicular to the electrode wall. Due to the steep temperature gradient near a cooled electrode, the chemistry must be modeled with finite rate kinetics. The conductivity drops steeply in the cool region near the wall. This situation is conducive to the onset of electro-thermal instability causing a switch from diffuse discharge mode to constricted discharge or arcing mode. Only the diffuse discharge is here modeled, providing background conditions for the study of arcs and some insight into the electro-chemistry responsible for the rapid deteriorization of the anode.

*Sponsored by the MHD Division, U.S. Dept. of Energy under Contract No. EX-76-C-01-2478.

AB-3

Voltage-Current Characteristics of Faraday MHD Generators - D. TRUNG, H.K. MESSERLE and J.J. LOWKE, University of Sydney, Australia - The steady state equations of the conservation of mass, momentum and energy have been solved for the plasma flow in the duct of a magnetohydrodynamic generator. Solutions are obtained of plasma velocity, temperature and pressure as a function of axial position. An iterative procedure is used to satisfy the split boundary conditions corresponding to (1) the condition of given stagnation pressures at the duct inlet and exit, and (2) the condition of constant mass flow with a given exit pressure. Volt-ampere characteristics are obtained for electrode pairs distributed axially in the duct for conditions of (1) equal currents, and (2) equal loading factors for each electrode pair. As the current is varied from open circuit to short circuit conditions, solutions are obtained for the three regimes corresponding to (1) subsonic flow, (2) a shock front existing within the duct, and (3) supersonic flow. The presence of a shock front within a duct causes a discontinuity to appear in the V-I characteristics. Characteristics for constant inlet stagnation pressure approach that of a constant current source for subsonic flow.

AB-4

Thermal Instability in MHD Channel

T.-M. FANG, Boston U. --Detailed MHD arcing phenomenon is studied. A general thermal instability criterion is obtained where the arc, or the current-carrying column before constriction starts, is treated as an open system rather than a solid cylinder with a fixed boundary. The total mass and the radius of the arc are now allowed to vary with the external perturbations. The response of the arc to the Joule heating and convective cooling can then be properly taken into account. Because of the complexity of the problem, the effect of the magnetic field on the arc is presently neglected. The crossed gaseous flow can pass freely into and out of an arc, thus the thermal term in the heat transfer equation should include the enthalpy change due to expansion and constriction of the arc. Using the general instability criterion developed in the present paper, an arc temperature of 4250°K is predicted in the AVCO MK VI MHD channel.

AB-5

The Ion Fly-Wheel Effect on the Electro-Thermal Instability in Non-Equilibrium MHD Hall Disc Generators* V.THIAGARAJAN, State University of New York at Buffalo—The electro-thermal instability has so far been studied in collisional time scales, neglecting the effects of the charge separation field. It has been treated here in an approximately collisionless time scale. Some energy will be transferred from the electrons to the ions by the charge separation field during the restoration of the charge neutrality. Part of the energy thus transferred can be stored in the azimuthal translational mode of the ions (referred to as "the ion fly-wheel", for simplicity); the energy thus stored will be transferred to the neutrals by ion-neutral collisions. There will be a consequent gain in the critical Hall parameter. The conditions for the transfer of energy from the electrons to the ion fly-wheel are ideally available in a non-equilibrium MHD Hall disc generator. It is predicted that the critical Hall parameter can be raised from 2 to 3 due to the ion fly wheel effect, if the pressure gradient is about 2 bars/m for the case of a K seeded argon plasma with T_e=2500°K and B=3 Tesla.

*Accepted for publication in Energy Conversion, Vol.18, No. 2.

AB-6

Radial Distributions of Electrical Conductivity in a Cesium Seeded, H_2-O_2 MHD Duct-S.Y. WANG, DOE/PETC*--A two-dimensional analysis of the NASA-Lewis cesium seeded, H_2-O_2 MHD duct flow has been performed by solving the boundary layer equations numerically. The axial pressure gradient is found using a predictor-corrector scheme. The variable transport properties are taken into account by incorporating an equilibrium program. For a range of seed fraction the radial distributions of electrical conductivity are calculated. These profiles are used to more accurately account for the thermal boundary layer in interpreting the experimental data of Wang and Smith[1].

*This work was started during residence in NASA-Lewis Research Center, Cleveland, Ohio.

[1]S.Y. Wang and J. Marlin Smith, 16th Symp. on the Eng. Asp.of MHD (1977).

AB-7

Identification of Positive and Negative Ion Species in Atmospheric Pressure Pulverized Coal/Alkali Combustion Plasmas*-J.C. WORMHOUDT and C.E. KOLB, Center for Chemical and Environmental Physics, Aerodyne Research, Inc.--Direct, coal-fired, alkali seeded MHD generators are now being developed as base-load electric power generation facilities. Inorganic impurities in coal have been predicted to form negative ion species which may significantly degrade MHD plasma conductivities and generator performance. This work presents initial mass spectrometric analyses of the positive and negative ions produced in atmospheric coal/alkali seed combustion plasmas. Negative ion species observed in the 1700-2000°K temperature range include PO_3^-, PC^-, OH^-, BO_2^-, and several transition metal oxide ions.

*Sponsored by the MHD Division, U.S. Dept. of Energy under Contract No. EX-76-C-01-2478.

SESSION BA

10:45 A.M. – 12:10 P.M., Tuesday, October 17

Embassy Room

RARE GAS HALIDE AND NUCLEAR PUMPED LASERS

Chairperson: L.F. Champagne,
Naval Research Laboratory

BA-1

Multiatmosphere Operation of a UV-Preionized Electric Discharge XeCℓ Laser - J. B. LAUDENSLAGER, R. V. SVOREC, AND T. J. PACALA, Jet Propulsion Laboratory, Pasadena, CA 91103 --High energy laser output was obtained from a small volume (76 cc) electric discharge excited XeCℓ laser when operated at multi-atmospheric (2 to 11 atm.) pressures. A UV-pre-ionized transverse-electric-discharge laser (EDL) device operating at high voltage (150 kv) was used to achieve glow discharge operation at high E/N. The output energy of the XeCℓ laser, with a fixed pressure of the Xe and HCℓ, increased with helium buffer pressure. The increase in laser output with helium buffer pressure may be due to the increased probability of the three-body ion-recombination formation channel for XeCℓ* and/or may be due to a more favorable matching of the gas discharge impedance to the discharge circuit. Efficient high E/N operation of EDL devices in the multi-atmospheric pressure region should prove useful for generating other lasers pumped by three-body reaction processes.

BA-2

Efficient Excitation of XeCl Laser by E-Beam and Discharge Pumping - D. E. ROTHE and J. B. WEST, Northrop Research & Technology Center, Palos Verdes, CA -- Intense laser output at 308 nm was obtained from XeCl in a Ne/Xe/HCl gas mixture at a pressure of 4 atm by e-beam excitation and by e-beam controlled discharge pumping. Efficiencies, based on energy deposited in the gas, were over 4 percent. The energy extraction per unit volume was 7 J/ℓ for e-beam excitation and 9 J/ℓ for the e-beam plus discharge. Similar results were obtained with KrF in the same device, indicating that under e-beam or e-beam controlled discharge excitation, XeCl is as efficient as KrF. A parametric study was performed of the variation of optical pulse energy, peak power, pulse width and pulse shape as a function of HCl and Xe concentrations. Results of these experiments are discussed with reference to the excitation and quenching kinetics and optical absorption processes predicted for this type of laser.

BA-3

Efficient Electron Beam Pumped XeCl Laser, L. F. CHAMPAGNE, Naval Research Laboratory--Experimental results for the electron beam pumped XeCl laser will be presented. Optical pulses ranging from 0.5 to 1.5 μs were obtained from mixtures of neon, xenon and HCl. Stimulated emission was observed on the (0,1) and (0,2) vibrational bands of the B-X transition. The small signal gain was measured to be 2.85%/cm under optimum pumping conditions and the saturation intensity is calculated to be ~ 0.35 MW/cm^2. Unlike KrF and XeF, no measurable degradation in output power is observed when a static fill of the laser mixture is irradiated several times. This suggests the possibility that closed cycle operation should be possible for this system. The absorption processes and laser performance will be discussed in depth.

BA-4

Energy Flow Kinetics in a Xenon-Chloride Laser,* L. J. PALUMBO, T. G. FINN,† and L. F. CHAMPAGNE, Naval Research Laboratory, A kinetics scheme has been obtained for electron-beam excitation of the xenon-chloride laser in neon diluent. The kinetics of XeCl formation and quenching processes have been investigated experimentally by e-beam excitation of Ne/Xe/HCl mixtures. The fluorescence efficiency and rates of dominant loss processes have been measured. The results of a computer model indicate the major energy pathways by which the upper-laser level is formed. Transient absorption and the role of the XeCl ground state will be discussed. The predictions of the numerical model agree well with the observed laser output power, gain and absorption.

*Work supported by DARPA

†Science Applications, Inc., Arlington, VA

BA-5

Dramatically Improved Performance of the XeCl Laser Using Ar as Diluent Gas-R.C. SZE, Los Alamos Scientific Laboratory*--Use of Ne or Ar diluents in place of He results in 30% improvement in output energy. Pressure dependence and comparisons with other RGH lasing performance can be explained through the change of the electron energy distribution as a function of different diluent gases and operating E/n. The sharply peaked pressure dependence (20 psia) is associated with the rapidly decreasing density for electrons above 8 ev as E/n is lowered when the filling pressure is increased. Kr- and Ar-H lasers operate poorly in Ar diluent because of low electron densities above the 13 ev required to excite the metastable state. Performance of different Xe-H lasers depend on the halide donor molecule due to the significant cooling of the electron temperature caused by the low lying vibrational levels. Similar discussion associated with Ne as diluent will be given.

*Work performed under the auspicious of the U.S. DoE.

BA-6

Laser Photodissociation of Cl_2 Observed as a Mechanism Responsible for the Long Static Fill Lifetime of the XeCl Exciplex Laser - ROBERT C. SZE and PETER B. SCOTT, Los Alamos Scientific Laboratory*--The difference in static fill lasing lifetimes between the KrCl and XeCl laser using HCl as the donor molecule has been investigated. After each firing of the laser, substantial H_2 and Cl_2 are formed from the HCl donor molecules. The photodissociation cross section of Cl_2 by the 308 nm XeCl laser is substantially larger than the 222 nm KrCl laser. The Cl atoms formed initiates the chain reaction in reactions with H_2, and H_2 and Cl_2 rapidly convert back to HCl. Experiments involving injection of the 308 nm laser into a KrCl laser cavity resulting in nearly full recovery of the KrCl initial lasing energy will be presented.

*Work performed under the auspices of the US Department of Energy.

BA-7

Production of XeF*(B) by Nuclear Pumping. G. H. MILEY, F. P. BOODY, S. J. S. NAGALINGAM, and M. A. PRELAS, Univ. of Ill., Urbana, IL--We have studied the formation of XeF*(B) in mixtures of $Ar/Xe/NF_3$, $Ne/Xe/NF_3$ and Xe/NF_3 excited by the MeV ions resulting from the $^{10}B(n,\alpha)^7Li$ nuclear reaction. Light output at 350 mm followed the input power density over periods up to 60 msec (i.e. quasi steady-state) and was ~ linear with power density from 5 to 40 W/cm^3. A fan was used to chop (spoil) the high-Q cavity, thus providing a means to measure the Stimulated Emission Ratio (SER).[1] For an optimum gas mixture ($Ar/Xe/NF_3$:99/0.5/0.2 at 300 T) an SER of ~8 was obtained at ~40 W/cm^3, corresponding to a maximum small-signal gain (corrected for absorption) of .015±.01% cm. This represents a conversion efficiency of ~50% from Ar* to 350-nm photons. Extrapolation of these data to high-flux reactors appears promising for laser applications. Present results will be interpreted in terms of differences between the kinetics of e-beam and nuclear pumping, including the initial ionization-excitation mechanism, dynamic effects associated with time scale, and electron-excited state densities.

[1]F. P. Boody, et al., Prog. in Astron. and Aero., Vol. 61, AIAA, (1978) 379-410.

BA-8

Recent Results with the Atomic Carbon Laser@ 1.4539μ - M. A. PRELAS, F. P. BOODY and G. H. MILEY, Fusion Studies Lab., Univ. of Ill., Urbana, IL--The nuclear pumped atomic carbon laser @ 1.4539μ ($C(3p^1P_1)$-$C(3s^1P_1^0)$) in $He-CO_2$, Ne-CO and $Ne-CO_2$ mixtures has demonstrated a unique delay between the peak of the laser signal and the peak of the neutron flux.[1] This laser is pumped by MeV ions from the $^{10}B(n,\alpha)^7Li$ reaction. Studies are in progress to identify the mechanisms associated with the delay from several possibilities in a $He-CO_2$ mixture including: 1) dissociation of CO_2 into the $C(2p^2\ ^1S_0)$ metastable state followed by penning ionization, recombination, and cascading into the upper laser level (ULL), 2) dissociation of CO_2 into vibrationally excited CO followed by relaxation and direct excitation into the ULL, 3) dissociation of CO_2 into vibrationally excited CO followed by penning ionization, recombination, and cascading into the ULL. Observation of spontaneous transitions which relax to the ULL, such as $C(4d\ ^1P_1^0) \rightarrow C(3p\ ^1P_1)$, have indicated that penning ionization-recombination is not the dominant process.

[1]M. A. Prelas, et al., Progress in Astronautics and Aeronautics, Vol. 61, AIAA, (1978).

BA-9

An Improved Kinetic Theory for Nuclear-Pumped Lasers - W. E. MEADOR and W. R. WEAVER, NASA, LaRC--Modeling of nuclear-pumped lasers requires accurate electron energy distributions for computing excitation, ionization, and recombination cross-sections and rate coefficients. Computation of the nascent-electron source term in the electron Boltzmann equation also requires accurate solutions of the fission-fragment equations. Previous solutions for both electrons and fragments have been obtained with the familiar P-1 approximation, which is inadequate for problems involving significant losses of particles by charge transfer or recombination. Although the solutions are substantially improved by including higher moments, such additions severely complicate an already complex situation if they are incorporated in the standard manner of Grad. A new method has been developed on the basis of assumed relations between moments and on the assumption that only the principal boundary conditions are necessary. The result is a model similar in form to two-function theories and of comparable simplicity, but with improved scattering and loss coefficients. Comparisons with exact numerical solutions of simple idealized problems verifies the accuracy of the method in extending P-1 theory to large charge transfer or recombination.

SESSION BB

10:45 A.M. – 12:10 P.M., Tuesday, October 17

Georgian Room

TRANSFER MECHANISMS IN ARCS

Chairperson: R.S. Bergman,
General Electric Cleveland

BB-1

Mechanism of Color Improvement in the Pulsed High Pressure Sodium Arc - PETER D. JOHNSON and T.H. RAUTENBERG, JR., General Electric Co. Corporate Research and Development--It has been discovered that the color temperature of the high pressure sodium arc can be increased from its usual value of about 2100°K when operated on a sinewave power supply to over 2500°K when operated in a pulsed mode at a pulse repetition rate of 500 to 2000 Hz and a duty cycle of 10 to 35%.[1] The enhancement of the radiative output in the blue region of the visible spectrum is due principally to radiation from the $nd^2D \rightarrow 3p^2P$ transitions of the sodium atom, where n=4 to 15. Excitation of these upper energy levels results from an unexpected transient non-steady state increase in plasma temperature to about 5400°K in the center of the arc. This temperature decays to a value near to that encountered in steady state excitation in a time commensurate with the previously determined plasma temperature decay rate for this discharge.[2]

1. M.M. Osteen, U.S. Patent Application, Serial No. 806301, June 1977.
2. T.H. Rautenberg, Jr. and Peter D. Johnson, J. Appl. Phys. 48, 2270 (1977).

BB-2

Net Radiation Emission of SF_6, Iodine and Sodium From Arc Measurements. R. J. ZOLLWEG, Westinghouse R&D Center.--The net radiation emission is an important transport property needed to calculate temperature profiles and other arc properties. We have used published experimental results of other investigators together with arc energy balance analyses to determine net radiation emission for arcs in a variety of different gases. The temperature measurements of Motschmann and of Popp for SF_6 arcs have been corrected for systematic error using recently improved determinations of atomic transition probabilities of S and F lines. The net radiation emission calculated by Liebermann and Lowke for 1 atm gives good agreement with the temperature profile and electric field for ~14,000°K (100A arc) but is a factor of two high for ~10,000°K (40A arc). The radiation emission of iodine is estimated from Neiger's measurements of axis temperature at three different arc currents. This is possible because atomic iodine is the dominant radiator and hence the temperature dependence of the emission is known. The sodium radiation emission was found from temperature profiles of ac arcs containing pure Na, Na + Hg and Na + Xe measured by deGroot. Calculated ac electrical properties of these arcs are in agreement with deGroot's measurements.

BB-3

The Radial Profiles of Current Density and Temperature in a Magnetically Confined Helium Arc.* TONY S. TAYLOR and GREGORY C. SMITH, Ohio State Univ.--A 4000A helium arc between an incandescent annular tungsten cathode of 16mm ID and 22mm OD and a flat water cooled anode is operated in an axial magnetic field of 2 to 10 kilogauss. The region of maximum current density near the anode corresponds closely to the emitting surface of the cathode at high field strengths and low helium pressures, although there is a conductive plasma in a cylindrical region of radius substantially larger than the outer radius of the cathode. With increase of helium pressure or decrease of the magnetic field intensity, the current profile at the anode broadens. The current density at the anode is of the order of $500 A/cm^2$. Although the current density is near zero on axis and peaks in the ring area defined by the emitting cathode surface, the temperature, estimated spectroscopically, is nearly constant from the axis of the arc to the outer edge of the current carrying region, and is close to 60000°K. Thus we appear to have in the core of the discharge column a dense, nearly homogeneous and isothermal plasma.

*Submitted by CARL E. NIELSEN

BB-4

Two Temperature Model of a Nonequilibrium Discharge in Argon. -J.P. NOVAK, IREQ, Quebec, F. HRON and E.S. KREBES, U. of Alberta.--A system of balance equations[1] for nonequilibrium discharges has been applied to a steady state discharge in argon at atmospheric pressure. Free convection was assumed to be the dominant mechanism of energy transfer between the discharge and the ambient gas. The system was solved numerically for discharge currents from 1 to 10 Amps corresponding to electron densities in the core of $0.6 - 2.0 \times 10^{15}$ cm^{-3}. The electric field decreased from 12 to 6.5V with increasing current while the temperature of the neutrals increased from 2500 to 6900°K. The electron temperature was approximately 11000°K, showing little dependance on discharge current. Radial profiles of electron density, temperature, heat flux and radial diffusion velocity, as well as gas temperature and heat flux were calculated for all cases. The profiles of electron density and temperature, and of gas temperature for a current of 5 A compare favorably with experimental values measured by Polak and Slovetskii[2].

1. J.P. Novak et al. J. Phys. D 10, L227 (1977).
2. L.S. Polak and D.I. Slovetskii, 12, 921 (1974).

BB-5

Additional Validation of the MTE Continuum Relation for Non-LTE Plasmas-T.L. EDDY and M.L. FENTRESS, West Virginia University--The MTE Continuum relation previously presented [1,2] is reexamined in light of more recent experiments in argon plasmas at high pressures, the diverse results of experimentally free-bound ξ factors are found to be largely due to variations in the atomic transition probability values used in the evaluation. Deviations between experimental and theoretical values are partially explained by the omission of energy levels in the free-bound Gaunt factor calculation.

[1] T.L. Eddy, C.J. Cremers and H.S. Hsia, Paper DA-7, 28th GEC, Rolla, Missiouri, Oct. 1975; Am. Phys. Society Series II, Vol. 21, No. 2, Feb. 1976.

[2] T.L. Eddy, C.J. Cremers and H.S. Hsia, JQSRT, Vol. 17, pp. 287-296, 1977.

BB-6

High Pressure Cataphoresis - R.S. BERGMAN and J.H. INGOLD, General Electric Co., Cleveland, Ohio 44112-In a previous analysis[1] of axial cataphoresis in a high pressure discharge consisting of a partially ionized sodium plasma immersed in a mercury-xenon background, it was shown that electron-neutral momentum transfer is important in determining the axial gradient in the sodium partial pressure when the discharge current is treated as the independent variable. In this previous work, however, the hard sphere approximation for the electron-neutral interactions was assumed, leading to qualitative but not quantitative agreement between calculation and measurement of the cataphoresis. In the present work, new expressions for the electron-neutral momentum transfer collision integrals for each neutral species are derived from energy dependent electron-neutral cross-section by the Legendre polynomial expansion method, leading to better agreement between theory and experiment.

[1] R.S. Bergman and J.H. Ingold, Bulletin of the American Physical Society, Vol. 23, p.133, 1978.

SESSION CA

1:30 P.M. – 3:05 P.M., Tuesday, October 17

Embassy Room

KINETIC PROCESSES IN RARE GAS HALIDE LASERS

Chairperson: J.H. Jacob,
Avco Everett Research Laboratory

CA-1

Ion Processes in Rare-Gas Halide Lasers*

W. L. NIGHAN, United Technologies Research Center.

Ion-ion recombination often dominates RGH* formation in rare-gas halide lasers, while absorption of laser radiation is significantly influenced by photodissociation of dimer ions. For these reasons knowledge of the nature and concentration of various ion species in laser mixtures is especially important. In the present work ion production and loss processes have been analyzed for conditions typical of e-beam controlled KrF*, XeF* and XeCl* lasers. Particular attention has been directed toward evaluation of the concentrations of rare-gas trimer ions and of rare-gas halide ions. Calculations show that the fractional populations of trimer ions can be substantial ($\sim$10%) for some experimental conditions. On the basis of these results the role of various ion species as absorbers of laser radiation has been analyzed and comparisons with experimental observations have been made. The implications of these results as regards laser properties will be presented. *This work was performed in part through the sponsorship of the Office of Naval Research.

CA-2

Positive Ions in Atmospheric Pressure Helium and Helium-Neon Mixtures, W. J. WIEGAND and R. H. BULLIS, United Technologies Research Center--Ions produced in helium and helium-neon mixtures at 760 torr and 300°K have been sampled employing a quadrupole mass spectrometer coupled to an atmospheric pressure ionization source. In helium, the dominant ions observed were He_2^+ and He_3^+ with an equilibrium coefficient consistent with existing low temperature-low pressure data.[1] For a mixture of helium with approximately 0.2 ppm neon the ions observed include He_2^+, He_3^+, Ne_2^+ and $HeNe^+$. Rate coefficients inferred from these measurements compare favorably with reported values. Of significance is the absence in these measurements of He_4^+ as reported by Gusinow et.al.[2] Furthermore, no significant concentration of heteronuclear trimers was observed. The implications of these results to rare gas halide laser processes will be presented.

1. P. L. Patterson, J. Chem. Phys. 48, 3625 (1968).
2. M. A. Gusinow, R. A. Gerber and J. B. Gerardo, Phys. Rev. Letts. 25, 1248 (1970).

CA-3

Electronic Structure and Photoabsorption Properties of Noble Gas Trimer Ions.-H.H. MICHELS and R.H.HOBBS, United Technologies Research Center*--A study of the electronic structure and absorption characteristics of the Ar_3^+ ion has been carried out to determine the relative importance of such species in the analysis of loss mechanisms in the noble gas-halide excimer systems. This study included detailed quantum mechanical calculations of the potential energy hypersurfaces for Ar_3^+ and prediction of the absorption bands. We find this ion to have trigonal symmetry with a bound $^2E'$ ground state ($^2A_1$ in C_{2v}). The vertical excitation spectra is $^2A_2'$ (.27 eV), $^2E''$ (.80 eV), $^2A_2''$(1.34 eV) and $^2A_1'$ (2.68 eV). The short wavelength transitions (300-500nm) are found to be weak for photoabsorption from the ground state. Similar results are predicted for the heavier noble gas trimer ions. These species are found in significant concentrations in high pressure(>10^3 torr) noble gas-halide excimer lasers. They are minor contributors to the total photoabsorption losses, which are dominated by the dimer ions.

*Supported in part by AFWL and AFOSR.

CA-4

Ultraviolet Laser Emissions and Fluorescence Enhancements in an E-Beam Excited Low Temperature and High Density Supersonic Flow*. B. FONTAINE and B. FORESTIER, Institute of Fluid Mechanics, Aix-Marseille U. 13003 Marseille, France -- Long Pulse ultraviolet laser emissions have been achieved following e-beam excitation (V = 240 kV, J = 10 A cm^{-2}, 600 ns) of mixtures of rare gases and NF_3 in supersonic flow at low temperature (80 or 120 K) and high density (1 amagat). Lasing was obtained near 350 nm on XeF in $Ne/Xe/NF_3$ mixtures and also on two NeII lines in Ne/NF_3, one of them had not been previously reported. These experiments have shown a lowering of absorption by excited species (Ne_2^+) near 350 nm when $Ne/Xe/NF_3$ and Ne/NF_3 mixtures are strongly cooled. Aerodynamic cooling has also allowed to obtain strong enhancement on several molecular bands at near UV and visible wavelengths from XeO*, $ArXeF^+$, ArXe* and Kr_2F* when mixtures of rare gases and oxidized or fluored compounds were e-beam excited. Effects of cooling on behaviour of these laser and fluorescence emissions will be discussed.

*Supported by D.R.E.T.

CA-5

Temperature Effects on the Quenching Kinetics of XeF^* in E-beam Pumped $Ne/Xe/F_2$ Mixtures#. Daniel W. Trainor, M. Rokni†, J. H. Jacob, and J. A. Mangano, Avco Everett Res. Lab., Inc. --Recent lasing experiments involving $Ne/Xe/NF_3$ mixtures have shown a factor of two improvement in laser performance when operated at elevated temperatures. Intrinsic efficiencies in excess of 5% have been observed[1]. To model these results, information on the various quenching processes is necessary. Some of these important kinetic processes were investigated in experiments which involved irradiating mixtures of $Ne/Xe/F_2$ with high energy ($\approx$ 150 keV) electrons[2]. The resulting fluorescence emanating from XeF^* formed in the various mixtures was monitored as a function of mixture ratio and total pressure at temperatures near 500°K. Rate constant information was thereby obtained for two and three body quenching processes of XeF^* with F_2, Xe and Ne.

Supported by ARPA and monitored by ONR

† Hebrew University of Jerusalem, Israel

1. J. C. Hsia, J. A. Mangano, M. Rokni, and J. H. Jacob, unpublished.
2. M. Rokni, J. H. Jacob, J. A. Mangano and R. Brochu, App. Phys. Lett. 30, 458, (1977).

CA-6

Radiative Lifetime and Collisional Kinetics of the XeF (II, 3/2) State - C.H. FISHER and R.E. CENTER, MSNW*--The effect of the XeF (II, 3/2) state has been neglected in models of the 351 nm XeF laser because of a lack of information, even though it may play an important role due to collisional mixing with the nearby (III, 1/2) upper laser level. In an effort to determine some of the needed information, we have employed a laser induced fluorescence technique to measure the radiative lifetime and to investigate the collisional formation and destruction of the XeF (II, 3/2) state. A short 351 nm laser pulse excites ground state XeF molecules to the (III, 1/2) state, some of which then undergo collisional transfer to the nearby (II, 3/2) state. The production and decay of the (II, 3/2) state is followed by monitoring the broadband (II, 3/2)→(I, 3/2) emission at 460 nm. The XeF (II, 3/2) state radiative lifetime determined in the present experiments is 90 nsec. Transfer and deactivation rate coefficients for the collision partners commonly present in XeF laser gas mixtures will be reported.

*Supported by DARPA under ONR Contract N00014-78-C-0343.

CA-7

Theoretical Study of Formation Rates of Rare Gas Halide Trimers--*V.H. SHUI and C. DUZY, Avco-Everett Res. Lab., Inc.--A scarcity of information on the rare gas halide trimers makes detailed calculations of their formation rates from the excited rare gas halides impossible. However, we have developed several approximate methods/models for determining these rate constants[1]. The range of applicability of these methods is discussed and rate constants for reactions of possible interest for the KrF^* and XeF^* laser systems are calculated. These reactions are:

(1) $KrF^* + Rg + Rg' \rightarrow KrRgF^* + Rg'$ and
(2) $XeF^* + Rg + Rg' \rightarrow XeRgF^* + Rg'$, where Rg, Rg' = Ar, Kr in Eq. (1) and Ne, Ar, Xe in Eq. (2).

*Work supported by Advanced Research Projects Agency.

[1]V.H. Shui, Appl. Phys. Lett. 31, 50 (1977).

CA-8

Kinetics of KrF^* and Kr_2F^* by Proton Excitation.† C.H.CHEN, M.G.PAYNE, and J.P.JUDISH, Oak Ridge Nat'l. Lab.--A 2-MeV proton beam with 10-nsec pulse width was used to excite Kr-F_2, Ar-Kr-F_2, and Ne-Kr-F_2 mixtures. The time interval between proton pulses and the number of protons in each pulse can be varied. The emitted vuv and near uv-visible photons are wavelength resolved and detected by time-resolved or time-integrated single photon counting techniques. The lifetimes of Kr_2F^* and KrF^* are given, and the mechanisms of production and quenching processes of KrF^* and Kr_2F^* are discussed. The quenching rate constants of KrF^* and Kr_2F^* for various quenching processes are listed, and the relative efficiencies to produce KrF^* by energy transfer processes and ion-ion recombination are presented. The difference of fluorescence efficiency between various gas mixtures is discussed.

†Research sponsored by the Division of Biomedical and Environmental Research, U.S. Department of Energy, under contract with the Union Carbide Corporation.

SESSION CB

1:30 P.M. – 3:05 P.M., Tuesday, October 17

Georgian Room

ARCS AND FLOWS I

Chairperson: G. Frind,
General Electric Corporate Research
and Development Center

CB-1

Correlated Electrical and Thermal Properties of Arcs in Gas Flow. G.R.JONES. Univ. of Liverpool, England*. - Experimental results are presented for the electrical and thermal properties of a 3kA A.C. arc burning in a 7 bar air blast. Measurements are given of the axial variation of local electrical conductance, the radial distribution of gas density and the cross-sectional area of the arc core, both at peak current and during the current zero period. The results have been obtained using voltage probing, laser fringe deflection and R.F. probing techniques. It is shown that the results correlate well, even close to current zero, with similar results for different arc forms using integral boundary layer theory parameters[1]. The role played by various fundamental arc properties during the extinction is identified and the behaviour of a model gas blast circuit interruptor is predicted.

*Supported by the Science Research Council, U.K.

[1] M.D.Cowley, J.Phys.D:Appl.Phys. 7, 2218 (1974).

CB-2

Arc Interruption Capabilities of Gases and Gas Mixtures-A. LEE and L.S. FROST, Westinghouse Research and Development Center*--Thermal recovery of several gases and gas mixtures have been measured after high current AC arcing: SF_6, CF_4, $CClF_2CF_3$, and mixtures of SF_6 with He, N_2 and $CClF_2CF_3$. The arc is initiated by contact separation in the nozzle-arc chamber under gas flow from an upstream piston chamber. The gas pressure in the compression chamber is monitored during each cycle. The recovery and the pressure rise data for rms arc currents from 10-20 kA lead to the interesting observation that contrary to expectation, gases with higher pressure rise in the compression chamber generally have lower interruption capabilities. Since gas flow is impeded by the arc, the pressure rise gives information on the arc size for different gases, and the residual effects of a larger arc channel overwhelm the benefits of a higher pressure differential and greater gas flow near current zero.

* This work was performed under Contract Number 847-1 with EPRI.

CB-3

Thermal Recovery Performance of Blown AC-Arcs in Various Gases and their Mixtures with SF_6-H.O. NOESKE, General Electric Corporate R&D, Philadelphia, PA.--The rate of rise of the voltage has been measured which is required immediately after current zero for ohmic reheating of the residual plasma of an AC arc which is quenched by the flow of highly pressurized gases in a supersonic nozzle. Its dependence on the type of gas at its mixture ratio with SF_6 has been determined for various gases and controlled conditions of nozzle inlet pressure and the dI/dt at current zero. The pressure drop in the nozzle was always sufficient for supersonic flow. An attempt is being made to explain qualitatively the peculiar dependence of the thermal recovery on the critical rate of rise of the voltage after current zero and the mixture ratio of the tested gases with SF_6. For this we consider the sonic velocity of the cold gas and a parameter which we assume to be important for the inhibition of the fusion of gas mixtures under existing extreme temperature and concentration gradients.

CB-4

Measurement of Critical Power Loss in Gas Blast Interrupters During Thermal Recovery - G. FRIND, L.E. PRESCOTT AND J.H. VAN NOY, General Electric R&D Center--Critical values for post zero current and for power loss during thermal re recovery were measured in an orifice type, gas blast interrupter, for the gases air and SF_6. Rate of current fall was varied between 10 and 35 amp/μsec. The measured values of critical power loss (at the failure limit) were for both gases one order of magnitude smaller than predicted by turbulent theory. The SF_6 power loss was at 14 amp/μsec only 500 watt. This suggests that critical cooling during thermal recovery was in our orifice type interrupter by laminar rather than by turbulent conduction.

CB-5

Model Calculations for Post Current Zero Thermal Behavior in Gas Blast Interrupters - R.E. KINSINGER, General Electric Corporate R&D Center--A simple channel model has been used to represent the critical region of a gas blast arc during the period of thermal recovery or reignition around current zero. The power loss term for the model can be chosen to represent either laminar or turbulent loss processes. When initial conditions (at current zero) are fixed by experimental measurements,(1) the calculated subsequent behavior of the arc as a circuit element is also in good agreement with the experiment if the power loss model used is laminar. For this agreement the arc diameters required are generally small ($\lesssim 0.2$ mm).

(1) G. Frind, "Measurement of Critical Power Loss in Gas Blast Interrupters During Thermal Recovery," to be presented in this Conference.

CB-6

Experimental and Theoretical Study of a D.C. Arc in an 8 Degree Conical Nozzle Flow.* H.T.NAGAMATSU, Rensselaer Polytechnic Institute and General Electric Co., and P.D. SYMOLON, Rensselaer Polytechnic Institute.-- The cold flow field for an 8° convergent-divergent nozzle was determined for subsonic, transonic, and supersonic flow velocities. D.C. arc voltage and current measurements were made for an arc gap of 5.52 cm and a current of approximately 100A. Arc voltage increased rapidly as the flow velocity increased from zero to supersonic velocity. Using a channel flow model with constant arc temperature and the energy integral for the convective cooling, analytical expressions were derived for the arc radius, electric field strength, arc voltage, resistance, and power as functions of the cold flow properties, current, and axial distance. Calculated arc voltages, resistances, and powers are in good agreement with the experimental data.

*Supported in part by EPRI under contract RP246-2

CB-7

Electric Arcs in Supersonic Flow - C.K. BHANSALI and D.M. BENENSON, State U. of NY at Buffalo*--Numerical solutions of the conservation equations are being obtained for a dynamic axial-flow arc immersed in a subsonic/supersonic flow field within a converging-diverging nozzle. Effects of real gas properties, turbulence, and (optically thin) radiation are included. The set of equations is solved using a two step second order finite difference method incorporating the concept of time splitting. Transformation of coordinates is employed. The general formulation permits use of the time dependent approach to obtain required initial (steady-state) solutions within the nozzle. Solutions are obtained for the case of a 10 bar (stagnation pressure), 700A (initial current) argon arc in a channel having 10mm throat diameter, ~8.5cm length (downstream of throat), and cold-flow exit Mach number ~2.4. For laminar (and initial steady-state) condition, the maximum centerline temperature, ~28,000K, is found near the upstream electrode; at the exit, T_e~23,000K. Arc diameter increases from ~4mm at the throat to ~7mm at the exit. Centerline axial velocity is ~5600m/s at the exit. Arc voltage is ~420V.

*Research supported by National Science Foundation Grant ENG 76-17009.

SESSION DA

3:20 P.M. – 5:10 P.M., Tuesday, October 17

Embassy Room

XeF KINETICS AND LASERS

Chairperson: D.L. Huestis,
SRI International

DA-1

Theoretical Study of XeF Vibrational Excitation and Dissociation-*C. DUZY and V.H. SHUI, Avco-Everett Res. Lab., Inc.--A combination of phase-space theory and semi-classical trajectory calculations[1] was used to determine rate constants for the dissociation of the ground state of XeF from specific vibrational levels; i.e., XeF(v) + Ne → Xe + F + Ne, where v = 0-5. Rate constants for collisionally induced transitions between these vibrational levels were also calculated. These rate constants were then incorporated into the ground state master equation which also contains radiative feeding (fluorescence/stimulated emission) from the $XeF^*(B)$ state. Results of these calculations are discussed in terms of their relevance to the behavior of XeF lasers[2].

*Work supported by Advanced Research Projects Agency.

[1]V.H. Shui, J. Chem. Phys. 57, 1704 (1972).

[2]M. Rokni, J.A. Mangano, J.H. Jacob and J.C. Hsia, IEEE J. Quant, Elec. 14, 464 (1978).

DA-2

XeF Ground State Dynamics-S.F. FULGHUM, I.P. HERMAN,* M.S. FELD, and A. JAVAN, MIT†--The time evolution of vibrational level populations in the XeF ground electronic state is determined by a laser induced fluorescence technique. Ground state XeF is produced by photodissociation of XeF_2 by an ArF laser pulse. Buffer gases are added to the XeF_2 cell as desired. A tunable pulsed dye laser, delayed by varying amounts from the ArF laser pulse, is then used to pump a selected XeF vibronic transition in the B↔X system, inducing fluorescence from the excited electronic state. The time evolution of the ground state vibrational level populations is obtained by measuring the relative fluorescence as a function of the time delay between the two lasers. Preliminary measurements on the v"=1 vibrational level in a He buffer indicate a multi-exponential decay with rates of from 1×10^4 sec^{-1} $torr^{-1}$ to about 3×10^4 sec^{-1} $torr^{-1}$.

*Present address: Lawrence Livermore Laboratory.
†Work supported by the Office of Naval Research.

DA-3

Lower Laser Level Removal in XeF.‡ K.Y. TANG and R.O. HUNTER, JR.,* Maxwell Laboratories Inc., and D.L. HUESTIS, Molecular Physics Laboratory, SRI International.--The collisional removal of XeF($X^2\Sigma^+$) has been investigated theoretically and experimentally. The gain during the excitation pulse, and absorption by ground state XeF during and after the excitation pulse, have been monitored in electron-beam pumped Ne/Xe/NF_3 mixtures. The absorption features are identical in position and shape to those observed in fluorescence under the same conditions, modified by the ground state vibrational Boltzmann factors. The ground state density is found to consist of two temporal components: (1) a time-decaying component arising from $XeF^* \rightarrow XeF^\ddagger + h\nu$; followed by $XeF^\ddagger + Ne \rightarrow Xe + F + Ne$; and (2) a time-independent component arising from $Xe + F + Ne \rightleftarrows XeF + Ne$. The rate coefficient for collision-induced-dissociation and the implications for laser performance will be discussed.

‡Supported by ARPA under Contract No. DASG60-77-C-0058 and DASG60-77-C-0028.

*Fannie and John Hertz Foundation Fellow, University of California, Irvine.

DA-4

The Influence of the Bound Lower Level on the XeF^* Laser Performance† M. ROKNI††, J. H. JACOB, J. A. MANGANO and J. C. HSIA, Avco Everett Res. Lab., Inc. -- The bound lower level of XeF could limit the extraction efficiency of the laser. We have investigated the effect of this on the laser kinetics and flux extraction, observing the depression of the side light fluorescence as a function of the intercavity flux. The intercavity flux was varied by introducing a cell containing $C\ell_2$ between the mirrors that formed the optical cavity. By varying the $C\ell_2$ pressure the cavity flux was varied continuously. The side light was monitored near the 95% output coupling mirror. By this means we could directly infer the cavity flux by measuring the laser power extracted through the output coupler. From these measurements it is apparent that the finite lifetime of the lower level plays an important role in the flux extraction. These measurements also give us an independent determination of the saturation flux.

†This work was supported by Advanced Research Projects Agency and monitored by the Office of Naval Research under Contract No. N00014-75-C-0062.

††The Hebrew University of Jerusalem, Israel.

DA-5

Improvement in XeF Laser Efficiency at Elevated Temperatures* J. C. HSIA, J. A. MANGANO, J. H. JACOB and M. ROKNI**, Avco Everett Res. Lab., Inc.--Improvement in E-beam pumped XeF laser efficiency is reported when the laser is operated at temperatures above 300°K. The improvement is due predominantly to improved energy extraction from the upper laser level as well as decreased lower level lifetime. The highest intrinsic laser efficiency (laser energy out/E-beam energy deposited in the active medium) observed at 3 amagats is 5.5%. The temperature at which the highest efficiency is achieved is observed to increase with increasing gas density.

*This work was supported by Advanced Research Projects Agency and monitored by the Office of Naval Research under Contract No. N00014-75-C-0062.

**The Hebrew University of Jerusalem, Israel.

DA-6

The Role of the Broadband Emission in the XeF Laser* M. ROKNI**, J. C. HSIA, J. H. JACOB and J. A. MANGANO, Avco Everett Res. Lab., Inc. -- We have investigated the broadband emission from XeF by monitoring the quazi-steady state fluorescence intensities as a function of both diluent and pressure in E-beam pumped gas mixtures. The observed pressure dependence of the ratio of broadband to B→X emissions cannot be explained by just collisional mixing of the B and C states. A possible explanation for these results is that there is another species that is emitting, i.e., triatomics. Laser sidelight measurements indicate that the energy stored in the broadband is recoverable under laser conditions. At low pressures when the collisional mixing is unimportant it appears that the B state is formed preferentially. The effects of these observations on the XeF* laser extraction efficiency will be discussed.

*This work was supported by Advanced Research Projects Agency and monitored by the Office of Naval Research under Contract No. N00014-75-C-0062.

**The Hebrew University of Jerusalem, Israel.

DA-7

Kinetic Operation of the XeF* Waveguide Laser Excited by a Capacitively Coupled Discharge--L.A. NEWMAN, United Technologies Research Center--The kinetic operation of this recently developed laser[1] is described by comparing the predictions of a detailed computer code to experimentally determined parameters. Of particular significance is that in order to explain the variation in the fluorescence efficiency of this device with pump power density, a quench process of XeF* which is proportional to pump density had to be invoked. Various quenching processes which could explain this observed effect are discussed and the implications of this process on the operation of larger scale devices is assessed.

[1]L.A. Newman: "XeF* and KrF* Waveguide Lasers Excited by a Capacitively Coupled Discharge" to be published in Appl. Phys. Letts.

DA-8

Screening of Fluorine-Bearing Gases for Self-Sustained Discharge Pumping of Rare Gas-Fluoride Lasers. L. J. DENES, P. J. CHANTRY, N. T. MELAMED and R. J. SPREADBURY, Westinghouse R&D Center.*--We have studied energy loading in 2 μs self-sustained discharges using XF:Ar:He = x:20:700 Torr mixtures where XF is the fluorine donor molecule. The energy loading showed a systematic decrease with increases in the attaching strength (or equivalently the dielectric strength) of the added gas, XF. The high energy loading capability (∿100 J/ℓ) of the weakly attaching gases offers the potential for efficient excited rare gas-fluoride (RgF*) production through the metastable channel $Rg^* + XF \rightarrow RgF^* + X$, rather than through the recombination of Rg^+ and F^-. F-donor candidates should therefore satisfy the energy requirement that $D(X\text{-}F) < D(Rg^*\text{-}F) \gtrsim 5$ eV where D is the strength of the bond indicated. Using this criterion, together with the preference for low dielectric strength, candidate fluorine-bearing molecules have been screened. The interesting gases include F_2, NF_3, SF_6, C_2F_6, CHF_3, CF_4 and CH_3F. Relative fluorescence intensity measurements have been made with 1 Torr of each gas added to a base mixture of 750 Torr He, 3 Torr Xe. XeF* fluorescence was observed in all cases.

*Work supported by U.S. Army BMD ATC.

DA-9

Energy Loading Limitations in 300 ns, Self-Sustained Rare Gas-Halide Discharges. L. J. DENES, J. L. PACK and L. E. KLINE, Westinghouse R&D Center.*-- A 25 cm^3 discharge apparatus has established limits on the arc-free energy loading for long-pulse (300 ns) UV-preionized self-sustained rare gas-halide discharges. The mixtures contained small concentrations of a strongly-attaching fluoride gas (SF_6 or NF_3) and a rare gas (Ar or Xe) in a high pressure ($\sim$1000 Torr) helium buffer. The discharge apparatus has an experimentally optimized electrode geometry and allows optimization of the circuit parameters for each mixture. With proper optimization, high energy loadings ($\gtrsim$ 30 J/ℓ atm) are obtained with attaching gas pressures up to a few tenths of a Torr. Modeling studies indicate that such NF_3 pressures will provide efficient XeF laser operation. Further increases (i.e. 0.3 to 0.6 Torr with NF_3 and 0.5 to 1.0 Torr with SF_6) cause an unexpectedly rapid decrease in the achievable energy loading. At higher concentrations, energy loading is low ($\sim$3 J/ℓ atm) and is insensitive to the actual amount of attacher present. The existence of this threshold phenomenon may provide further insight into the mechanism of the glow-to-arc transition in attaching gas mixtures.

*Work supported by U. S. Army BMDATC.

DA-10

Self-Sustained Discharge Pumped XeF Laser and Discharge Kinetics - L. E. KLINE, L. J. DENES, S. G. LESLIE and R. R. MITCHELL, Westinghouse R&D* -- U.V. preionized, self-sustained discharges in NF_3:Xe:He mixtures are used to pump the XeF laser. Measured discharge voltage and laser output waveforms agree with computer simulation results obtained by simultaneously solving differential equations for charged and neutral species densities, circuit currents and voltages, and the laser cavity flux. Predicted efficiencies are: a) XeF* pumping(energy into XeF*/electrical energy in) of 5-15%, b) extraction (laser energy out/energy into XeF*) of $\sim$10%, and c) overall of 0.5 to 1.5% in agreement with experiment. The model predicts that the XeF* pumping efficiency is determined primarily by the gas mixture proportions, and that the low extraction efficiency results from the short (30 ns) discharge pulse and the bound lower laser level in XeF. The extraction efficiency can be increased to 40%, with a corresponding overall efficiency of 2-6%, by increasing the discharge pulse length to 300 ns.

*Work supported by U. S. Army BMDATC.

DA-11

X-Ray Preionization for Electric Discharge Lasers.* J. I. LEVATTER and S. C. LIN, Univ. of Cal., San Diego--Using x-ray of 50-100 keV photon energy as an ionizing radiation source in a transmission-line-driven, low-inductance discharge chamber, we have recently succeeded in generating spatially-homogeneous pulsed avalanche discharges of up to 100 nsec duration over several liter volume at greater than 1 atm pressures in a number of well-known gas mixtures for the CO_2 ir laser and the XeF, KrF uv lasers. The observed laser power outputs from some of these exploratory experiments are already found to be comparable to or better than those reported in the literature for e-beam-controlled discharges at the same total rate of energy deposition. The ionization kinetics, overall efficiency, and potential advantages of this new method for initiating homogeneous avalanche discharges in certain high power laser applications will also be discussed in this paper.

*Jointly supported by ONR and DARPA under Contracts N00014-77-C-0692 and N00014-76-C-0116.

SESSION DB

3:20 P.M. – 5:10 P.M., Tuesday, October 17

Georgian Room

ARCS AND FLOWS II

Chairperson: A. Lee,
Westinghouse Research & Development Center

DB-1

Theory of Arc Clogging in Nozzles - P. KOVITYA, J.J. LOWKE and A.D. STOKES - University of Sydney, Australia - One dimensional solutions have been obtained of the equations of mass, momentum and energy for an arc in a nozzle over which there is an imposed pressure drop. It is assumed that radial pressure gradients are negligible and that the gas surrounding the arc is isothermal at room temperature. As the current is increased three current domains are distinguished, (1) when the arc diameter is less than the nozzle diameter, (2) nozzle clogging, when the arc fills the tube and the plasma pressure is influenced by ablation products from the wall, (3) nozzle blocking, when the pressure in the nozzle is so large that back flow occurs. Derived volt-ampere curves are only slightly sensitive to the gross changes in gas flow characteristics that occur between domains. For domain (1), V-I characteristics are slightly positive or negative depending of whether the nozzle throat is near the nozzle entrance or exit. Calculations indicate that the Mach number of the plasma is approximately equal to the Mach number of the gas surrounding the arc. The nozzle first "clogs" at the downstream end of the nozzle.

DB-2

Temperature Measurements in Turbulent Arcs* - Y.K. CHIEN and D.M. BENENSON, State University of New York at Buffalo--Experiments are being carried out to more quantitatively determine the distributions of temperature and its fluctuations in turbulent arcs. Initial tests are being conducted with DC argon arcs in a cylindrical channel 1cm diameter, ~15cm long. The arc is operated at (nominally) atmospheric pressure, ~100A, and with mass flows from laminar to turbulent regimes. Integrated intensity distributions are obtained using a high speed rotating mirror to freeze out effects of gross motion of the arc during data acquisition. The data acquisition system, which includes transient recorder and microcomputer units, permits rapid recording, transfer, storage and processing of the many traverses of the arc. Radiation is monitored from the argon I 4159Å and 6965Å lines, together with their adjacent continuua. Using a data reduction procedure previously developed for turbulent flows - which procedure requires local (spatial) information on time-averaged emission coefficients from two lines and one continuum - the time-averaged radial distributions and mean square fluctuations can be found.
*Supported by National Science Foundation Grant ENG 76-17009 and by Electric Power Research Institute Contract RP 246-2.

DB-3

Free Convection in Horizontal High Pressure Mercury Arcs. D.K. MCLAIN and R.J. ZOLLWEG, Westinghouse R&D Center.--When high pressure mercury arcs are operated horizontally in enclosed cylindrical quartz tubes the arc bows upward because of buoyancy forces. The magnitudes of these buoyancy forces and of the wall-stabilizing forces have been measured at different mercury pressures and as a function of power loading by visual observation of arc position as a function of applied transverse magnetic field. The two-dimensional (r,z) vertical arc convection model developed by Lowke[1] has been modified such that the arc position, temperature profile and convective gas flow are calculated numerically for a two-dimensional (r,θ) horizontal arc cross section using material transport properties determined previously.[2] Calculated arc positions are in good agreement with experiment as are the displacements when a transverse magnetic field is applied. Gas flow direction in the arc core is reversed with a significant transverse magnetic field.

[1]J.J. Lowke, Bull. of APS 21(2), 134 (1976).

[2]R.J. Zollweg, J. Appl. Phys, 49(3), 1077 (1978).

DB-4

Simple Theory of Free Burning Arcs - J.J. LOWKE, University of Sydney, Australia - Analytic expressions are derived to give approximate properties of free burning arcs. Expressions are given for the arc voltage, electric field, arc radius and plasma velocity in terms of the arc length, current, gas pressure and temperature. The energy balance equation relates arc temperature with current. The expressions involve the material functions of the arc plasma, so that predictions can be made for any arc medium whose material functions are known. Properties of free burning arcs for low currents, e.g., less than 25 A for air, are controlled by natural convection, it being assumed that the arc is vertical. At higher currents properties become controlled by convection induced by the self magnetic field of the arc and depend on the current density at the cathode, which is assumed to be constant with current. Although gross simplifications are made such as assuming that arc temperature is isothermal with radius, the major predictions for arcs in air for currents ranging from 1 to 20,000 A are in fair agreement with experiment for a distance of 1 cm from the lower electrode. At smaller distances electrode effects, and at larger distances turbulence effects not included in the simple theory make predictions increasingly inaccurate.

DB-5

Emission of a Sound Wave from a 0.01 to 80 kA AC Arc - F. NADEAU, and M.G. DROUET, Direction Sciences de base, IREQ, Varennes, Québec -- The amplitude of the pressure wave produced by an atmospheric 60 Hz arc has been measured for current varying between 10 and 80,000 A and arc length between 0.01 and 6 m. For low values of the arc power the amplitude of the sound wave is found to be proportional to the time rate of change of the electrical power dissipated in the arc, in agreement with recent studies[1]; however, for high values of the electrical input, a very large departure from this relation is observed. It is attributed to non-linearity in both the production and the propagation of the sound wave evidenced in particular by the stronger absorption of the high frequency components of the sound wave for increasing amplitude of the wave, in agreement with theoretical considerations[2].

[1]M. Fitaire, T.D. Mantei, Phys. Fluids, 15, 464 (1972).
H. Dadgar, thèse, Orsay, France, 1977.
H. Dadgar, M. Fitaire, A. Pilorget, to be published.

[2]R.B. Lindsay, Mechanical Radiation, McGraw Hill, 1960.

SESSION E

7:30 P.M., Tuesday, October 17

Embassy Room

WORKSHOP ON FUNDAMENTAL PROCESSES IN EXCIMER LASERS

Moderator: C.K. Rhodes,
University of Illinois at Chicago Circle

E-1

Ab Initio Calculations on HgCl and HgBr: Application of the Relativistic Effective Core Potential Methods-W.R. WADT, Los Alamos Scientific Laboratory--The recent development of relativistic effective potential by Kahn, Hay and Cowan* allows one to extend ab initio quantum chemical techniques to molecules involving very heavy atoms (Z>54). The effective core potential method will be reviewed and illustrated by application to the mercury halide laser systems. Potential energy curves, spectroscopic constants and radiative properties will be reported for HgCl and HgBr. The strengths and limitations of the results will be outlined. The effects of spin-orbit coupling of the mercury halide systems will be considered using a simple, effective, one-electron model. The theoretical data will be synthesized to give theoretical emission spectra and lifetimes and compared with experiment. Preliminary results on the photodissociation of $HgCl_2$ and $HgBr_2$ will be discussed.

*L.R. Kahn, P.J. Hay and R.D. Cowan, J. Chem. Phys., 68, 2386 (1978).

E-2

The Dominant Kinetic Processes in XeF Laser Media*-D.L. HUESTIS, SRI International--The XeF laser, operating at 351 and 353 nm, has the longest wavelength of any of the rare gas halide lasers. In electron-beam pumped $Ne/Xe/NF_3$ mixtures, substantial output energies have been obtained at reasonable efficiencies. However, the efficiencies are well below the theoretical maximum of 13% based on the ratio of the 3.5 eV XeF photon to the 27 eV primary excitation energy in neon. Before the ultimate efficiency and scaling potential can be assessed, three major classes of kinetic processes must be comprehensively characterized: (1) Production of the excited state--The substitution of Ne for Ar as the host gas to reduce the absorption due to Ar_2^+ has necessitated understanding the input kinetic chain of the $Ne/Xe/NF_3$ mixture; (2) Excited State Mixing and Quenching--It has recently been established that the upper laser level [XeF($B\frac{1}{2}$)] is not the lowest excited state; and (3) Removal of the lower laser level sustained laser action depends on the depletion of the XeF($X^2\Sigma^+$) ground state vibrational manifold by dissociation induced by collisions with the background rare gas.

*Supported by the Defense Advance Research Projects Agency under Contract DASG60-77-C-0028 through U.S. ArmyBMDATC.

E-3

Applications of Rare-Gas-Halide Lasers to Multiquantum Spectroscopy and Nonlinear Optics - D.J. KLIGLER* and J. BOKOR**, Stanford University, Stanford CA, W.K. BISCHEL and C.K. RHODES, SRI International-- Multiple photon absorption, photodissociation, and parametric conversion using rare-gas-halide lasers open up a new, previously inaccessible region of the atomic and molecular energy scale to study. The high power and efficiency of these lasers make it possible to create large excited state densities using nonlinear processes and thus offer great promise as pump sources for new VUV and even XUV lasers. In our laboratory, we have studied a number of simple atomic and molecular systems in this way. Excitation of H_2 and CO has been studied using flourescence emission spectroscopy. Photolysis of OCS, N_2O and OCSe has been studied with a view toward efficient production of (^1S) excited group VI atoms. Further, Kr and Xe have been selectively excited allowing detailed kinetic studies of the rare-gas-halide and rare gas dimer systems. The results of these experiments will be discussed as well as very promising possibilities for the future.

* National Science Foundation Graduate Fellow
**Fannie and John K. Hertz Foundation Graduate Fellow

SESSION FA

8:30 A.M. – 10:00 A.M., Wednesday, October 18

Embassy Room

ELECTRODE EFFECTS AND VACUUM ARCS

Chairperson: J.V.R. Heberlein,
Westinghouse Research & Development Center

FA-1

Microwave Diagnostics of a Vacuum Arc Plasma- M. ROSENFELD, R. DOLLINGER, and C.N. MANIKOPOULOS, St. U. of N.Y. at Buffalo*--A comprehensive microwave plasma diagnostics study has been undertaken on a vacuum arc device employing coaxial electrodes+. Unlike conventional geometries, a hollow ring anode (17.5 cm I.D.) surrounding an axially positioned solid cathode (1 cm O.D.) is utilized. Experiments with and without an axial magnetic field applied to the plasma were performed with 3 different cathode materials. Using microwave interferometry and reflection measurements at 10 GHz, the temporal density variation of the arc plasma was monitored. Plasma density was found to increase by a factor of 10 for an equivalent increase in arc current. This is consistent with the work of others. However, the magnitude of plasma density was 3 orders below that found in vacuum arcs with opposing butt electrodes. As a result of the hollow ring anode, a larger volume is available for the plasma to expand. This is believed to be responsible for lower densities. Plasma densities exceeding 10^{12} cm^{-3} as evidenced by cutoff, were demonstrated.

*Supported in part by the Electric Power Research Institute and Sandia Laboratories

+Studies done at SUNY and Gould, Inc., Greensburg, PA

FA-2

Neutral Temperatures and Densities in a Copper Vacuum Arc with a Ring Anode- W. CROMPTON, F.N. YAO, J. L. LEE, R. DOLLINGER, D.P. MALONE and D.M. BENENSON, State University of N.Y. at Buffalo.*--The anode of the vacuum arc consists of a large, open cylinder (17.5 cm I.D.) which surrounds a small cylindrical, copper cathode (1 cm I.D.). A series of spectroscopic measurements of the visible Cu I line intensities were made at several different axial and radial positions. The densities and temperatures were calculated from the time averaged line intensities. The temperature was found to have a value of $\sim 6000^{\circ}K$ that was independent of position and peak values of arc current ($\sim$6 kA). One might expect the density near the anode to be about 10^{8} times less than near the cathode because the volume of the plasma in the anode region is about 10^{8} times the volume of the cathode spots where all of the plasma is generated. However, it was found that the vacuum chamber was uniformly filled to a density of $10^{13} cm^{-3}$. Copper ions were found only in the axially oriented plasma plume produced by the cathode.

*Supported by the Electric Power Research Institute and Sandia Laboratories.

FA-3

Cathode Material Study with a Hollow Anode - P. R. SCHWARTZ, R. DOLLINGER, A.S. GILMOUR and D.P. MALONE, State University of N.Y. at Buffalo.*--A vacuum arc with a round, hollow anode (17.5 cm I.D.) exhibits a series of repetitive voltage spikes and an average arc voltage of several kV. Neither phenomenon is seen in a typical vacuum arc with opposing butt contacts where the arc voltage is essentially constant ($\lesssim$100 V). In contrast, the arc current of a vacuum arc with a hollow anode (under certain conditions) is essentially constant ($\sim$1 kA). Therefore, a study using 13 different cathode materials was done in order to determine which cathode materials produce voltage spikes and high average arc voltage. It was found that a vacuum arc with a vanadium cathode was the best at producing these phenomena and aluminum, titanium, niobium and molybdenum were second best. These results were compared to those material properties that have historically been of interest in typical vacuum arcs. A correlation was found between erosion rate and molecular weight which will be discussed.

*Supported by the Electric Power Research Institute

FA-4

Voltage Fluctuations in Low Current Atmospheric D.C. Arcs - M.G. DROUET, Direction Sciences de base, IREQ, Varennes, Québec; R. HAUG, and M. GOLDMAN, Laboratoire de Physique des Plasmas, SUPELEC, Gif-sur-Yvette, France -- The voltage fluctuations associated with the metallic-gaseous transition in an arc produced by the separation of current carrying contacts has been studied previously[1]. A very similar phenomena has been observed for a low current D.C. arc, 5 mm in length and burning in air between Cu/Cu or Cu/Ag electrodes. The voltage fluctuations correspond, in our case, to fluctuations in the release of metallic vapor from the anode surface as evidenced by spectroscopic observation of the light emission from the anode region. This discontinuous release of metallic vapor is attributed to successive explosive releases of metal from the anode separated by long period of heating of the anode surface during which the Cu or Ag lines are absent while the N_2 lines are increased. We expect a similar phenomena to be associated with the formation of craters at the cathode.

[1]M.F. Hoyaux, C.W. Kimblin, Electrical Contacts (Illinois Inst. of Tech.) p. 218 (1969).
E.W. Gray, J. Appl. Phys. 43, 4573 (1972).

FA-5

Dynamic Measurements of Cathodic Emission on Oxide Films - H. MERCURE, and M.G. DROUET, Direction Sciences de base, IREQ, Varennes, Québec -- Recent experiments have shown that oxide layers play a dominant role in delineating the basic emission features. Such findings have been deduced primarily by using S.E.M. records[1]. However, real-time measurements of individual site current, with a time resolution better than 10 ns, have been made possible by a novel technique[2] which exemplifies the impulsive nature of cathodic emission. This same technique is being applied to an investigation of the fine structure of current emission on controlled copper oxide layers (25 - 1000 Å) in atmospheric air. Trends in emission features are analysed and correlated with oxide thickness. The use of this current sampling method in conjunction with T.E.M. or S.E.M. observations is believed to be essential in order to define a consistent emission model.

[1]A.E. Guile, A.H. Hitchcock, Proc IEE, 125, 251 (1978).

[2]M.G. Drouet, S. Gruber, IEEE Trans. PAS-95, 105 (1976).

FA-6

Cathode Current Densities and Current per Cell in a Copper Cathode Vacuum Arc-G.P. SMITH, D.P. MALONE, R. DOLLINGER and A.S. GILMOUR, State University of N.Y. at Buffalo.*-- High speed, framing photographs (2.5μs/frame) of a ∿700 A copper cathode vacuum arc are used to obtain experimental values for the area of the cathode spots as a function of time, current, current density (J) and rate of change of current. The current per cell (or microspot) was calculated from the present data and three previously proposed theoretical cell areas. These present values of current per cell (3.9 A to 5.3 A) were found to compare favorably to the earlier values obtained by others even though the earlier work was done using single cell arcs (∿10 A) and the present work used multi-spot/multi-cell arcs (∿7 spots or ∿ 70 cells). It was observed that the current changed smoothly in time but that J was discontinuous because the number of spots changed only in integral steps. The current per spot was found to range from 20 A to 182 A depending on J and the statistical nature of spot size.

*Supported by the Electric Power Research Institute

FA-7

Power Flux to the Cathode of a dc Mercury Vacuum Arc. GISELA ECKHARDT, Hughes Research Labs -- The power dissipated in the cathode of a dc mercury vacuum arc has been measured for a range of discharge currents and linear current densities. A molybdenum cone with a 90°-cone angle served as the container for the continuously replenished liquid mercury and as the external anchor for the cathode spots. All spots were anchored at the intersection between molybdenum cone and mercury pool surface, forming a circular pattern around the pool. It was found that the net power flux into the cathode was independent of the total discharge current between 30 and 84A but showed a weak dependence on the linear current density I' (= total discharge current divided by the perimeter length of the cathode spot pattern). The energy balance for the mercury cathode spots will be discussed in this context.

FA-8

A Simple Classical Analysis for Particle-Surface Energy Accommodation - L. P. HARRIS, General Electric Corporate R&D--A simple two-stage classical analysis is given for the energy accommodation and possible condensation that occurs when a low energy atomic particle strikes a solid surface. In the first stage, the particle-surface forces are approximated with a parabolic potential well and the solid by an elastic continuum. The particle-surface interaction is then mathematically equivalent to a transient in a simple RLC electrical circuit. In the second stage, the "spring constant" parameter of the potential well is adjusted as a function of the ratio of particle incident kinetic energy to the binding energy of the condensed particle. The results give the energy accommodation coefficient in terms of two dimensionless parameters, the energy ratio and the ratio of the incident particle mass to the solid mass uncovered by sound waves while the particle reflects from the surface. For conditions at vacuum arc electrodes, impact of a metal atom on the parent metal gives high energy accommodation and condensation.

SESSION FB

8:30 A.M. – 10:00 A.M., Wednesday, October 18

Georgian Room

ELECTRON AND ION TRANSPORT

Chairperson: J.J. Lowke,
University of Sydney

FB-1

Three-Temperature Theory of Gaseous Ion Transport - L. A. Viehland, S. L. Lin* and E. A. Mason*, Parks College of St. Louis University A three-temperature kinetic theory of gaseous ion transport through neutral atomic gases, valid for electric fields of arbitrary strength without restriction on the ion-atom mass ratio or interaction potential, is presented. The theory is based on the use of a set of basis functions in which the ions are allowed to have different temperatures parallel and perpendicular to the field, neither of which is necessarily equal to the gas temperature, and for which the ion velocity distribution is displaced from the origin. Although the theory is more difficult to use than are earlier theories, it has the important advantage of yielding accurate results in low orders of approximation to quantities that are intrinsically anisotropic, notably ion diffusion coefficients. Numerical results are presented for both model and real data.

*Permanent address: Brown University

FB-2

Diffusion of Ions in Oxygen, Nitrogen, Carbon Monoxide and Carbon Dioxide - J.A. REES and S.R. ALGER, Liverpool Univ. (U.K) --- Experimental data have been obtained for the ratio D_T/μ (D_T is the ion diffusion coefficient perpendicular to the direction of the applied electric field and μ is the ion mobility) for O_2^+ ions in oxygen, N^+, N_2^+, N_3^+ and N_4^+ ions in nitrogen, CO^+ CO ions in carbon monoxide and O^- and CO_3^- ions in carbon dioxide. The results have been fitted using generalised Einstein relationships with the ratio of the diffusion and viscosity collision cross-sections for the ions treated as an adjustable parameter. The values chosen for the parameter also lead to acceptable values of the longitudinal diffusion coefficient D_L in those cases for which experimental data are available.

FB-3

The Drift Velocity of Electrons in Mercury Vapour, M.T. ELFORD, Electron and Ion Diffusion Unit, Australian National University, Canberra - The drift velocity of electrons in mercury vapour at 573K has been measured over the E/N range 0.1 to 3 Td and at pressures ranging from 5.4 to 14.5 kPa. The experimental techniques are described and the absolute errors are estimated to be less than 2%. The drift velocities show a linear dependence on pressure which is ascribed to the presence of dimers. A momentum transfer cross section has been derived using drift data extrapolated to zero pressure. The resonance was found to occur at approximately 0.45 eV and to have a magnitude of approximately 200 $\AA^2$.

FB-4

Electron Drift and Diffusion in Polyatomic Gases*. P. KLEBAN, Univ. of Maine, and H. TED DAVIS, Univ. of Minnesota - We describe recent results[1,2] on electron drift and diffusion in polyatomic gases. A new kinetic mechanism for the drift velocity maximum (negative differential conductivity) observed in methane is proposed. Good agreement with experiment is obtained with the use of model scattering cross sections. The Boltzmann equation is solved directly by an iterative numerical technique. Drift velocities and (anisotropic) diffusion constants for CH_4, CD_4, and related models are calculated with this method.

1. P. Kleban and H. Ted Davis, Phys. Rev. Letters, 39, 456 (1977).
2. P. Kleban and H. Ted Davis, J. Chem. Phys. 68, 2999 (1978).

*Work supported in part by grants from the National Science Foundation and the Donors of the Petroleum Research Fund.

FB-5

Model of Drift Velocity Enhancement and Differential Negative Conductivity in Molecular Gas-Rare Gas Mixtures - M. R. STAMM, W. F. BAILEY, A. GARSCADDEN, Air Force Aero Propulsion Laboratory, Wright-Patterson AFB, Ohio 45433--An analytic model is presented to explain the influence of small amounts of molecular gases on the electron drift velocity, W_e, in rare gases. In argon at low E/N, W_e is enhanced typically by a factor of 4 due to the presence of a few percent of molecular gases such as H_2 or N_2. Furthermore rare gas-molecular gas mixes may exhibit differential negative conductivity, in which an increase of E/N causes a decrease in W_e. It is demonstrated that both effects depend on the energy thresholds, E_{th}, of the inelastic processes and the energy dependence of the elastic and inelastic cross sections near E_{th}. The details of the W_e variation with E/N also depend on the nature of the inelastic collision (resonant or nonresonant). The necessary conditions for W_e enhancement and for the occurrence of differential negative conductivity are given. Comparisons are made with available experimental data and with numerical solutions of the collisional Boltzmann equation.

SESSION GA

10:15 A.M. – 12:05 P.M., Wednesday, October 18

Embassy Room

ION INTERACTIONS AND MOBILITIESI

Chairperson: P.C. Cosby,
SRI International

GA-1

Ion-Molecule Reaction Studies Using a New Flow-Drift Tube. - W. LINDINGER, E. ALGE, H. STÖRI, and R.N. VARNEY, Atomphysik, U. of Innsbruck. --

An apparatus for study of ion-molecule reactions having certain new features has been built. The features include: (1) The ion source is a hollow cathode discharge tube from which ions emerge through a 50-μm hole directly into a drift tube. (2) The drift tube may contain a buffer gas that is the same as or different from that in the HC. (3) A reactant gas of still a different type can also be added to the drift space. (4) Both primary ions and product ions leave the drift space through a sampling hole 150 μm in diameter and are then mass analyzed and counted. New reaction rate coefficients have been determined for Ar^{++} in O_2, CO_2, N_2, CH_4, NO_2, C_2H_2, and H_2. The results with H_2 disclosed a high degree of sensitivity to whether the Ar^{++} is in a ^3P or a ^1D state. The data in addition show that the transverse diffusion coefficient for Ar^+ ions in Ar is essentially constant for E/N from nearly 0 to 400 Td.

GA-2

Reactions of Excited Ions of the Rare Gases - M. GROSSL, H. HELM, M. LANGENWALTER and T.D. MARK, Inst. f. Atomphysik, Univ. Innsbruck, Austria--In their parent gas atomic rare gas ions $R^{+2}P_{3/2}$ are converted in three body collisions into stable bound molecular ions $R_2^+(II1/2_u)$. The upper state $^2P_{1/2}$ is regarded to be lost in three body collisions as well. However the molecular state directly accessible to it, $R_2^+(III/2_u)$ is weakly bound and may decay into gerade states of the $R^{+2}P_{3/2}$ + R^1S_o configuration. It has been proposed that the rate of loss of $R^{+2}P_{1/2}$ ions is governed by the balance of radiative decay and thermal dissociation of the weakly bound molecular ion†

$$R_2^+(II1/2_u) \xrightarrow{\tau} R_2^+(\text{gerade}) + h\nu \qquad (1)$$

$$R_2^+(II1/2_u) + R \xrightarrow{k} R^{+2}P_{3/2} + 2R \qquad (2)$$

We have measured the rate of loss of singly charged atomic ions of Ar and Kr in a stationary afterglow experiment and found evidence for reactions (1) and (2). The experiment is sensitive to the ratio of the lifetimes of ions in (1) and (2), $\tau.k.N$, where N is the gas density.

†H. Helm and R.N. Varney, J. Chem. Phys. 68 (1978) 5301

GA-3

Ion-Molecule Association Reactions, F.C. FEHSENFELD, T.J. BROWN, and D.L. ALBRITTON, NOAA/ERL, Boulder CO*--Ion-molecule association reactions that produce weakly bound "cluster" ions play an important role in high-pressure, low-temperature ionized gases. Rate constants for the association of O^- and O_2^- with N_2 and O_2 and Ar^+ with Ar have been measured as a function of temperature in a variable-temperature flowing afterglow. In addition, equilibrium constants for the association of NO^+ with N_2 and Ar_2^+ with Ar have been determined between 100 K and 200 K. From these results, the heats of formation and entropy of $NO^+ \cdot N_2$ and Ar_3^+ are deduced. The results will be reported and their implication briefly discussed.

*This work has been supported in part by DNA.

GA-4

Ion-molecule Reactions of Singly and Multiply Charged Atomic and Molecular Ions in Kr and Kr + Cl_2 Discharges.- F. HOWORKA, I. KUEN, and R.N. VARNEY, Atomphysik, U. of Innsbruck, Austria.--The partial charge exchange rate constant of multiply charged Kr^{n+} ions (n = 2,3,4) was determined in a low pressure hollow cathode discharge in pure krypton: Kr^{2+} :$k<5 \times 10^{-13}$, Kr^{3+}: $k = (1.9 \pm 0.7) \times 10^{-11}$. Kr^{4+}: $k \simeq (1 \pm 0.7) \times 10^{-10}$ $cm^3 s^{-1}$. The formation of $KrCl^+$ in Kr-Cl_2 mixtures was found to be due to three energetically possible processes with the rate constants k:

$Kr^+ + Cl_2 \rightarrow KrCl^+ + Cl$ $\quad k = 1 \times 10^{-12}$ $cm^3 s^{-1}$

$Kr^{++} + Cl_2 \rightarrow KrCl^+ + Cl^+$ $\quad k = 1 \times 10^{-11}$ $cm^3 s^{-1}$

$Cl^+ + 2Kr \rightarrow KrCl^+ + Cl+Kr$ $\quad k = 4 \times 10^{-28}$ $cm^6 s^{-1}$

If more than one process is responsible, the above k values are to be considered upper limits.

GA-5

Measurements of the Reaction $He^+ + H_2 \rightarrow He + H^+ + H$ at Low Temperatures* - A. K. CHEN, R. JOHNSEN, and M. A. BIONDI, Univ. of Pittsburgh -- Bimolecular and termolecular rate coefficients have been determined for the dissociative charge transfer process $He^+ + H_2 + (H_2) \rightarrow He + H^+ + H + (H_2)$ using a temperature-variable drift tube/mass spectrometer apparatus at temperatures from 77 to 330 K. The results indicate that the two body rate coefficient decreases from 1.5×10^{-13} cm^3/sec to 1.1×10^{-13} cm^3/sec as the gas temperature is raised from 77 K to 330 K. A three-body contribution to the charge transfer rate is found to have a rate coefficient of 1.8×10^{-30} cm^6/sec at 77 K and $\sim 4 \times 10^{-31}$ cm^6/sec at 330 K. The corresponding reaction with deuterium has also been studied and is found to exhibit considerably smaller rate coefficients. The results will be compared with previous experimental and theoretical results.

*This research has been supported, in part, by the National Aeronautics and Space Administration (NGL39-011-137).

GA-6

Reactions of Drift-Induced Vibrationally Excited Ions, W. LINDINGER, D.L. ALBRITTON, and F.C. FEHSENFELD, NOAA/ERL, Boulder CO 80303*--A flow-drift tube has been used to study the reactions of vibrationally excited O_2^+ and CO_2^+ ions with several gases. The vibrational excitation is collisionally induced at high E/N in an argon buffer gas. The excitation does not occur for ions drifting in a helium buffer. It is found that vibrational excitation promotes the otherwise-slow reactions of O_2^+ and CH_4 and CO_2^+ with O_2 and inhibits the fast reaction of CO_2^+ with H_2. The drift-induced vibrational excitation of O_2^+ and CO_2^+ is rapidly quenched by a few percent of O_2 and CO_2, respectively, in the argon buffer gas, allowing one to study separately the effects of kinetic and ionic vibrational energy on the reaction rate constant.

*This research was supported in part by DNA.

GA-7

The Production of $NO^+(a\ ^3\Sigma^+)$ in the Reaction of N^+ with O_2, D.L. ALBRITTON, A.A. VIGGIANO, I. DOTAN, and F.C. FEHSENFELD, NOAA/ERL, Boulder, CO 80303*--It is well-known that the O_2^+ and NO^+ product channels each constitute about 50% of the total rate constant for the reaction

$$N^+ + O_2 \rightarrow O_2^+ + N$$
$$\rightarrow NO^+ + O.$$

The $NO^+(X\ ^1\Sigma^+)$ and $NO^+(a\ ^3\Sigma^+)$ products are both energetically possible. A selected-ion flow tube has been used to determine the percentage of $NO^+(a\ ^3\Sigma^+)$ ions. It is known from separate studies that $NO^+(a\ ^3\Sigma^+)$ reacts rapidly with N_2 to form N_2^+; therefore, the separate addition of N_2 and the search for an N_2^+ signal provide a monitor for the $NO^+(a\ ^3\Sigma^+)$ product. It was found that $NO^+(a\ ^3\Sigma^+)$ production was less than 5% of the total rate constant.

*This research was supported in part by DNA.

GA-8

The Determination of Thermal Energy Rate Constants using a Modified Version of the Selected Ion Flow Tube (SIFT) Technique, G.I. MACKAY, G. VLACHOS, H.I. SCHIFF and D.K. BOHME, York University. The selected ion flow tube (SIFT) originally reported by Adams and Smith[1] has been modified to permit increased ion signals and versatility in ion production. The reactant is produced in known energy states by chemical ionization in a miniature flowing afterglow. It is separated from other ions by a quadrupole filter. A venturi aspirator is used to inject the mass-selected ion beam into the carrier gas of the main reaction tube. Both He and H_2 have been used as the carrier and aspirator gases. Reaction of these ions with the neutral reagent introduced downstream is monitored in the usual manner. Previous difficulties encountered with the conventional flowing afterglow such as extended sources of reactant ions, interferences from reactions of the parent or product ion with buffer gas or of the neutral reagent with other ions produced in the source region are avoided. Examples will be given to illustrate how these advantages can be exploited.

1. N.G. Adams and D. Smith, Int. J. Mass Spectrom. Ion Phys., 21 349 (1976).

GA-9

Mobililty of Ions in Methane Gas--M. SAPOROSCHENKO--Southern Illinois University-Carbondale-- The mobilities of $C_4H_9^+$, $C_5H_9^+$, $C_6H_{11}^+$, and $C_8H_{15}^+$ ions in methane gas have been measured using a Tyndall double shutter device. Gas pressure in the drift tube was 1.8-2.2 torr range. The ions have been identified mass-specrometrically simultaneously with measurement of the mobility. The mobility, extrapolated to zero field and atmospheric pressure, is 1.17 cm^2-$volt^{-1}$-sec^{-1} for $C_4H_9^+$ ion and few percent lower for the higher order ions. Drift velocities have been measured for the secondary and tertiary ions in methane gas.

GA-10

Ionic Polymerization in CH_4 - M. SAPOROSCHENKO, Southern Illinois University-Carbondale--A large number of positive ions in methane gas formed in a chain of consecutive ion-molecules reactions were observed in the drift tube mass spectrometer. Cross sections for the reaction of seventeen ions with methane molecules were determined from the exponential attenuations of the normalized intensities of the ions with increasing drift distance at constant gas pressure and constant electric field intensity. Rate constants for the reactions of the following ions: $C_2H_5^+$, $C_3H_5^+$, $C_3H_7^+$, $C_4H_9^+$, $C_5H_9^+$, and $C_6H_{11}^+$ with methane gas were obtained from the experimentally measured ion drift velocities and cross sections. Extensive ionic polymerization in CH_4 through long chains of consecutive low energy ion-molecule reactions was studied. Ions containing up to twenty carbon atoms were observed.

SESSION FB (continued)

10:15 A.M. – 10:45 A.M., Wednesday, October 18

Georgian Room

ELECTRON AND ION TRANSPORT

Chairperson: J.J. Lowke,
University of Sydney

FB-6

On the Diffusion Approximation of the Boltzmann Equation for Slow Electrons* J.H. JACOB, B.N. SRIVASTAVA, M. ROKNI**, J.A. MANGANO, Avco Everett Res. Lab., Inc.--The applicability of the lowest order diffusion or P_1 approximation of the Boltzmann equation is investigated. The analysis which is performed by considering a narrow beam of electrons in energy space shows that for stable high pressure discharges the P_1 approximation is valid for all the cases considered. This result is a direct consequence of the fact that the electron production in high pressure discharges is due to distributed source of electrons for which the spatial derivative in the Boltzmann equation can be neglected. For cases where spatial derivative cannot be neglected, e.g., for spatially localized source of electrons, the region of validity of the P_1 approximation is much more restrictive. Electrons generated for swarm experiments are examples of a spatially localized source of electrons.

*Supported by ARPA Contract N00014-75-C-0062.

**The Hebrew University of Jerusalem, Israel.

FB-7

Theory of Electron Drift and Diffusion in Neutral Gases in an Electrostatic Field* - S. L. LIN, R. E. ROBSON,† and E. A. MASON, Brown U. - We develop a rigorous theory of electron transport in neutral gases in an electrostatic field, which does not require approximating the electron distribution function by the first two terms of an expansion in spherical harmonics. The method is a modification of the procedure developed by Viehland and Mason[1] for ion transport. There is no restriction upon the field strength or cross section, and both elastic and inelastic collisions are considered. In cases such as electrons in methane, where inelastic collisions are dominant, the inadequacy of the two-term approximation is especially pronounced, and the present method is directly applicable. However, in other situations where no inelastic collisions occur, even where the elastic cross section has a deep Ramsauer minimum, the two-term approximation suffices.

*Supported in part by the US Army Research Office.

†Permanent address: James Cook U., North Queensland, Australia.

[1]L. A. Viehland and E. A. Mason, Ann. Phys. (N.Y.) 110, 287 (1978).

FB-8

Analytic Solutions for Electron Energy Distributions in Gas Discharge Lasers. P.E. NIELSEN, T.E. GIST, and E.D. SEWARD, AF Inst of Tech, WPAFB OH 45433.--We develop approximate analytic solutions to the Boltzmann equation for the number of electrons $f(\varepsilon)d\varepsilon$ within $d\varepsilon$ of ε arising from an electron beam applied to a neutral gas in the presence of an electric field. These solutions complement more detailed numerical solutions to the Boltzmann equation in several ways: they may be used in a general assessment of direct vs discharge pumping in gas lasers, they provide a priori knowledge of the zoning necessary for an accurate numerical solution, and when input as an initial condition to numerical programs, they allow rapid relaxation to the true solution. We discuss these and other applications in detail.

SESSION GB

10:45 A.M. – 12:05 P.M., Wednesday, October 18

Georgian Room

GLOW DISCHARGES

Chairperson: J.T. Verdeyen,
University of Illinois

GB-1

A General Characteristic Equation for a Diffusion-Controlled Positive Column of Arbitrary Shape with One- and Two-Step Ionization. GERALD L. ROGOFF, Westinghouse R&D Center--A simple expression characterizes the electrical properties of a steady-state positive column of arbitrary cross-sectional shape with electron loss by diffusion and production by one-step and/or two-step electron-impact ionization, i.e., with production rates linear or quadratic in electron density. This equation relates the ionization and diffusion coefficients (or applied electric field), the total number of electrons per unit column length (or electron current), the area of the column cross section, and the cross-sectional shape, which is represented by a single dimensionless number. For the limiting case of one-step ionization only, the equation indicates that the field depends on the cross-sectional area and is independent of the number of electrons per unit length. However, in the limit of two-step ionization only, the dependence is completely reversed; the field varies with the number of electrons per unit length (and thus with current) but is independent of the cross-sectional area. Thus, for two-step ionization and constant electron current, the operating field varies only with the shape of the cross section.

GB-2

Behavior of Neon Discharges- R.M.M. SMITS, Eindhoven U.,The Netherlands--The positive column of a neon discharge has been investigated in the region $0.50<p_oR<10$ torr.m, $0.01<I/R<10$ A/m. A numerical model has been set up for the positive column in this region. The electron energy distribution function has been calculated from the Boltzmann-equation. Balance equations for the excited atoms and the electrons have been solved together with the gas and electron temperature equations. Taking into account the alterations in some plasmaparameters due to a nonlinear striation development above certain pressure and current values, the sudden constriction of the column may be explained with this model. The calculations are in agreement with the experiments. The electron density and temperature have been measured using the electron-atom continuum radiation. Excited atom densities have been measured with the fluorescence technique, using a c.w. dye-laser. With this laser also reaction coefficients for transitions between 2p-levels by atomic collisions have been measured. The dependence of these coefficients on the gas temperature has been evaluated from these measurements with the aid of the numerical model. All coefficients were proportional to T_G^n with $0\leq n\leq 2.5$. (A simple estimation gives n=1.5 for a special case).

GB-3

Model Calculations on the Positive Column of Hg-Noble Gas Discharges. F.A.S. LIGTHART, Philips Research Labs, Eindhoven, The Netherlands.--Model calculations have been carried out on the positive column of low-pressure Hg-noble gas discharges. The atomic states 6^1S_o, $6^3P_{0,1,2}$ and 6^1P_1 and the ions Hg^+ and Hg_2^+ are included. In addition to direct and two-step electron-impact ionization we also include ionization via mutual collisions between 6^3P-atoms.[1] The electron-impact rates are calculated using a modified two electron group model. The calculated electric field strengths, UV-efficiencies and electron temperatures reproduce experimental data within 5-10% for a set of conditions relevant to fluorescent lamps (noble gas: argon or neon, R=1.8 cm, p=0.5-20 Torr, T_{wall} = 20-80°C, I=.1-.8A). The inclusion of excited-state collisional ionization leads to much better agreement as compared to prior calculations, in particular at the higher wall temperatures. The application of the two electron group model gives better agreement, particularly at low current values.

[1]L. Vriens, R.A.J. Keyser and F.A.S. Ligthart, J. Appl. Phys., in press.

GB-4

Electron Density Distributions in a Low-Pressure Discharge Tube Containing an Array of Dielectric Fibers. GERALD L. ROGOFF, Westinghouse R&D Center--Steady-state electron density (n_e) distributions have been calculated numerically for positive columns of circular cross section containing an array of dielectric fibers parallel to the axis, a structure similar to the glass or quartz wool used[1] to enhance the rate of electron-ion surface recombination. The fibers are treated as regions of zero electron density in the boundary conditions for the electron continuity equation, which includes terms for production by one-step ($\propto n_e$) or two-step ($\propto n_e^2$) electron-impact ionization and loss by diffusion. For one-step ionization the calculated distribution is fairly diffuse, similar to that with no fibers. However, for two-step ionization the column is highly constricted, much more so than with no fibers. The latter distribution is also more constricted than those calculated by Hasker[1] with stepwise ionization but with the effect of the fibers distributed continuously by a loss term added to the continuity equation. The calculated constricted distribution agrees qualitatively with experimental observations.

[1]J. Hasker, Appl. Phys. Lett. 28, 586 (1976); J. Illum. Eng. Soc. 6, 29 (1976).

GB-5

Average Loss Rate of Electron Energy in Positive Column of Oxygen Glow Discharge - K. NOBATA, T. KAKISHIMA, and M. KANDO, Shizuoka U. -- Both the electric field E and the electron temperature T_e have been measured by Langmuir probes in the positive column of oxygen glow discharge. The values of E/p at the pressure higher than about 5 Torr where the contraction occurs are found to be much smaller than those at the pressure bellow about 2 Torr where the positive column does not contract, under the condition of same values of T_e. This implies that the average loss rate of energy at each collision of an electron with gas molecule, κ, becomes smaller at higher gas pressure than about 5 Torr. The amount of the dissociation of the oxygen molecules is estimated not to be large at 10 Torr rather than at 2 Torr by spectroscopic measurements. The change of κ is reasonably explained by increasing of excited molecules. The ratio of the number of molecules excited to a metastable state to that of ground state, x, is calculated against the pressure by providing a parameter of the probability of excitation. The change of κ against the pressure is explained by the change of x against pressure at a certain value of excitation probability.

GB-6

Electron Energy Relaxation in Low-Pressure Gas-Discharges-F.A.S. LIGTHART and R.A.J. KEIJSER, Philips Research Labs.,Eindhoven, The Netherlands--The Fokker-Planck formalism has been used to derive expressions for the rate of electron energy relaxation between the so-called bulk and tail electrons in a two electron group model approach[1]. The electron energy distribution used is continuous at the bulk-tail boundary. The effects of diffusion and drift of the electrons in energy space are both taken into account. The earlier relaxation rates[1,2] were calculated using (i) a stopping power approach which only accounts for the continuous slowing down (drift) of the electrons and (ii) a discontinuous electron energy distribution. We find that the diffusion effect is dominant, but that the too small relaxation in the earlier approach is largely compensated by the use of the discontinuous function. The new rates are used to calculate excited state densities in a low-pressure Hg-Ar discharge. Good agreement with experiment is obtained.

[1]L. Vriens, J. Appl. Phys. 44, 3980 (1973).
[2]L. Vriens and F.A.S. Ligthart, Philips Res. Repts. 32, 1 (1977).

SESSION HA

1:30 P.M. – 3:05 P.M., Wednesday, October 18

Embassy Room

ION INTERACTIONS AND MOBILITIES II

Chairperson: H. Helm,
Universität Innsbruck

HA-1

Inelastic Processes in 5-500 eV He^+-Li Collisions - G.D. MYERS, and J.J. LEVENTHAL, Univ. of Mo.-St. Louis*--Excited state production in 5-500 eV He^+-Li collisions has been studied by observing uv-optical-near ir radiation emanating from the collision region of a beam apparatus. The dominant feature of the collision produced spectra at all kinetic energies was the 671 nm. LiI resonance line. At elevated energies, endothermic charge transfer, yielding HeI emissions, was observed. Although there are no restrictions on the spin states of the product species, only HeI triplet radiation was observed. The absence of singlet HeI radiation is attributed to nearly inaccessible crossings of the $He^+(1\ ^2S)$-Li $(2\ ^2S)$ potential energy curve with other singlet $[HeLi]^+$ curves.

*Work performed under ONR Contract No. N00014-76-C-0760

HA-2

Mobilities of He^{++}, Ne^{++}, Ar^{++} and Xe^{++} in Their Parent Gases* - RAINER JOHNSEN and MANFRED A. BIONDI, Univ. of Pittsburgh. -- Mobilities of the doubly charged rare gas ions He^{++}, Ne^{++}, Ar^{++}, Kr^{++}, and Xe^{++} in their parent gases have been determined using a drift tube/mass spectrometer apparatus. The observations of more than one mobility for each of the doubly charged ions (except for He^{++}) is attributed to the presence of the ^1D and ^1S low-lying metastable states as well as the ^3P ground state of these ions. At 300 K the reduced mobilities (in units of $cm^2/V\text{-}sec$) extrapolated to zero field have the values (accurate to ± 3%); $\mu_o(He^{++}$ in He) = 18.3; $\mu_o(Ne^{++}$ in Ne) = 6.5 (^1D), 7.0 (^3P), 8.5 (^1S); $\mu_o(Ar^{++}$ in Ar) = 2.7 (^3P), ~ 2.2 (^1D); $\mu_o(Kr^{++}$ in Kr) = 1.11 and 1.28, $\mu_o(Xe^{++}$ in Xe) = 0.65 and 0.75. The measured mobilities of He^{++} in He are in quite good agreement (5%) with those calculated by Wadehra and Bardsley.

*This work has been supported, in part, by the U. S. Army Research Office (DAAG-29-77-G-0079).

HA-3

Radiative and Non-radiative Charge Transfer Reactions of Doubly Charged Rare Gas Ions with Rare Gases* RAINER JOHNSEN and MANFRED A. BIONDI, Univ. of Pittsburgh. -- Radiative and fast charge transfer of doubly charged rare gas ions, X^{++}, with rare gas atoms has been studied at thermal energies in a drift tube/mass spectrometer. The measured rate coefficient of 4.8×10^{-14} cm^3/sec for $He^{++} + He \rightarrow 2\ He^+ + h\nu$ agrees well with the calculations of Cohen and Bardsley. Slightly smaller rate coefficients, dependent on the state of the ion (^1S, ^1D, ^3P), are found for the corresponding reactions in the heavier rare gases. Three body contributions with rate coefficients from 10^{-31} to 10^{-30} cm^6/sec are found to contribute to the charge transfer which become more important in the heavy rare gases and at reduced temperature. Rate coefficients ranging from 10^{-15} to 10^{-9} cm^3/sec have been obtained for the heteronuclear reactions $X^{++} + Y$ several of which result in doubly charged products. Similar reactions with molecules to produce ions of ionospheric interest and their reactions ($O^{++} + N_2$, O_2) will be discussed briefly.

*This work has been supported, in part, by the U. S. Army Research Office (DAAG-29-77-G-0079).

HA-4

Interactions of α Particles with He Atoms - J.N. BARDSLEY, J.S. COHEN, and J.M. WADEHRA, Los Alamos Scientific Laboratory*--Ab initio calculations on the lowest three states of He_2^{++} were performed by the valence bond method which is particularly appropriate for studies of long-range interactions. The mobility of α particles in He was computed using the lowest order of transport theory to be about 5% lower than the experimental values of Johnsen and Biondi. The dependence of the mobility on field strength is in good agreement. The probability of radiative transitions between the lowest ungerade and gerade states was evaluated and the rate for radiative charge transfer in α-He collisions was estimated by the JWKB approximation to be 4.4×10^{-14} $cm^3\ s^{-1}$. Calculations incorporating quantal treatment of the resonances in these collisions will also be reported.

*Supported by NSF, DOE and ARPA.

HA-5

Potential Surfaces Govern Processes In Ionized Gases - D.G. HOPPER, Science Applications,Inc.*--The rates of various processes in ionized gases may be interpreted in terms of and rigorously calculated from a sufficient knowledge of the relevant molecular adiabatic potential energy surfaces. A program of ab initio state-of-the-art calculations to advance the knowledge of such surfaces for atmospheric molecules, clusters, and their ions is currently underway at Science Applications,Inc. Multiconfiguration self-consistent-field calculations with extended configuration interaction for several electronic states of the N_2O^+,O_3,NO_2^+, and CO_3^- systems will be outlined as examples. The presentation will stress the use of these calculated surfaces to interpret, to assign, and/or to predict (a) reactivity such as in the O^+/N_2 and $O+O_2+M \rightarrow M+O_3^*$ reactions, (b) vibrational (IR) spectra, (c) electronic (UV and vis) spectra and (d) molecular geometries and properties. In skilled hands such a priori calculative procedures must now be considered instruments for data obtention in ionized gases. Hereinafter the acquisition of molecular property and rate data by such calculative instruments will more and more frequently precede acquisition by any other instruments available for the study of basic phenomena in ionized gases. *Work supported in part by AFOSR.

HA-6

Switching Reactions of Solvated Hydroxyl Ions - J.F. PAULSON, Air Force Geophysics Laboratory* -- Cross sections have been measured in the energy range from 0.3 to 10 eV for reactions in which the negative hydroxyl ion, stabilized by clustering with water, is further stabilized by bimolecular switching reactions with CO_2, SO_2, and NO_2, leading to HCO_3^-, HSO_3^-, and HNO_3^-, respectively. The product of the reaction with CO_2, i.e. HCO_3^-, undergoes a subsequent switching reaction with SO_2. The cross sections for these solvent exchange reactions are large, e.g. 30×10^{-16} cm^2 at collision energies below 1 eV, but decrease as roughly the negative fifth power of energy above 2 eV. Cross sections were also measured for charge exchange and collisional dissociation in the interaction between $OH^- \cdot H_2O$ and NO_2.

*Supported in part by the Defense Nuclear Agency

HA-7

Energetics and Structures of the Excited and Ground States of CO_3^- R. L. C. WU and T. O. TIERNAN, Wright State U.*--Accurate translational energy thresholds have been determined for collision-induced dissociation of CO_3^- to give O^- and CO_2, using ion beam techniques. The projectile ion, CO_3^-, was produced from pure CO_2, and from a mixture of N_2O and CO_2 by the three body association process, $O^-(CO_2,CO_2)CO_3^-$. A mixture of O_3 and CO_2 was also utilized to generate CO_3^-, and in this case, CO_3^- is formed by the particle transfer reaction, $O_3^-(CO_2,O_2)CO_3^-$. It was observed that CO_3^- projectile ions formed in the O_3^-/CO_2 reaction exhibit a dissociation energy of 2.5 eV, while some fraction of the CO_3^- ions produced by the O^-/CO_2 reaction has a lower dissociation energy (1.8 eV). This is indicative of an excited state of CO_3^- which is not effectively collisionally deactivated, even at relatively high source pressures. The excitation functions for the isotopically labelled ions, $C^{16,16,18}O_3^-$ and $C^{16,18,18}O_3^-$, impacted on He, were also determined. The implications of these experiments with respect to the structure and thermochemistry of CO_3^- will be discussed.

*Supported by AFOSR Contract No. F44620-76-C-0007.

HA-8

Negative Ion Chemistry in Air-Like Gas Mixtures* V.A. MOHNEN and J.A. KADLECEK, Atmospheric Sciences Research Center, State University of New York at Albany

A drift tube mobility analyzer coupled with a quadrupole mass spectrometer was used to investigate the development of ion sequence in air-like gas mixtures containing known additions of oxides of nitrogen, sulfur dioxide, ammonia and, most importantly, ozone. The drift tube was operated at atmospheric pressure. Dominant negative ions observed in the mass spectrometer include the hydrated species of NO_3^-, CO_3^-, NO_2^-, SO_5^- and SO_4^-. If ozone is present in the system, a dramatic shift of the ion spectra is observed towards SO_5^- (mass 112). Possible reaction mechanisms leading to these ions and implications to stratospheric ion chemistry will be discussed.

*Supported by NSF Contract ATM76-81264 and ONR Contract N00014-76-C-0283.

SESSION HB

1:30 P.M. – 3:05 P.M., Wednesday, October 18

Georgian Room

DIAGNOSTICS AND AFTERGLOWS

Chairperson: D.P. Malone,
State University of New York at Buffalo

HB-1

Near-resonant light scattering from ground-state and excited Na atoms in a gas discharge. L. VRIENS and J. de RUYTER, Philips Research Labs, Eindhoven, The Netherlands.--We report on the collision-induced spectral redistribution and depolarization of light scattered from a low-pressure Na-Ne discharge. A single-mode cw dye laser was tuned near the $3^2S_{1/2}$-$3^2P_{3/2}$, $3^2P_{1/2}$-$4^2D_{3/2}$ and $3^2P_{3/2}$-$5^2S_{1/2}$ transition frequencies of Na. Rayleigh and Raman scattering (RS) and collision-induced fluorescence (CIF) were observed. The RS is dominant in scattering from the ground-state atoms, see also[1]. For the excited atoms the (spectrally) integrated CIF signals are found to be almost two orders of magnitude larger than those for the RS. A quantitative analysis is made to explain this difference in terms of the various broadening mechanisms (spontaneous decay, Lorentz (Ne), Stark (e)), level mixing, quenching and radiation trapping. As an application of the analysis, we determine local gas temperatures from the line width of the CIF from the excited states.

[1]L. Vriens, J. Appl. Phys. 48, 653 (1977).

HB-2

Use of Collisional-Radiative Model for Plasma Diagnostic Purposes-AMIT K. HUI, Vanderbilt U. -- Collisional-Radiative model was used for the study of diffusion in a hydrogen plasma across an axial magnetic of moderate strength. The magnetic field was varied and relative intensity of first three Balmer lines was measured. Recently calculated Collisional -Radiative coefficients were used for determination of electron density and variation of electron temperature from measured line intensities. Diffusion was found to be collisional in nature.

The work constitutes a part of author's doctoral dissertation submitted to Indian Institute of Technology, Kanpur.

HB-3

Interaction Between Vibrationally Excited Molecular Nitrogen and Atomic Cesium, R. CHANDRA, N. SHAH, C.H. LEE, C.N. MANIKOPOULOS and D.T. SHAW, SUNY at Buffalo.* -- Both a flowing system with a glow discharge and a stationary system with a hot cathode have been utilized to study the interaction of N_2^* with Cs.[1] Measurements have been carried out for a variety of mixing ratios, molecular nitrogen pressures in the range of 1 to 50 torr and cesium pressures between 0.01 and 0.2 torr have been employed. Spectroscopic measurements of the line emissions have been carried out as a function of discharge current as well as a function of position in the interelectrode gap. Studies of the discharge current-voltage characteristics and the corresponding line emissions of the excited species indicate the production of Cs ionization by collisions with vibrationally excited molecules.

* Supported by NASA and NSF.

[1] D.T. Shaw, C.H.Lee and C.N. Manikopoulos, Proceedings 11th Intersociety Energy Conversion Engineering Conf. Sept. 1976, Vol. II, pp. 1625-1629.

HB-4

Pulsed Discharge of Cesium Seeded Molecular Nitrogen, M. HATZIPROKOPIOU, F. RADPOUR, C.N. MANIKOPOULOS, and D.T. SHAW, SUNY at Buffalo*-- The behavior of a pulsed mixture of molecular nitrogen and atomic cesium has been studied for a variety of mixing ratios in the plasma afterglow. The nitrogen pressure was in the range of 1 to 100 torr while the cesium pressure was between 0.01 to 0.1 torr. A hot tungsten cathode was employed with an interelectrode separation of several millimeters. The characteristic emission lines of the excited species in the decaying plasma were studied as a function of position in the interelectode gap for each mixing ratio. The plasma density was also monitored in the afterglow using plasma probes. The proper analysis of the emission lines of N_2 allowed for the deduction of the vibrational temperature of N_2 in the afterglow as a function of position. Indications were seen of cesium electronic excitation by vibrationally excited nitrogen.

* Supported by NASA and NSF.

HB-5

Laser Initiated Afterglow in a High Pressure K-Kr Mixture.*-L.K. LAM and L.D. SCHEARER, U. of Missouri-Rolla--We ionized K atoms in a K-Kr ([K] = 6×10^{14} cm^{-3}, [Kr] = 2×10^{19} cm^{-3}) mixture with a 120 μJ, 404 nm dye laser pulse in a resonance absorption-photoionization process and monitored the K fluorescence spectra as a function of time. We saw a fast (∿20 ns) initial component due to electron excitation and a slow decay tail (∿10 μs) due to electron-ion recombination. Electron temperatures and densities in the afterglow decay are obtained from the spectra assuming LTE. The electron density decay obtained compares favorably to that obtained from a simple energy loss collisional-radiative model.

*This research supported in part by ONR.

HB-6

Studies of Population Inversions in MPD Arc Generated Helium Plasmas* - T.B. SIMPSON, T.M. YORK**, W.F. VON JASKOWSKY, K.E. CLARK, R.G. JAHN, Princeton U. -- Population inversions during the recombination of an expanding and cooling argon plasma have been demonstrated to be large enough to support laser oscillations (1). The application of this expansion-recombination mechanism to a helium plasma is of interest due to the possibility of steady vacuum ultraviolet lasing. This work examines the possibility of using a quasi-steady MPD arcjet to produce population inversions in helium, primarily in the n=3-2 transition of HeII at 1640Å. Theoretical studies using the collisional-radiative quasi-equilibrium model including absorption indicate a range of T_e and N_e where inverted distributions can exist. Experimental studies of the radiative properties of the helium MPD discharge, along with magnetic and double Langmuir probe measurements, show that the desired ranges of T_e and N_e may be obtained in the exhaust flow of the MPD accelerator.

(1) Applied Physics Letters, Vol. 30, No. 11, 1 June 1977.

*Supported by NASA Research Grant NGL-31-001-005

**Permanent Address: The Pennsylvania State University

HB-7

Electron Collision Frequencies in Ar, He, Ne Gases and Their Relation to the Volume Recombination Controlled Plasma Afterglow - J.S. CHANG, P. BAILLE, G.L. OGRAM, K. KESKINEN and R.M. HOBSON, YORK U. -- The electron-neutral collision frequency ν_{eff} in Ar, He, Ne gases has been calculated using recent numerical results for momentum-transfer cross sections[1] by assuming Maxwellian electron energy distributions. The electron temperature T_e relaxation and plasma density N_e decay have also been calculated using present results for ν_{eff} in Ar, He, and Ne. A r.f. discharge tube with single and triple probe and mass spectrometer was used for experimental confirmation. The results show that: (1)ν_{eff} has a power-law dependence of 0.56 and 0.82 for He and Ne gas, respectively in the range of 0.01-0.5 eV: therefore for larger T_e the T_e relaxation and Ne decay show discrepancies with the approximate theory for Ne[2]; (2) The T_e dependence of ν_{eff} for Ar has a dependence different from the mono-energetic case. The afterglow theory using the mono-energetic expression[3] should be reconsidered; (3) The effect of T_e relaxation on volume recombination has been examined by numerical calculation and experiment.

[1]Yau et al, J. Phys. B. 11, (in press) (1978).
[2]Chang et al, J. Phys. B. 11, 1675 (1978).
[3]Bochknova et al Sov. Phys. J.E. T.P. 19, 475 (1974).

HB-8

Electronic Recombination of He^+ - J.F. DELPECH and J. BOULMER, U. Paris XI, Orsay, France--Experimental rate coefficients for excitation transfer due to collisions with electrons and neutrals have been recently measured in detail in helium. These experimental results have been used to solve the system of first-order differential equations which described the relaxation of a partially ionized gas[1]. The recombination rate coefficients from 300 to 600 K, with and without 10.6 μm laser irradiation, are found to be in excellent agreement with previously reported experimental results[2].

1 J. Stevefelt, J. Boulmer and J.F. Delpech, Phys. Rev. A12, 1246 (1975).

2 J. Boulmer, J.F. Delpech and J. Stevefelt, Phys. Rev. A15, 1502 (1977).

SESSION I

3:20 P.M., Wednesday, October 18

Embassy Room

WORKSHOP ON DISSOCIATIVE RECOMBINATION

Moderator: M.A. Biondi,
University of Pittsburgh

I-A

Dissociative Recombination of Vibrationally Excited N_2^+ Ions-E. C. ZIPF, University of Pittsburgh.--Absolute laser photofluorescence techniques are used to study the dissociative recombination of N_2^+ ions in specifically identified rotational and vibrational levels. The N_2^+ density and spatial distribution, and the rotational and vibrational temperature of the $X^2\Sigma_g^+$ ground-state ions are determined from the fluorescence radiation. The optical measurements show that rotational equilibrium is achieved rapidly ($T_{rot} \sim 300"$ K) but that N_2^+ ions remain vibrationally excited throughout the afterglow period with an approximate vibrational temperature of 1100° K in a gas mixture consisting of 0.25μ N_2 in 6 torr of Ne. By combining these results with simultaneous measurements of the average electron density by microwave methods and of the composition of the decaying plasma by ion mass spectroscopy, we have measured the dissociative recombination coefficients, $\alpha(v')$, for N_2^+ ions in the $v' = 0,1$, and 2 vibrational levels. The experiment shows that $\alpha(v' = 0,1,2) \simeq 2.8 \times 10^{-7}$ cm^3 sec^{-1} at 300° K in agreement with the averaged value obtained by Mehr and Biondi[1].

[1]F. J. Mehr and M. A. Biondi, Phys. Rev., 181, 264, 1969.

I-1

Electron and Ion Temperature Dependence of the Dissociative Recombination Coefficients of H_3O^+ and D_3O^+ -G.L. OGRAM, JEN-SHIH CHANG, J.B. HOYE and R.M. HOBSON, York U. Toronto--The dissociative recombination coefficient of H_3O^+ and D_3O^+ was measured for ion temperatures between 800°K and 3500°K and electron temperatures between 800°K and 10,000°K. The r.f. produced plasma was shock heated in a 4 cm I.D. low pressure shock tube. The electrons were heated independently of the gas and ions by using a pulsed, focused microwave beam. The charge density decay and electron temperature were measured using cylindrical double and triple electrostatic probes, respectively. The experimental results have shown: (1) that if we express the dependence of coefficient on ion temperature T_i as a power-law, ie $T_i^{-\gamma}$, no single power-law dependence holds over the range of measurement, γ ranges between 0.7 and 1.1 for H_3O^+, γ increasing with temperature. The previously unmeasured coefficient for D_3O^+ was found to have a similar dependence on T_i. (2) that these temperature dependences do not exceed the upper limits of γ given by the simple theory of dissociative recombination of vibrationally excited ions given by O'Malley[1].

[1]T.F. O'Malley Phys. Rev. 185, 101 (1969)

SESSION JA

8:30 A.M. – 10:15 A.M., Thursday, October 19

Embassy Room

ELECTRON IONIZATION AND EXCITATION

Chairperson: J. Mazeau,
Université Pierre et Marie Curie

JA-1

Electron Impact Double Ionization Cross Sections of K^+ Ions.* R.K. FEENEY and W.E. SAYLE, II, Georgia Institute of Technology.--Absolute cross sections for the electron impact double ionization of K^+ ions have been measured as a function of incident electron energy from below threshold to approximately 2.9 x 10^{-18} cm^2 at approximately 150 ev electron energy. The measurements were accomplished with a crossed beam facility operating in the pulsed beam mode. The electron source utilized an oxide cathode and operated with typical currents of 1 mA. A thermionic-type ion source produced a collimated ion beam of approximately 100 nA. After undergoing collisions with the electron beam, the ion beam charge state components were separated in a two-stage parallel plate electrostatic analyzer. Two stages of analysis were used to improve the signal-to-noise ratio. The two beam current distributions were determined by means of a movable slit scanner. Numerous consistency checks were performed to evaluate possible sources of error.

*Work partially supported by USDOE.

JA-2

Electron Excitation of the S and D States of Li. A. ZAJONC and ALAN GALLAGHER,* JILA, Univ. of Colo. and NBS.--Optical excitation functions for the 3D, 4D, 4S, and 5S states of Li have been measured in a crossed-beam apparatus. The intensities of the radiation from these states have been measured relative to the 6708 Å, resonance-line intensity. Since the resonance line intensity has been accurately normalized to the Born theory at high energy,[1] we thereby obtain normalized cross sections for the S and D state excitations. These cross sections rise very abruptly at threshold, almost as fast as our ~0.3 eV energy resolution. At energies above 30 eV, we observe constant QE (cross section times energy), indicating convergence to the Born theory. This convergence is more rapid than is characteristic for resonance-line excitation.

*Staff Member, Quantum Physics Division, National Bureau of Standards.

1. D. Leep and A. Gallagher, Phys. Rev. A 10, 1082 (1974).

JA-3

Excitation and Predissociation of Triplet States in H_2 and D_2 Measured by Electron-Photon Coincidences - N. BOSE, U. of Kaiserslautern, Germany*--The excitation of hydrogen triplet states by a beam of monoenergetic electrons is investigated by the energy loss technique. A direct detection of predissociated triplet states is possible by coincidence measurements between energy loss electrons and Ly α photons.

$$H_2(X\,^1\Sigma_g^+)+e^-(E>14.7\ eV)\rightarrow H_2\ (\text{Triplet})+e^-_{\text{loss}}$$

$$\downarrow\ \text{Prediss.} \qquad \uparrow$$

$$H(2p)+H(1s)$$

$$\downarrow$$

$$\text{Ly}\ \alpha \qquad \text{coincidence}$$

Using selection rules and known data about triplet potential curves, the predominant influence of heterogeneous predissociation is shown. For one state above ionization limit the measured coincidence peak could unambiguously be associated with the predissociation of $k\,^3\pi_u$ $v = 4$.

*Present address: U. of Toronto.

JA-4

Electron Impact Ionization of Rare Gas Dimers and Atoms - H. HELM, K. STEPHAN and T.D. MARK, Inst. f. Atomphysik, Univ. Innsbruck, Austria--An ion source-mass spectrometer combination has been used to measure relative partial single and multiple ionization cross section functions of He, Ne, Ar, Kr and Xe. Single electron impact ionization of Ar_2, ArKr and Kr_2 has also been studied in our electron energy range (< 180 eV). In order to optimize extraction and transmission conditions the total ion current from the source was measured without mass spectrometer and compared with previous studies. Relative partial cross sections were summed up using our measured cross section ratios and calibrated with the total cross section reported by Rapp and Englander-Golden†. Total cross section functions thus obtained agree in shape with those of Rapp and Englander-Golden. No previous data for the ionization cross section of Van der Waals dimers exist.

†D. Rapp and P. Englander-Golden, J. Chem. Phys. 43 (1965) 1464

JA-5

Excitation of $N_2(A^3\Sigma_u^+)$ by Electrons.* D. LEVRON and A. V. PHELPS,† JILA, Univ. of Colo. and NBS.--Rate coefficients for electron excitation of the metastable $N_2(A^3\Sigma_u^+)$ state were determined from lifetimes[1] and densities of the v=0 vibrational state obtained from absolute intensity measurements of 276 nm emission. Experimental rate coefficients vary from 2.6×10^{-19} cm^2 at an electric field to density ratio E/N = 4.7×10^{-16} V cm^2 to 1×10^{-16} cm^2 at E/N = 2×10^{-15} V cm^2. Excitation rate coefficients at low E/N are determined by cross sections for vibrational excitation and are nearly independent of cross sections for electronic excitation.[2] The derived vibrational excitation cross sections are about two times those obtained previously.[3] This value disagrees with the factor of about 1.5 we obtain from analyses of electron transport data.

*Work supported in part by ARPA/ONR.
†Staff Member, Quantum Physics Division, NBS.

1. D. Levron and A. V. Phelps, J. Chem. Phys. (Sept. 1978).
2. D. C. Cartwright, S. Trajmar, A. Chutjian and W. Williams, Phys. Rev. A 16, 1041 (1977).
3. A. G. Engelhardt, A. V. Phelps and C. G. Risk, Phys. Rev. A 135, 1566 (1964).

JA-6

Electron-Impact Dissociation of O_2: Excitation of the OI Quintet States-M. R. GORMAN, E. C. ZIPF, and R. W. MCLAUGHLIN, University of Pittsburgh,--The absolute cross sections for the excitation of the quintet states of atomic oxygen by electron-impact dissociation of O_2 have been measured. The direct cross sections for the specific ns $^5S^o$, np ^5P, and nd $^5D^o$ terms were evaluated from these results by relying on the OI oscillator strengths given by Pradhan and Saraph[1] in order to calculate the cascade contributions. For a given principal quantum number, n, the $^5S^o$, ^5P, and $^5D^o$ terms are found to be excited with equal probability. The total excitation cross section for the OI quintet system has a value of 6.9×10^{-18} cm^2 at 100 eV; this value also applies to the excitation of the metastable OI(3s $^5S^o$) state which is populated for the most part by cascade radiation from the other quintet levels. From an analysis of the variation of the specific cross sections $\sigma_n(^5S^o, ^5P, ^5D^o)$ as a function of n, we have determined the total cross section for the excitation of the high-lying OI quintet Rydberg states ($n \geq 10$) produced by electron impact dissociation of O_2. At 100 eV $\sigma_R = 1.9 \times 10^{-21}$ cm^2.

[1]A. K. Pradhan and H. E. Saraph, J. Phys. B: Molec Phys. 10, 3365 (1977).

JA-7

Metastable Fragmentation of NH_3 Induced by Electron Bombardment-B. L. CARNAHAN and E. C. ZIPF, University of Pittsburgh.--The production of metastable fragments resulting from electron impact on ammonia has been investigated in a series of time-of-flight and excitation function measurements spanning the bombardment energy range from threshold to 200 eV. The observed time-of-flight spectra were dominated by the detection of excited atomic hydrogen in the 2s state and in long-lived Rydberg levels. Over the range of incident energies investigated, four separate processes were identified as sources leading to the production of H(2s) atoms, while the hydrogen Rydberg signal was found to proceed through at least three distinct dissociation paths. The results to be presented will include a summary of the threshold energies which were measured for these various processes and a set spectra for both the 2s and Rydberg fragments which trace the development of their respective kinetic energy spectra with increasing electron energy.

JA-8

Photoabsorption Spectrum of CF_3I by Electron Impact* - S.K. SRIVASTAVA and S. TRAJMAR, Jet Propulsion Lab., and N.W. WINTER, Lawrence Livermore Lab.--Photo absorption spectrum of CF_3I in the wavelength region between 653Å and 3757Å has been generated by utilizing electrons as pseudo photons (high energy and low angle scattering). In the present experiment, electrons of 100, 150, and 200 eV impact energies were scattered by a CF_3I beam at scattering angles of 0, 5, and 10 degrees. The energy loss spectra between 3.3 and 19 eV were recorded. From these spectra, it was concluded that the energy loss spectrum at 200 eV impact energy and 0° scattering angle could be converted to represent the photoabsorption spectrum of CF_3I with a fair accuracy. The spectrum of CF_3I was known only up to about 1100Å. In the present work it has been extended to 653Å. Three new spectral features have been found which represent hetherto unknown electronic transitions. These and the previously known features will be interpreted with the help of Hartree-Fock self consistent field (HCF) calculations and the improved virtual orbital method.

*Supported by the National Aeronautics and Space Administration under Contract NO. NAS7-100 to the Jet Propulsion Laboratory.

JA-9

A Study of Excited Fragment Emission from the Electron Impact Dissociation of Volatile Mercury (II) Halides - J. ALLISON and R. N. ZARE, Stanford U.--Emission resulting from collision of 5-200eV electrons with gaseous HgX_2 and CH_3HgX (X=Cℓ,Br,I) in the 3800-5500 Å region was characterized. Absolute cross-sections for formation of HgX B-X emission as a function of electron energy were determined. The formation of electronically excited mercury atoms in these systems and cross-section trends are discussed in terms of a simple charge transfer model.

SESSION JB

8:30 A.M. – 10:15 A.M., Thursday, October 19

Georgian Room

RARE GAS EXCIMERS AND GROUP VI LASERS

Chairperson: H.T. Powell,
Lawrence Livermore Laboratory

JB-1

Time Resolved Spectroscopy of Krypton and Xenon Excimers Excited by Synchrotron Radiation.* T.D. BONIFIELD, F.H.K. RAMBOW, G.K. WALTERS, Rice University, M. V. McCUSKER, D.C. LORENTS, Molecular Physics Laboratory, SRI International, and R. A. GUTCHECK, Stanford Synchrotron Radiation Lab. Time dependences of the lowest 0_u^+ and 1_u states of Kr_2 and Xe_2 were taken following excitation using monochromatized synchrotron radiation from SPEAR. Pure gases and mixtures with argon were studied from 100 to 10,000 torr. Direct excitation into the molecular wells was possible as well as excitation of selected atomic states. The measured lifetimes, molecular formation rates, and rates for vibrational relaxation and collisional mixing of the 0_u^+ and 1_u states will be reported. Results for xenon generally agree with those obtained with low level e-beam excitation. For krypton, however, it is found that excitation in the $^1P_1$ level is not relaxed to the 1_u state within the 1_u lifetime, for pressures below 5,000 torr, accounting for the peculiar pressure dependence of the $Kr_2(1_u)$ decay in experiments employing e-beams.

*Supported by Office of Basic Energy Sciences, DOE.

JB-2

Fluorescence Studies of Kr_2^* at 1457 Å.* - M.J.W. BONESS and C. DUZY, Avco-Everett Res. Lab., Inc. -- Experimental and theoretical fluorescence studies of the krypton excimer system at 1457 Å pumped by a high energy E-beam are reported. A 450 kV electron beam with a foil aperture of 4x100 cm^2, current capability of 1-20 amps/cm^2 and pulse length of 1.5 μsec has been employed to pump pure krypton contained in a clean stainless steel cavity at pressures from 1-10 atms. Measurements of the temporal behavior and the absolute efficiency of the fluorescence have been performed. These results are compared with the predictions of a comprehensive computer code which has been developed to model the system. This code contains both heavy particle and electron kinetics and can be used to model either fluorescence or lasing.

*Work supported by Department of Energy.

JB-3

Kr_2^* Fluorescence Studies for Low Current, Long Pulse Electron-Beam Pumping.* D.J. ECKSTROM, H.H. NAKANO and D.C. LORENTS, SRI International, and J.A. BETTS, TRW, Inc.--Absolute fluorescence intensity measurements as a function of absolute electron-beam pump rate have been made for Kr pressures up to 4 atm and electron beam currents up to 30 A/cm^2 for $\sim$ 1 μsec pulses. Fluorescence yields of 100% were measured for higher pressures. However, electron interactions severely modify the fluorescence behavior at low pressures, resulting in suppression of peak intensities and lengthening of the afterglow. The fluorescence intensity increases after termination of the electron beam in certain cases. The local fluorescence intensity is reduced more than the integrated fluorescence intensity for a given condition. Experimental results will be compared with results from a numerical model, and suggested kinetic processes and rates will be discussed.

*Supported by the Department of Energy, Division of Laser Fusion.

JB-4

Electron Density Measurements in Kr Pumped by a Low Current, Long Pulse E-Beam.* T. ROTHEM, H.H. NAKANO, D.C. LORENTS, and D.J. ECKSTROM, SRI International, and J.A. BETTS, TRW, Inc.--A cw CO_2 laser has been used to measure electron density histories in e-beam-pumped Kr plasmas by the inverse bremsstrahlung technique. Kr pressures were $\leq$ 3 atm, electron beam currents were $\leq$ 20 A/cm^2, the beam pulse lengths were $\sim$ 1 μsec, and the excitation path length was 100 cm. Absorption coefficients ranged up to several percent per cm. The highest absorptions were observed at the lowest pressures, suggesting that higher electron temperatures exist under those conditions. High T_e would reduce the electron-ion recombination rate and increase the bremsstrahlung absorption cross section. Comparison of the measurements with the results of computer modeling studies will be presented.

*Supported by the Department of Energy, Division of Laser Fusion.

JB-5

Kinetic Processes in Selenium Atom Lasers-M.J. SHAW, Rutherford Laboratory, UK--Lasers operating on the forbidden transitions $^1S \rightarrow {}^1D$, $^1S \rightarrow {}^3P$ in atomic selenium seem good candidates for high energy storage with applications to laser fusion[1]. Excited selenium atoms are produced by photolysis of carbonyl selenide at wavelengths less than 200 nm $OCSE + h\nu \rightarrow Se(^1S) + CO$. Photolysis by ArF laser at 193 nm has a number of advantages over Xe_2^* photolysis at 172 nm in that photoionization of $Se(^1S)$ is excluded and vacuum UV conditions and materials may be avoided. Measurements of the yields of various selenium atom states resulting from ArF laser photolysis and their effects on the kinetics of the system will be described. Ways of increasing the yield of ^1S atoms will be discussed together with measurements of two-photon ionization processes in the donor molecule.

[1] J.R. Murray and C.K. Rhodes, J Appl. Phys. 4, 5041 (1976)

JB-6

Sulfur $^1S_0 - {}^1D_2$ Laser By OCS Photodissociation
H. T. POWELL, D. PROSNITZ, and B. R. SCHLEICHER, Lawrence Livermore Laboratory* - Laser oscillation was previously reported[1] for the forbidden $^1S_0 - {}^1D_2$ and $^1S_0 - {}^3P_1$ lines of selenium using 172 nm photodissociation of OCSe. Strong lasing has now been obtained for the 772.5 nm, $^1S_0 - {}^1D_2$ line of sulfur by photodissociation of OCS at 146 nm using Kr_2^* radiation. The buffer gas has been optimized to minimize ^1S atom deactivation by photoelectrons[2] employing moleculer buffers which provide both electron cooling and electron attachment. The $S(^1S)$ decay time is longer that 10^{-6}s for excited concentrations greater than 10^{16} cm^{-3}. An output energy of 9 mJ was obtained from a 6.5 cm^3 laser volume to be compared with 80 mJ possible by extracting one 772.5 nm photon for each OCS molecule in that volume.

*Supported by US ERDA Contract E (11-1)-2176

[1] H. T. Powell and J. J. Ewing, Appl. Phys. Letters 33, 165 (1978)
[2] H. T. Powell and A. U. Hazi, to be published Chem. Phys. Letters.

JB-7

Electron Energy Distributions in Photolytically Pumped Lasers-R.D. FRANKLIN, W.L. MORGAN, and R.A. HAAS, Lawrence Livermore Laboratory.*--Photolysis of OCS or OCSe by Kr_2^* or Xe_2^* vuv excimer radiation produces S or Se atoms in the (^1S) electronic state. Photoionization of these (^1S) atoms by the excimer radiation produces electrons which can be rapidly heated by superelastic collisions with (^1S) atoms. Electron multiplication by impact ionization is greatly enhanced by this heating. Catastrophic loss of the (^1S) states has been observed[1] in these systems and has been attributed to electron multiplication and the resulting superelastic quenching. The Boltzmann energy equation has been solved for mixtures of S and Se (^1S) atoms with CO and Xe added as buffer gases. The calculations show that highly non-Boltzmann electron energy distributions can result from superelastic electron heating, and cooling by inelastic excitation of CO vibrational levels and Xe electronic states. The impact of these distributions on media kinetics has been assessed.

*Work performed under the auspices of the U.S. Department of Energy by the Lawrence Livermore Laboratory under contract number W-7405-ENG-48.

[1]Powell, H. and Hazi, A., to be published, Chem.Phys.Lett.

SESSION KA

10:30 A.M. – 11:25 A.M., Thursday, October 19

Embassy Room

BREAKDOWN*

*This session is dedicated to the memory of Leonard B. Loeb.

Chairperson: L.H. Fisher,
California State University at Haywood

KA-1

Theory of Low Pressure Spark Buildup.* EUGENE J. LAUER, DAVID M. COX, SIMON S. YU, LLL--The low Pd branch of the Paschen curve for spark breakdown is numerically modeled with a one-dimensional code (x, t). The vacuum E-field is assumed, and the frictionless runaway condition is used for particles. The model includes charge exchange between energetic ions and gas molecules, gas ionization by electrons, ions and neutrals, secondary electron emission from the cathode due to impact of ions and neutrals, and back scattering of electrons from the anode. The predicted threshold sparking parameters for H_2 gas agree with published measurements.

Work Jointly Supported by U.S. DOE under contract No. W-7405-Eng-48 and Department of the Navy under contract No. N00014-78-F0012.

KA-2

Ultraviolet Laser Induced Gas Breakdown. ROBERT R. BUTCHER and SHYAM H. GURBAXANI, Los Alamos Graduate Center*--Experiments[1] reported here are designed to extend laser induced gas breakdown data to shorter wave lengths than have previously been reported. Energy outputs of greater than 250 mJ/pulse have been measured at 248nm with KrF and 120 mJ/pulse at 193nm with ArF. Preliminary results indicate the threshold for air breakdown to be approximately 10^{10} watts/cm^2 at 248nm, with work presently being pursued at 193nm. Results are in general agreement with some aspects of energy transfer mechanisms previously reported.[2]

*Operated by U of NM under U of Calif. contract.

[1] Shyam H. Gurbaxani and R. R. Butcher, to be published.

[2] Shyam H. Gurbaxani, Bull.Am.Phys.Soc., 18,465 (1973).

KA-3

2-D Breakdown Isolators for Laser-Fusion Lasers - R.J. BJURSTROM and C.J. ELLIOTT, Los Alamos Scientific Laboratory*--Optical breakdown which naturally occurs within large CO_2 laser-fusion lasers had been found to provide protection against retropulse damage of the power amplifier thereby obviating the need for expensive Faraday-rotator technology. This phenomena occurs near mirror surfaces where the retropulse turns back on itself and traces out a region which partially overlaps that traced out by the incident pulse. This partial beam overlap has been described by a 2-D propagation code DAMCO which includes inverse-bremsstrahlung absorption, electron generation (computed on the basis of Boltzman codes), pulse propagation, and recombination on an (x,z,t) grid. Results are given for evaluation of the design used in Antares, the LASL 100 KJ laser system, and the difficulties of using this mechanism for wavelengths shorter than 10μ are described.

*Work performed under the auspices of the United States Department of Energy.

KA-4

The Radial Distribution of Space Charge Within a Filamentary Discharge Channel. E. MARODE*, D. HILHORST†, I. GALLIMBERTI** and B. GALLIMBERTI**, *Lab. Phys. Déch. CNRS-ESE Gif/Yvette France, †Mathemat. Centrum, 2°Boerhaaverstraat 49 Amsterdam, Holland, **Instituto di Elettrotecnica-University di Padova Italia--The formation of a discharge in free space leads often to the build-up of a weakly ionized plasma channel; evidence of a longitudinal field arises from the current and potential measurements. On the other hand the equipotential behavior of a plasma should prevent the existence of a large field in it. It has been therefore necessary to analyze how the space charge, defining the longitudinal field, is distributed within a cylinder of ionized and positively charged gas. The steady state distribution of a cloud of electrons within a gaussian shaped cloud of positive ions at rest was studied under the assumption that no radial current flows out of the cylinder. The mathematical analysis[1], together with the numerical solution of the problem leads to the conclusion that a purely positive charge appears around a quasi-neutral plasma forming the discharge core, the transition layer being of the order of the debye screening length.

[1]O.Diekmann, D.Hilhorst and L.A. Peletier-Mathemat. Cent. Tw 1 74/78. Amsterdam.

KA-5

Criteria for Maintenance of Spatial Homogeneity during the Formative Phase of a Pulsed Avalanche Discharge.* S. C. LIN and J. I. LEVATTER, Univ. of Cal., San Diego--The effects of finite voltage rise time on charge redistribution near the cathode during the formative phase of an otherwise homogeneously preionized, large-volume, pulsed avalanche discharge are examined. Approximate formulae are derived for calculating the rate of growth of the electron-deficient cathode layer and for determination of the critical track length corresponding to development of strong local space-charge fields around primary electron avalanche patches which may lead to secondary avalanche processes and subsequent streamer formation. Criteria are then proposed for establishing certain relationships between the voltage rise time and the initial plasma conditions which may eliminate the possibility of streamer formation throughout the formative phase of the discharge.

*Supported by the Defense Advanced Research Projects Agency (DARPA), Contract N00014-76-C-0116.

SESSION KB

10:30 A.M. – 11:25 A.M., Thursday, October 19

Georgian Room

NOVEL LASER PUMPING TECHNIQUES

Chairperson: C.B. Collins,
University of Texas at Dallas

KB-1

The Atomic Fluorine Laser using a Hollow Cathode Discharge, J.K. CRANE and J.T. VERDEYEN, Gaseous Electronics Laboratory U. of Illinois*--It is possible to obtain uniform, stable, long pulse excitation ($\geq$ 100 μsec) in gas mixtures involving highly electronegative constituents (SF_6, $CC\ell_4$, NF_3, I_2). Such a system was used to investigate the atomic Fluorine laser. In the hollow cathode, lasing on Fluorine transitions in the doublet system lasted for up to 80 μs with no signs of the self-termination as reported previously in positive column devices. The excitation process of the laser appears to depend heavily upon the Fluorine donor utilized. For instance, a single step process is involved when NF_3 is used whereas a two step process is evident for SF_6. The details will be discussed.

*Supported by NASA Contract NGR-14-005-200

KB-2

CO_2 Laser-Produced Plasma-Initiated Recombination Laser Studies in Ar, Cl, Kr, N, and Xe - W. T. Silfvast, L. H. Szeto, and O. R. Wood, II, Bell Tel. Labs. --This paper describes the results of a detailed study of a number of CO_2 laser-produced plasma-initiated recombination lasers in which initially ionized plasmas rapidly expand and cool resulting in high recombination rates and population inversions in the neutral species. Nine near-infrared, neutral-gas lasers, with wavelengths between 1.27 - 3.65 μm have now been produced by such a process. In addition, by incorporating a periodic spatial variation in the 10.6 μm pumping radiation, small-signal gains exceeding 55%/cm at 2.03 μm in xenon have been achieved. These results strongly suggest that powerful and efficient near infrared lasers can be developed using this technique. Although the population inversions described in this paper were achieved in the near infrared, scaling of the same physical processes to higher ionization stages should be possible. This eventuality would have important implications for the development of short-wavelength lasers.

KB-3

Electron Collisional Laser in Pb^+ Populated by Recombination - W. T. SILFVAST, L. H. SZETO, and O. R. WOOD II, Bell Laboratories--Laser oscillation has been achieved on two transitions in highly excited Pb^+ where the inversion is shown to be established via electron thermalization within two "bands" of levels. As the electrons cool in the afterglow of a pulsed discharge, the population distributions within these bands are shown to shift to the lower lying levels of each band producing a quasi-steady-state[1] inversion. The inversions in Pb^+ occur in the infrared at wavelengths of 1.16μm ($6f\,^2F_{5/2} - 7d\,^2D_{3/2}$) and 1.32μm ($6f\,^2F_{7/2} - 7d\,^2D_{5/2}$). However, for ions of much higher ionization potential (i.e., highly stripped ions) a similar inversion would occur in the vacuum uv or soft x-ray region.

[1] D. R. Bates, A. E. Kingston and R. W. P. McWhirter, Proc. R. Soc. A267, 297 (1962).

KB-4

The Production of Excited Metal Atoms by Fragmentation of Metal Carbonyls and Other Metal-Encapsulated Compounds - J. ALLISON, Z. KARNY, R. NAAMAN and R. N. ZARE, Stanford U.--The luminescence from excited metal atoms in the 3300-6500 Å region from excitation of a number of metal-containing compounds was characterized. Excitation was performed by a number of methods including electron impact, multiphoton fragmentation using ArF and KrF lasers, and collisions with rare gas metastables. In the case of $Fe(CO)_5$, emission from selected J levels of a number of triplet and quintet states of the metal atom is observed. Some mechanisms are suggested for the formation of these excited atoms.

SESSION LA

1:45 P.M. – 3:30 P.M., Thursday, October 19

Embassy Room

ELECTRODE RELATED DISCHARGE PHENOMENA*

*This session is dedicated to the memory of Leonard B. Loeb.

Chairperson: W.L. Borst,
Southern Illinois University

LA-1

Comparison of Monte Carlo and Boltzmann Calculations of Electron Diffusion to an Anode - G.L. BRAGLIA, Universita Parma, Italy and J.J. LOWKE, University of Sydney, Australia - Calculations have been made of the effect of an absorbing metal anode on a continuous stream of electrons travelling in a gas in a uniform electric field. The absorbing boundary influences the electron energy distribution which becomes a function of position near the boundary. The effective electron drift and diffusion coefficients also become a function of position so that the electron density distribution is no longer given by the solution of the electron continuity equation using the usual equilibrium drift and difussion coefficients appropriate to the applied electric field and gas pressure. Predictions obtained using both Monte Carlo calculations and a solution of the Boltzmann transport equation are in fair though not exact agreement. The calculations for a momentum transfer cross-section proportional to electron speed give an enhancement of the average electron energy of almost a factor of two at the boundary.

LA-2

Negative Oxygen Ions in a Cylindrical Hollow Cathode, R.N. VARNEY, I. KUEN, and F. HOWORKA, Atomphysik, U. of Innsbruck, Austria - The negative-ion density distribution of O^- and O_2^- across the negative glow of a hollow cathode discharge in O_2 shows a sharp maximum near the sheath edge where the ions are trapped in a shallow potential well. Whereas the distribution of O_2^- is nearly independent of the extraction potential of the sampling probe, a second maximum of O^- ion current appears on the axis of the discharge when the potential of the probe exceeds 10 V. This is due to dissociative attachment of slow plasma electrons which are accelerated toward the probe and create O^- ions in the orifice. The dependence of the spatial ion density distribution on discharge current, discharge pressure and probe voltage leads to a better understanding of the discharge in electro-negative gases.

LA-3

Model of the Hollow Cathode Discharge Using a Two-Fluid Theory, B. E. WARNER and K. B. PERSSON*, Univ. of Colorado & NBS/Boulder† - The use of the hollow cathode discharge as a laser medium has increased interest in understanding the mechanisms in this discharge. A one-dimensional, two-fluid approach to modelling the discharge is presented. Special attention is focused on the ionization source and the description of the electron distribution function. The resulting set of non-linear, coupled differential equations pose problems in numerical solution due to a region of instability. Application of the plasma approximation avoids the numerical instabilities and permits integration to stable regions where the full set of equations are used. The resulting ion and electron density profiles, and potential distributions compare favorably with measurements in a planar hollow cathode.

†Supported by ONR Contract N00014-77-F-0026
*Staff Member, Time and Frequency Division, NBS

LA-4

Power Deposition in the Cathode-Fall and Negative Glow Regions of a Discharge - S.B. HUTCHISON and J.T. VERDEYEN, Gaseous Electronics Laboratory, U. of Illinois*--The cathode fall voltage multiplied by the discharge current represents a minimum power necessary to sustain a discharge. Is this power directly coupled to the ions generated in the cathode dark space or is it primarily transferred to the "beam" electrons which have gained energy comparable to the cathode fall voltage? One is motivated to ask this question, because the answer determines the limiting efficiency of a hollow cathode discharge laser. Two theories are discussed which support contradictory viewpoints but which are otherwise in agreement with known facts about the cathode region. In order to distinguish between these theories, calorimetric probe measurements of the cathode fall and negative glow regions of a planar d.c. discharge in helium have been made in an effort to explore the problem of power deposition in the cathode region. These measurements have yielded quantitative data concerning power deposition as a function of position in such a discharge.

*Supported by DAHC04-75-G-0132.

LA-5

Steady-State Cathode Fall Model with Transverse Gas Flow* - W. H. LONG, JR., Northrop Research and Technology Center, Palos Verdes, CA -- The cathode fall of a glow discharge is characterized by steep gradients in the electric field and particle number densities. Electrons are accelerated through this region so rapidly that they never reach local equilibrium. Ion mobility is limited by charge and momentum transfer, which is also the principal source of gas heating. Transverse flow provides cooling through a turbulent boundary layer. The present model begins with a solution of the Boltzmann equation for electrons in position and velocity space, which is coupled self-consistently with the field equations, the moment equations for positive ions, and the boundary layer equations for the gas, including heat addition. Results confirm the distinct nonequilibrium behavior of electrons in this region and reveal a severe depression of the neutral number density near the cathode surface. The derived current-voltage characteristics indicate that an extended cathode sheath cannot exist in high pressure gas flows, the preferred steady-state solution being an arc.

*Work supported by AFAPL, Contract F33615-77-C-2048.

LA-6

Observations of Density Disturbances in the Cathode Region of Electron-Beam Sustained Discharges - E. MARGALITH and W.H. CHRISTIANSEN, Univ. of Washington* -- A plasma diode e-beam gun is used as an external ionization source in a sustained discharge. Power densities in excess of 200 w/cm^3 were obtained in N_2 at densities from 0.2 to 0.4 amagat for pulse lengths on the order of 200 μsec. Using holographic interferometry, the density in the vicinity of the cathode is observed. In addition to the density disturbance normally associated with the cathode shock, density variations of more than 50% are observed at the cathode vicinity following the initiation of the discharge. A characteristic propagation rate of the disturbance and related gas velocity are examined. The layer thickness reaches 5 mm to 10 mm in 100 μs depending on the discharge conditions and the gas pressure. The velocity varies in the range of 10 to 20 m/s away from the cathode and is found to be related to the ratio of the discharge current to the gas pressure. Enhanced diffusion, which is a result of nonuniform heating at the cathode, is suggested to explain the observed phenomenon. Good agreement is obtained with theoretical calculations when a diffusivity two orders of magnitude larger than the gas kinetics value is introduced.

*Supported by AFOSR Grant 74-2650.

LA-7

TEA CO_2 Laser Performance Using Two Current Excitation Pulses, R. TURNER, and R. A. MURPHY, Applied Physics Laboratory, Johns Hopkins U.*--Two current excitation pulses (< 50 nsec) 0 to 50 msec apart have been used to study the glow to arc transition in a small TEA CO_2 laser. The operating conditions are adjusted to give a uniform discharge in a 10% He-CO_2 mixture at 300 Torr with a 50 msec separation between excitation pulses. For this condition, the effective gas resistance is high ($\approx$ 10 Ω); the inductance is low (a uniform discharge); the velocity of the cathode to anode ionization wave is high (> 10^9 cm/sec); the emission from CO, O, and Al is small and of equal intensity for each current pulse. As the spacing between excitation pulses is reduced to 1 msec the gas resistance drops ($\approx$ 1 Ω); the electron density increases; the inductance decreases (a non-uniform discharge); the ionization wave velocity decreases to 3.5×10^7 cm/sec; the emission from CO, O, and Al due to the second current increases $\approx$ 10 times; the filamentary structure becomes more pronounced and finally a single arc forms. The conditions leading to the arc form within 10 nsec after the excitation and are attributed to cathode heating.

*Supported by U.S. Navy Contract N00024-78-C-5384

SESSION LB

1:45 P.M. – 3:30 P.M., Thursday, October 19

Georgian Room

PHOTON INTERACTIONS

Chairperson: D.L. Albritton,
NOAA

LB-1

Cooling of Resonant Absorbers by Photon Pressure, R. E. DRULLINGER, D. J. WINELAND and F. L. WALLS, National Bureau of Standards, Boulder, CO. -- We report the first observation of radiation pressure cooling of a system of resonant absorbers which are elastically bound to a laboratory fixed apparatus. Ground state Mg^+ ions are stored in an electromagnetic Penning trap where the trapping time is the order of days and the rate of collisions with the neutral background gas is the order of hours. Irradiation of the $^2S_{1/2} \rightarrow {}^2P_{3/2}$ ($M_j = +1/2 \leftrightarrow M_j = +3/2$ or $M_j = -1/2 \leftrightarrow M_j = -3/2$) resonance transition with the output of a frequency doubled, single-mode, dye laser tuned to the low frequency side of the Doppler broadened line profile has produced cooling to a few degrees Kelvin. On this transition where $\tau^{-1} \sim 10^8$, a cooling rate of approximately 100°/sec can be achieved with $1 mW/cm^2$ and a temperature limit of $\sim 10^{-3}K$ is predicted.

LB-2

Coaxial Beams Photofragment Spectroscopy of O_2^{+*} - P.C. COSBY, J.B. OZENNE, and J.T. MOSELEY, Molecular Physics Laboratory, SRI International, and D.L. ALBRITTON, NOAA Aeronomy Laboratory--Photodissociation of O_2^+ has been studied in a coaxial ion beam-single mode laser apparatus in which the photofragment O^+ ions produced with a specified kinetic energy in the center-of-mass frame are collected. Several hundred transitions in the ($b^4\Sigma_g^-, v'=4$, $N'=9$-23) $\leftarrow$ ($a^4\Pi_u, v''=4,5$) bands of $^{16}O_2^+$ and $^{16,18}O_2^+$ were measured with a sub-doppler resolution of 0.003 cm^{-1} and comparable accuracy. Transitions to O_2^+ ($b^4\Sigma_g^-, v'=5$) were also studied. Linewidths of the absorptions, which range from 175 to 2000 MHz, reflect the predissociation lifetime of the $b^4\Sigma_g^-$ state and depend on the vibrational, rotational and fine structure levels of this state, and the isotopic composition of the O_2^+. In addition, high resolution kinetic energy spectra of the O^+ photofragments show marked differences between predissociations resulting from Q-branch transitions ($\Delta J=0$) and those from P or R-branches ($\Delta J = \pm 1$).

*Research supported by NSF and ARO.

LB-3

Two-Photon Photodetachment of C_2^-.* PATRICK L. JONES, ROY D. MEAD and W. C. LINEBERGER,† Dept. of Chem., Univ. of Colo. and JILA, Univ. of Colo. and NBS.--A new band system to the low frequency side of the previously observed $^2\Sigma - ^2\Sigma$ transition of C_2^- has been seen using resonant two-photon photodetachment.[1,2] A mass analyzed beam of C_2^- from a discharge ion source was crossed with the intracavity beam of a cw tunable dye laser. Electrons and neutrals produced by photodetachment were counted as a function of laser frequency with the resultant cross section being highly structured due to the saturated transition to the intermediate bound state of C_2^-. Vibrational frequencies and a characterization of the intermediate state will be presented.

*Supported by the National Science Foundation.
†Camille and Henry Dreyfus Teacher-Scholar.

1. G. Herzberg and A. Lagerquist, Can. J. Phys. 46, 2363 (1968).
2. W. C. Lineberger and T. A. Patterson, Chem. Phys. Lett. 13, 40 (1972).

LB-4

Photodissociation and Photodetachment of Ions in $O_2/CH_4/H_2O$ from 4000 to 8600 Å.* L.C. LEE and G.P. SMITH, Molecular Physics Laboratory, SRI International.--The photodestruction cross sections for O^-, O_2^-, $O_2^- \cdot H_2O$, O_3^-, $O_3^- \cdot H_2O$, O_4^-, OH^-, and OD^- have been measured in the 4000-5400 Å and 6900-8600 Å regions. The ions were produced in a drift tube mass spectrometer and interacted with a dye laser or ion lasers inside the laser cavity. The photodetachment cross sections for O^- and $OH^-(OD^-)$ have sharp onsets at wavelengths near 8480 and 6795 Å, respectively, and at shorter wavelengths their values are nearly constant. The photodestruction cross sections for O_2^-, O_4^-, and $O_2^- \cdot H_2O$ increase monotonically with increasing photon energy. In contrast, the photodestruction cross section for O_3^- shows structure over the wavelength region observed. The processes for creation and photodestruction of the various negative ions will be discussed. Comparison is made with other measurements.

*Supported by Atmospheric Sciences Laboratory, U.S. Army Electronics Command, White Sands Missile Range, NM.

LB-5

Photodissociation Cross Sections of Atmospheric Positive Ions 3500-8600 Å.* G.P. SMITH and L.C. LEE, Molecular Physics Laboratory, SRI International.--Photodissociation cross sections have been measured for many positive atmospheric cluster ions at ion laser and dye laser wavelengths between 3500 and 8600 Å, using a drift tube mass spectrometer. Structureless cross sections were observed for the dimer ions O_4^+, $NONO^+$, N_4^+, and $CO_2CO_2^+$, and for CO_4^+, $O_2^+ \cdot H_2O$, and $O_2^+ \cdot 2H_2O$. The nature of the electronic states involved is discussed. Evidence of a second dissociative state for O_4^+ and for $O_2^+ \cdot H_2O$ in the ultraviolet is presented. Upper limits on the cross sections of $COCO^+$, N_2H^+, $NO^+ \cdot N_2$, $NO^+ \cdot CO_2$, $NO^+ \cdot H_2O$, $NO^+ \cdot 2H_2O$, and $H_3O^+ \cdot nH_2O$, n=0-3 below 1 x 10^{-19} cm^2 were established at many wavelengths.

*Supported by U.S. Army Research Office.

LB-6

Photodestruction of Ions Formed in O_2/SO_2/Ar Gas Mixtures.* R. V. HODGES† and J. A. VANDERHOFF, Ballistic Research Lab.--Measurements of photodestruction cross sections for SO_2^-, $O_2 \cdot SO_2^-$, and $O_2 \cdot SO_2^+$ have been extended to cover the photon energy range 1.6 to 3.5 eV.[1] Cross sections for $SO_2 \cdot SO_2^-$ and $SO_2 \cdot SO_2^+$ have also been determined over this energy range. The cross section for SO_2^- increases smoothly with photon energy from 0.9 to 2.4 x 10^{-18} cm^2. This behavior is consistent with direct photodetachment. $O_2 \cdot SO_2^-$ has a measurable cross section only at photon energies greater than ~ 3 eV. The photodestruction spectra of the remaining ions consist of broad, structureless bands characteristic of transitions to repulsive, excited states.

*Research supported by DNA.

†NRC/BRL Resident Research Associate

[1] J. A. Vanderhoff, Bull. Am. Phys. Soc. 23, 155 (1978).

LB-7

Multiphoton Ionization of Cs-Inert Gas Excimers*
M.A. CHELLEHMALZADEH and C.B. COLLINS, Univ. of Texas at Dallas—In this work a more sensitive, multiphoton technique has been introduced for the study of the electronic transitions of alkali-inert gas excimers. In situ detection of the photoionization resulting from illumination with a tunable dye laser had made possible the detection of absorption in CsAr and CsKr at levels as low as $10^{-4}cm^{-1}$ with S/N=40. Dispersion curves have been interpreted in terms of available potential curves.

*Research supported in part by NSF Grant ENG74-06262 and in part by the Organized Research Fund of the University of Texas.

LB-8

Multiphoton Ionization of Cs_2 Dimers Through Dissociative Molecular States*. J.A. ANDERSON and C.B. COLLINS, Univ. of Texas at Dallas, D. POPESCU, Institute of Physics of Bucharest, I. POPESCU, Univ. of Bucharest, Romania--Hybrid resonances observed in the multiphoton absorption spectrum of cesium and rubidium dimers have contributed to an improved understanding of the interatomic potentials of the heavy alkalis.[1,2] Such resonances generally occur through dimer or excimer states of a collision complex and those reported here have been excited by superimposed beams from two separately tunable dye lasers. The wavelength of one was fixed on an atomic transition resonance while the other was scanned through the visible wavelengths. Four new transitions from $^1\Sigma_g$ and two from $^3\Sigma_u$ states of Cs_2 to states dissociating to $5^2D_{3/2}$ and $5^2D_{5/2}$ were found.

*Conducted as part of the U.S.-Romanian Cooperative Program in Science and Technology, supported by NSF Grant INT76-18982.

1. C.B. Collins, B.W. Johnson, M.Y. Mirza, D. Popescu, and I. Popescu, Phys. Rev. A10, 813 (1974).
2. C.B. Collins, S.M. Curry, B.W. Johnson, M.Y. Mirza, M.A. Chellehmalzadeh, J.A. Anderson, D. Popescu and I. Popescu, Phys. Rev. 14, 1662 (1976).

SESSION MA

8:30 A.M. – 10:30 A.M., Friday, October 20

Embassy Room

ATTACHMENT

Chairperson: A. Herzenberg,
Yale University

MA-1

H^- Negative Ion Beam Direct Extraction from a Hydrogen Multipole Plasma - M. BACAL, A.M. BRUNETEAU, H.J. DOUCET and A.M. MARECHAL, Ecole Polytechnique 91128 Palaiseau Cedex (France).-- Large concentrations of negative ions in hydrogen multipole and diffusion type plasmas have been previously reported[1]. Direct extraction of negative ions from a multipole plasma of 10^{11} cm^{-3} substantiates previous negative ion density measurements effected using electrostatic probes.

[1]M. Bacal, E. Nicolopoulou and H.J. Doucet, Bull. Am. Phys. Soc. 23, 141 (1978).

MA-2

Dissociative Attachment from Vibrationally and Rotationally Excited H_2 by Electron Impact - M. ALLAN and S.F. WONG, Yale U.*--Previous studies of dissociative attachment in excited molecules (e.g. O_2, N_2O, CO_2 ...) are limited to temperature dependences in cross sections.[1] We report here dissociative attachment cross sections in H_2 for different initial vibrational levels v=0-3 and for selected rotational levels J=0-7 for electron energies 2-18 eV. The apparatus used is an electron impact mass spectrometer[2] with changes in ion optics and incorporation of an oven source for excited molecules. In the 3.75 eV resonance region the threshold cross sections for H^-/H_2 show an increase by more than a factor of ten with each increase in vibrational quantum and a three-fold increase from J=0 to J=7. The detailed comparison between experiments and a recent theoretical calculation of Bardsley and Wadehra will be discussed. The experimental findings in the 11-18 eV region and the isotope studies in D_2 will also be presented.

*Supported by US ARO, NSF, and Swiss NSF.
[1]H.S.W. Massey, Negative Ions, Cambridge U. Press (1976)
[2]Stamatovic and Schulz, J. Chem. Phys. 53, 2663 (1970).

MA-3

The Dependence of the Dissociative Attachment on the Vibrational and Rotational State in e-H_2 Collisions, J. M. WADEHRA, and J. N. BARDSLEY, University of Pittsburgh*--The analysis of H^- production in the negative ion sources for injection into controlled thermonuclear devices requires cross sections for dissociative attachment of hot H_2 molecules by electron impact. Resonant scattering theory with semi-empirical parameters is used to provide estimates of these cross sections near threshold for several vibrational-rotational states of H_2. Typical values just above threshold, in cm^2, are 2.8 (-21) for the ground state (v=0, J=0), 8.3 (-20) for (1,0), 1.0 (-18) for (2,0) and 3.5 (-20) for (0,10). The effect of rotational excitation is found to be significant, although not as large as suggested by Chen and Peacher.

*Supported by National Science Foundation and Advanced Research Projects Agency.

MA-4

Measurements of Attachment Coefficients and Ionic Mobilities in NF_3-N_2 Mixtures, V.K. LAKDAWALA and J.L. MORUZZI, Department of Electrical Engineering and Electronics, University of Liverpool, Liverpool, U.K.--Measurements have been made of the attachment coefficient α_a and mobilities of negative ions in NF_3-N_2 mixtures in a pulsed drift tube over the range of $1.0 \leq E/p \leq 15$ V cm $^{-1}$ torr^{-1}. The electrons were released in a pulse of short duration from a rear illuminated palladium coated photocathode and the time dependence of the negative ion current arriving at the collector was used to measure α_a. For better S/N ratio the amplified ion current was recorded in a MCA. Measured values of α_a/p_{NF3} at 20°C varied between 40.0 to 120.0 cm^{-1} per torr and was found to peak at E/p of V cm^{-1} torr^{-1}. At least two distinct ion peaks were observed in the waveform with reduced zero field mobilities of 1.54 and 1.87 cm^2 V^{-1} s^{-1} respectively. The overall accuracy of the measurements is estimated to be better than $\pm$ 10%.

MA-5

Dissociative Attachment Cross Section Measurements in F_2 and NF_3 - P. J. CHANTRY, Westinghouse R&D Center*--An apparatus which permits total ion current measurements and mass identification of the ions has been used to measure the magnitude of the attachment cross section between zero and 10 eV for the title gases. Above 0.25 eV the result in F_2 is in good agreement with the curve calculated by Hall[1], but exceeds it by approximately an order of magnitude at zero electron energy, where the present measurements reveal a sharp peak. The dependence of the attachment rate coefficient $k_a(F_2)$ on electron mean energy $\bar{\varepsilon}$ predicted from the present data agrees acceptably with the measurements of others made above $\bar{\varepsilon} \simeq 0.3$ eV, but disagrees significantly with other lower energy measurements[2]. The cross section in NF_3 is dominated by a single broad peak centered at 1.6 eV which causes $k_a(NF_3)$ to peak at $\bar{\varepsilon} \simeq 2$ eV. The ions F^-, F_2^-, NF_2^- and NF^- are produced with relative peak intensities of approximately 100:3:1.4:0.02.

*Supported in part by ARPA, Contract DASG60-77-C-0023.

1. R. J. Hall, J. Chem. Phys. 68, 1803 (1978).
2. G. D. Sides, T. O. Tiernan and R. J. Hanrahan, J. Chem. Phys. 65, 1966 (1976).

MA-6

Electron Attachment and Ionization Rates, and Electron Drift Velocities in Rare Gas - Halide Gas Mixtures* - S.R. HUNTER, K.J. NYGAARD, S.R. FOLTYN, and H. BROOKS, University of Missouri-Rolla--Electron attachment and ionization coefficients have been measured in gas mixtures containing F_2-Ar, F_2-He, NF_3-Ar and Cl_2-Ar with varying halide concentrations over a wide range of E/N (electric field/gas number density). An argon fluoride laser has been constructed (λ=1930A; pulse width $\simeq$ 20 nsecs.) allowing the above coefficients and the electron swarm drift velocities to be measured, from which the reaction rates for these processes have been obtained.

*Supported in part by ARPA/ONR.

MA-7

Temperature Dependence of the Attachment Reaction Rate in I_2-He Gas Mixtures.* H. BROOKS, S.R. HUNTER, and K.J. NYGAARD, University of Missouri-Rolla.--Electron dissociative attachment reaction rates have been measured in gas mixtures containing I_2 and He in a pulsed Townsend discharge experiment using a kryton fluoride laser as a photo-electron source. The measurements have been made with varying I_2 concentrations from 1% to 10% over a wide E/N range, with gas temperatures between approximately 20°C and 100°C. The variation in the gas temperature allows the importance on the observed attachment reaction rates of varying percentages in the population of the vibrational levels of the I_2 molecule to be observed. This knowledge is of importance in the understanding of the operation of I_2 lasers currently under development.

*Supported in part by ARPA/ONR.

MA-8

Dissociative Attachment Of Electrons To F_2 - C. A. Brau, A. E. Greene, S. D. Rockwood, B. I. Schneider, Los Alamos Scientific Laboratory.*-- Results of a joint theoretical and experimental effort to determine electron dissociative attachment rates and cross sections for F_2 will be reported. Experimentally the rate of dissociative attachment to F_2 in N_2 and Ar has been measured over the electron mean energy range from 0.9 to 4 eV. The rate is about 7×10^{-9} cm^3/s at a mean energy of 1 eV, and decreases like $(\text{mean energy})^{-3/2}$. Theoretically we have taken two approaches. Qualitatively we have examined the electron attachment to F_2 in terms of potential energy curves of F_2 and F_2^- and the compound state model of Bardsley, Herzenberg and Mandl. Quantitatively we have used a computer program which solves the Boltzmann equation to find electron energy distributions and dissociative attachment cross sections. This latter analysis has been applied to our own experimental results and those of other investigators in search for a mutually consistent set of cross sections. We conclude that no such set of cross sections is possible. We will also comment on the sensitivity of electron energy distributions to the fluorine concentration.

*Work performed under the U.S. Department of Energy.

MA-9

Electron Attachment Rate Constant for $C\ell_2$ at Room Temperature and 250°C * M.ROKNI**, J.H.JACOB and J.A.MANGANO, Avco Everett Res. Lab., Inc. -- The electron attachment rate constant for $C\ell_2$ has been measured in mixtures of $N_2/C\ell_2$ and $Ar/C\ell_2$ at room temperature and at 250°C in an electron beam controlled discharge. From these measurements and the use of a numerical solution of the Boltzmann equation we have been able to calibrate the relative electron attachment cross-section of $C\ell_2$ that has been measured by Tam and Wong, and by Kurepa and Belic. The peak value of this cross-section that gives the best fit to our data is 2.2×10^{-16} cm^2 at room temperature.

*Work supported by the Advanced Research Projects Agency and monitored by the Office of Naval Research under contract No. N00014-75-C-0062.

**The Hebrew University of Jerusalem, Israel.

MA-10

Electron Attachment to Chlorofluoromethanes.* D.L. McCORKLE, A.A. CHRISTODOULIDES, and L.G. CHRISTOPHOROU,† University of Tennessee--Electron attachment rates, $\alpha w(E/P_{298})$, for CCl_3F and $CClF_3$ mixed in small concentrations with N_2 and Ar were measured as a function of E/P_{298}, the pressure-reduced electric field, at 298°K. Electron attachment cross sections, $\sigma_a(\varepsilon)$, were deduced as a function of electron energy, ε, for those molecules from the measured $\alpha w(E/P_{298})$, and will be reported. The attachment cross section for CCl_3F showed maxima at 0.22 and 0.75 eV with $\sigma_a(\varepsilon = 0.22$ eV$) = 1.1 \times 10^{-15}$ cm^2 and $\sigma_a(\varepsilon = 0.75$ eV$) = 7.5 \times 10^{-16}$ cm^2. The $\sigma_a(\varepsilon)$ for $CClF_3$ exhibited a pronounced maximum at 1.45 eV with $\sigma_a(\varepsilon = 1.45$ eV$) = 2.4 \times 10^{-18}$ cm^2. The number and positions of negative ion resonances for these halocarbons at subexcitation energies will be compared with literature values on chlorofluoromethanes. These data are of practical interest because of the occurrence of chlorofluoromethanes in the atmosphere.

*Supported by DOE Contract EY-76-S-05-4703.

†Also, Oak Ridge National Laboratory

MA-11

Negative Ions Formed by Electron Impact on Fluorocarbons. I. SAUERS, L.G. CHRISTOPHOROU, and J.G. CARTER, Oak Ridge National Laboratory*--Negative ions resulting from low-energy (0-10 eV) electron impact on 2-C_4F_8, c-C_4F_8, 2-C_4F_6, and c-C_4F_6 have been studied using a time-of-flight mass spectrometer. Observed fragment ions include: $C_4F_7^-$* (∿0.0), $C_4F_6^-$* (∿0.0, 0.7), $C_3F_5^-$* (2.3, 4.2), $C_3F_3^-$ (5.1), $C_2F_3^-$ (5.4), CF_3^- (5.3), and F^- (5.2) from 2-C_4F_8; $C_3F_5^-$ (4.1), $C_2F_3^-$ (4.9, 7.9), CF_3^- (4.8), and F^- (4.8, 6.5, 7.9, 10.2) from c-C_4F_8; $C_3F_3^-$ (1.5, 5.0), CF_3^- (5.9), and F^- (5.3) from 2-C_4F_6; $C_4F_5^-$ (4.8, 7.0), $C_3F_3^-$ (1.9, 4.0, 7.0), and F^- (4.1, 6.0, 6.7, 7.6, 8.3) from c-C_4F_6. Values in parentheses are the energy positions of resonance maxima and the asterisk indicates metastable (>10^{-6} sec) fragments. No cleavage was observed at the multiple bonds. Although at high (∿5 eV) energies negative ion states multiply fragment, only 2-C_4F_8 exhibited fragmentation at ∿0.0 eV. The parent ions 2-$C_4F_8^-$*, c-$C_4F_8^-$*, 2-$C_4F_6^-$* and c-$C_4F_6^-$* form at ∿0.0 eV and are by far the most abundant; their lifetimes against autodetachment were found to be 11, 5, 9, and 6 μsec respectively.

*Operated by Union Carbide Corporation under contract W-7405-eng-26 for the U.S. Department of Energy.

SESSION MB

8:30 A.M. – 10:30 A.M., Friday, October 20

Georgian Room

PLASMA CHEMISTRY AND INFRARED LASERS

Chairperson: J.W. Rich,
Calspan Corporation

MB-1

Analysis of Ozone Generation Processes at Atmospheric Pressure in E-Beam controlled Discharges* - D. PIGACHE, G. FOURNIER, and G. GOUSSET, Office National d'Etudes et de Recherches Aérospatiales, 92320 Châtillon France and M. LECUILLER, CNRS-ESE, 91190 Gif-sur-Yvette, France - - Ozone generation rates greater than dissociation rates (dissociative attachment +8.4 eV dissociative excitation) were previously reported in an E-beam controlled discharge in pure O_2[1]. These measurements are confirmed at atmospheric pressure. In order to explain this discrepancy a 3 body reaction ($O_2 {}^1\Sigma_g^+ + O_2 {}^1\Sigma_g^+ + O_2 {}^3\Sigma_g^- \longrightarrow 2O_3$) was first suggested. However, the time evolution of the ${}^1\Sigma_g^+$ concentration and the dependance of ${}^1\Sigma_g^+$ concentration and ozone generation rate on initial ozone concentration are not entirely explained by this assumption. Accordingly, it is deduced that the excitation processes labelled 4.5 eV and 6 eV should be partly dissociative.

* Submitted by J. Taillet

(1) G. Fournier, R. Lucas, D. Pigache, and M. Lécuiller, Bul. Am. Phys. Soc. 23 (1978), 146.

MB-2

Ozone Production in Fast Pulsed High Voltage Dielectric Barrier Discharges in O_2 - L.A. ROSOCHA, Univ. of Wisconsin,* and W.A. FITZSIMMONS, Nat'l Research Group, Inc, Madison, Wisconsin.-- We have studied dielectric barrier discharges in O_2 produced by 50 to 100 KV, 4 ns rise time, high voltage pulses from flat plate Blumlein circuits. Ozone densities of 10^{14} to 10^{15} per cm^3 per pulse are produced with ½ cm electrode spacing and 2 mm thick glass dielectric barrier for O_2 pressures between 25 and 760 Torr. Our analysis includes the Townsend ionization of the gas coupled to the Blumlein circuit, along with 59 rate equations which describe the kinetics of O_3 production. The measured growth rate and absolute yield of O_3 as functions of O_2 density, charge voltage, and other electrical parameters are in excellent agreement with the calculations. Our results indicate the most efficient production of Ozone occurs when E/P is between 50 and 100 V/cm·Torr with an energy cost of about 5 eV/O_3 molecule.

*Supported in part by University of Wisconsin Graduate School.

MB-3

An Experiment to Investigate Plasma Chemistry in E-beam Pumped Closed Cycle CO_2 Lasers - P. BLETZINGER and C. A. DeJOSEPH, Air Force Aero Propulsion Laboratory, Wright-Patterson AFB OH 45433 and Universal Energy Systems, Dayton OH--Many medium and high power flowing gas laser applications would benefit from a closed-cycle gas supply. However the high energy E-beam as well as the discharge may produce gas species which affect laser operation. Several experimental and theoretical investigations have been performed of low pressure CO_2 laser discharges but there is little experimental information on the plasma chemistry effects at the higher pressures used in medium or high power lasers. Of particular interest are the generation rates of the various nitrogen-oxide compounds, known to cause deterioration of the discharge and laser characteristics. We will describe an experiment using a small E-beam and a very high vacuum closed cycle loop designed to minimize the influence of the leak and contamination characteristics of the vacuum system. Diagnostics include electrical probes, on-line and off-line IR spectroscopy and masspectroscopy. Preliminary results indicate that indeed also in an atmospheric CO_2N_2He mixture (1:2:3 pressure ratio) NO_x compounds are generated in the ppm range.

MB-4

Discharge Characteristics in CW CO_2 EDLs - D.L. SMITH, C.M. LEE, T.W. MEYER and P.D. TANNEN, USAF Weapons Lab - An atmospheric pressure electron-beam sustained discharge was used to investigate the performance of CW subsonic CO2 EDLs. Specific energy loading in the 8:7:1:0.3 ($He:N_2:CO_2:O_2$) gas was as high as 210 kJ/lb. Discharge efficiency was improved by reducing the discharge spreading. Different cathode arrangements were very effective in reducing the spreading thus restricting the energy loading to the desired volume. Measurements of small signal gain with a solid cathode sheet showed a maximum gain of 0.45%/cm; a slightly recessed cathode with helium blanket improved the gain to 0.6%/cm with the same energy loading. Current-voltage characteristics of the discharge with electron beam current densities ranging from 50 to 250 $\mu amp/cm^2$ for the various cathode arrangements showed that the higher gains correlated to higher E/N values, $0.9 - 1.1 \times 10^{-16}$ V - cm^2. The impact of the more efficient energy loading is shown in the laser output. Far field beam quality measurements of the square output pattern imply a 1.04 times diffraction limited beam without the use of corrective optics.

MB-5

Transverse Electrodeless Discharge Excitation of a CO_2 Laser, C. P. CHRISTENSEN, Univ. of Southern Calif.*--A pulsed electric discharge between two dielectric sheets is used to excite a CO_2 laser. This type of discharge inherently exhibits good spatial homogeniety since the dielectric functions as a distributed capacitive ballast. Energy deposition into the laser medium is limited by the dielectric constant and breakdown voltage of the dielectric material. However, it is shown that pump energy densities of the order of 100 J/L can be achieved with an appropriate choice of dielectric. A CO_2 laser utilizing this technique has been constructed which operates without preionization at pressures extending to 600 torr. A simple L-C circuit is employed for laser excitation, and barium titanate is used for the discharge dielectric.

*Supported by NSF Grant ENG-77-00123

MB-6

The 16 μm CO_2 Bending Mode Laser. L. H. TAYLOR and R. B. FELDMAN, Westinghouse R&D Center*--A computer model yields a detailed description of the 16 μm ($02^00 \rightarrow 01^10$) CO_2 laser. The electrical excitation of the gas is followed by the collisional transfer of energy from the excited N_2 to the 00^01 level of CO_2. A 9.4 μm optical pulse stimulates the transfer of stored energy from the 00^01 level to the 02^00 level, causing a short-lived population inversion relative to the 01^10 level, with a resultant 16 μm laser pulse. The latter two levels involve only the bending mode of the CO_2 molecule; their populations are therefore very dependent on collisional relaxation processes. The rotational state populations collisionally relax very quickly to the Boltzmann equilibrium values. The effect of the collisional processes on laser performance has been studied as a function of pressure and temperature. For a 1:2:25=CO_2:N_2:He mixture, an optimized output energy of 170 mJ/ℓ (at an efficiency of 0.8%) is predicted at 50 Torr and 200 K. The latter two values yield the best compromise between the desired fast rotational relaxation and slow vibrational relaxation of the bending mode.

*Supported, in part, by US DOE Contract EW-78-C-04-4199.

MB-7

CO Laser Operating on 1st Overtone Infrared Band. R.C. BERGMAN, J.W. RICH, Calspan Corporation*-- During the past year, powerful laser action on the $\Delta V = 2$ vibrational bands of CO has been observed in electric-discharge-excited systems. Both a c.w. supersonic flow laser[1] and a cryogenically cooled, non-flowing pulsed device [2] have recently been reported. The present paper reports additional experiments on the performance and operating characteristics of the supersonic flow system. The dependence of the output power and spectral distribution on discharge parameters, including current, gas mixture, and temperature, has been measured. The laser now operates at approximately 1% electrical efficiency, with power distributed over ten $\Delta V = 2$ band components from 2.7 to 3.1 μm. The present results are compared with the predictions of theoretical models of CO overtone lasers. Means of increasing the efficiency and extending the spectral range are discussed.

*Supported by USAF Avionics Lab. and Calspan I.R.& D.

[1] R.C. Bergman and J.W. Rich, Appl. Phys. Lett. 31, 597 (1977).

[2] V.Danilychev, Paper K 11, 10th International Quantum Electronics Conf., Atlanta, GA, 29 May-1 June 1978.

SESSION NA

10:45 A.M. – 11:55 A.M., Friday, October 20

Embassy Room

ELECTRON SCATTERING

Chairperson: J.N. Bardsley,
Los Alamos Scientific Laboratory

NA-1

Decay of Feshbach Resonances in NO: Electronic and Dynamic Coupling, J. MAZEAU, Université P. et M. Curie, Paris, France - Decay of the first four vibrational levels of long lived NO^- ions has been observed in the vibrational levels of the ground state up to $v = 18$. This decay is well described by the product of a Franck-Condon factor and a bielectronic coupling term which depends on the final energy of the scattered electron. Decay into the Rydberg states is also observed. When the exit channel is the parent state of the resonance, decay occurs through a monoelectronic process and a $\Delta v = 1$ selection rule. The decay intensity increases as $v+1$ of the final state. This decay is forbidden in the Born-Oppenheimer and pure electronic coupling approximation and is interpreted as an interaction between electronic and nuclear motion.

NA-2

Temporary Negative Ion Formation in Alkali Vapors.* A.R. JOHNSTON and P.D. BURROW, University of Nebraska.--An electron transmission experiment[1] has been used to study resonances in the total scattering cross section of Na, Rb, and Cs. In Na a low energy ^3P shape resonance was observed at 0.10±0.03 eV, which is in good agreement with theory.[2,3] In Rb evidence was found for the existence of a shape resonance below 0.05 eV. In each element a progression of Feshbach resonances was observed from energies near the first excited state to the lowest ionization potential. The classification of these resonances will be discussed.

*This work supported by the National Science Foundation.

[1]L. Sanche and G.J. Schulz, Phy. Rev. A 5, 1672 (1972).
[2]D.L. Moores and D.W. Norcross, J. Phys. B 5, 1482 (1972).
[3]A.L. Sinfailam and R.K. Nesbet, Phy. Rev. A 7, 1987 (1973).

NA-3

Inelastic Electron Collisions at Very Low Energies Using a Magnetically Collimated Electron Beam - WING-CHEUNG TAM* and S.F. WONG, Yale U.†--A new type of electron impact spectrometer using an axial magnetic field for electron collimation has been developed. This makes it possible to obtain a uniform incident electron beam and to characterize the analyzer transmission down to near zero energy simultaneously. The capability of this new apparatus for collision studies at very low impact energies (0.1-15 eV) will be demonstrated with energy-loss and constant-residual-energy spectra, as well as energy dependences of vibrational and electronic excitation in N_2, CO,[1] and C_2H_2. Potential applications and limitations of this experimental approach will be discussed.

*Present address: Div. of Phys. NRC, Ottawa, Ont., Canada K1A OR6.

†Supported by US ARO and NSF.

[1]G.J. Schulz, Principles of Laser Plasmas, edited by G. Bekefi (Wiley Interscience, N.Y., 1976) Chap. 2

NA-4

Low Energy Electron Scattering in Methane and Other Saturated Hydrocarbons.* P.D. BURROW, University of Nebraska and J.A. MICHEJDA†, Yale University.--An electron transmission[1] study of methane, ethane, propane, butane and cyclohexane reveals sharp structure in the total scattering cross sections at energies below 1.5 eV. In contrast to unsaturated hydrocarbons in which structure is due to temporary negative ion formation, no appropriate low lying unfilled orbitals are available in these compounds. Energetically, the features appear to be associated with the thresholds for excitation of certain of the vibrational modes. A trapped electron experiment[2] was also carried out and vibrational excitation at these thresholds was observed directly.

*This work supported by PRF.

†Present address, Bell Laboratories, Allentown, PA

[1]L. Sanche and G.J. Schulz, Phys. Rev. A 5, 1672 (1972).
[2]G.J. Schulz, Phys. Rev. 112, 150 (1958).

SESSION NB

10:45 A.M. – 11:55 A.M., Friday, October 20

Georgian Room

REACTIONS OF EXCITED SPECIES

Chairperson: R.E. Drullinger,
NBS Boulder

NB-1

Measurement of the Rate Coefficients for the Bimolecular and Termolecular Charge Transfer Reactions of $He(2^3S)$, $He_2(^3\Sigma_u)$ and Ar_2^+*. C.B. COLLINS and F.W. LEE, Univ. of Texas at Dallas--This work continues[1] the measurement in afterglows of e-beam discharges into high pressure gas mixtures of rate coefficients for energy transfer reactions of inert gas metastables and ions. The bimolecular reactions of 2^3S compared favorably with the NOAA results[2] at low pressures. Termolecular components measured for reactions of 2^3S varied from $\leq 10^{-30}$ for Kr to 15×10^{-30} cm^6sec^{-1} for $CC\ell_3F$. Termolecular rates for reactions of $He_2(^3\Sigma)$ were generally smaller and those for Ar_2^+ were below the limit of detection. Bimolecular rates were found to agree with the NOAA results[3] when available.

*Research supported by NSF Grant ENG 74-06262.

1. F.W. Lee, C.B. Collins and R.A. Waller, J. Chem. Phys., 65, 1605 (1976); F.W. Lee and C.B. Collins, J. Chem. Phys., 65, 5189 (1976); 67 2798 (1977); 68, 1391 (1978).
2. W. Lindinger, A.L. Schmeltekopf, and F.C. Fehsenfeld, J. Chem. Phys. 61, 2890 (1974).
3. D.K. Bohme, N.G. Adams, M. Mosesman, D.B. Dunkin, and E.E. Ferguson, J. Chem. Phys. 52, 5094 (1970).

NB-2

Quenching of Neon Metastable Atoms in Pure Neon Afterglows. R.A. SIERRA* and A.J. CUNNINGHAM, Univ. of Texas at Dallas. -- We report the results of a room temperature study of the quenching of neon metastable atoms in pure neon afterglow plasmas. The experiments were conducted over the pressure range 20 - 400 Torr. using resonance absorption techniques to monitor the temporal evolution of the absolute population density of the $^3P_0$, $^3P_1$, $^3P_2$ and $^1P_1$ lowest excited states. Two and three body rate coefficients for the destruction of the $^3P_0$ and $^3P_2$ states are compared with the values reported by Phelps. New results are reported for the $^1P_1$ state and the role of quenching by electrons discussed.

*Supported by University of Texas at Dallas' organized research funds.

NB-3

Kinetic study of Ar*-CO_2 transfer. Possibility of CO Cameron Laser. J.P. GAUYACQ, F. COLLIER and P. COTTIN - Lab. de Marcoussis (France)† - Dissociation of the CO_2 molecule by collision with metastable argon ($^3P_2$) has been shown a few years ago[1] to almost uniquely lead to the excitation of the first vibrational levels of the metastable $a^3\pi$ state of CO. This efficient energy transfer suggests the possibility of lasing action on the Cameron bands (λ=210 nm, $\tau_{rad} \sim 7$ ms). A kinetic study of Ar-CO_2-N_2 mixtures excited by an e-beam has been undertaken using the $C^3\pi_u - B^3\pi_g$ (λ=337 nm) emission of N_2. Because of its rather long decay time, the CO $a^3\pi$ state flourescence yield is very low; in contrast, the $C^3\pi u$ state of N_2, which is associated with the same kinetics as CO ($a^3\pi$) provides important signals and can thus be used as a tracer of the kinetic chain. Furthermore, using different pressure ratios, it is possible to separately study the decay rates of each kinetic step. The kinetic constants for energy transfer from Ar^+ (or Ar**) and Ar* to CO_2 have been measured. This allows for a detailed investigation of the feasibility of a CO Cameron laser.

†work supported by DRET -

[1]G.W. TAYLOR and S.W. SETSER, Chem. Phys. Let. 8, 51 (1971)

NB-4

Ionization and Energy Pooling in Laser-Excited Na Vapor - G.H. BEARMAN, and J.J. LEVENTHAL, Univ. of Mo.-St. Louis*--Energy transfer and energy conversion processes occurring in laser-excited Na vapor ($\sim 10^{13}$ cm^{-3}) have been investigated using a cw dye laser tuned to one of the D lines, emission spectroscopy and mass analysis. Both Na^+ and Na_2^+ ions were observed as was radiation from high-lying Na states. These experiments eliminate superelastically heated electrons as the source of the ions and excited states as had been suggested.[1] The Na^+ ions probably result from two photon ionization of Na(3p) and/or laser induced Na(3p)-Na(3p) processes; the high-lying radiating states are formed in energy pooling reactions.

*Supported by US DOE Contract EY-76-5-02-2718

[1]S. Geltman, J. Phys. B 10, 3057 (1977).

NB-5

Excitation of $O(^3S)$ Resonance Radiation in Inelastic Collisions Between $O(^5S)$ Metastables and O_2 Molecules.* J. FRICKE, H. K. KIEFL, and W. L. BORST+, University of Würzburg, Germany.--Strong emission of O(1304 Å) resonance radiation was observed according to the reaction

$$O(^5S) + O_2 \longrightarrow O(^3S) + O_2 \longrightarrow O(^3P) + O_2 + h\nu.$$

The cross section for this endothermic process was measured for $O(^5S)$ energies from threshold to 8 eV. It rose steeply from the minimum threshold of 0.36 eV (c.m. system) to a plateau of 3×10^{-17} cm^2 near 3 eV, from where it decreased slightly. The $O(^5S)$ metastables were produced by electron dissociation of O_2, velocity-selected by a time-of-flight technique, and monitored by in-flight radiative decay at 1356 Å. The resulting $O(^3S)$ atoms were detected by 1304 Å resonance radiation. A gas filter technique, uv-transmitting filters, and single photon counting were used to monitor the uv-photons. The possible experimental errors were carefully assessed. In contrast to O_2, the use of N_2 as a target gas did not result in any significant uv-production. The present results are applicable to auroral processes.

*Supported, in part, by Deutsche Forschungsgemeinschaft.
+On leave from Southern Illinois University, Carbondale.

NB-6

The Effect of Spin-Orbit Coupling on Quenching of $O(^1D)$ by Rare-Gas Atoms. J. S. COHEN, W. R. WADT, and P. J. HAY, Los Alamos Scientific Lab.*--Thermal-energy rate constants for the quenching reaction,

$$O(^1D_2) + Rg \rightarrow \begin{cases} O(^3P_2) + Rg \\ O(^3P_0) + Rg \end{cases}$$

with Rg = Ar, Kr, and Xe, have been determined. The inelastic transitions are mainly due to the spin-orbit couplings of the $^1\Sigma^+(^1D)$, $^3\Sigma^-(^3P)$, and $^3\Pi(^3P)$ states of RgO. Calculations reported earlier showed the necessity of a careful treatment of the spin-orbit operator. We have now evaluated the matrix elements using accurate CI wave functions with the approximate operator

$$V_{SO} = \frac{1}{2}\alpha^2 \sum_{i_k,k} (Z_k^{eff}/r_{i_k k}^3)\, \vec{\ell}_{i_k k} \cdot \vec{s}_{i_k}$$

where k = Rg or O, i_k = electrons of k, and Z_k^{eff} is chosen to reproduce the splittings of $^1Rg^+(p^5)$ or $O(p^4)$. Charge-transfer character in the $^1\Sigma^+(^1D)$ state has been found to increase the effective coupling by factors of ~ 4 and ~ 8 for Kr and Xe respectively.

*Work performed under the auspices of the U.S.DOE.

NB-7

Analysis of the $N_2(C^3\Pi_u)$ Excitation by $Ar(^3P_2)$ and $Ar(^3P_0)$ Metastable Atoms. T.D. NGUYEN and N. SADEGHI, Laboratoire de Spectrométrie Physique-U.S.M.G. 38041-GRENOBLE, France. -The energy transfer reaction between $Ar(^3P_2$ and $^3P_0)$ metastable atoms and $N_2(X^1\Sigma_g^+)$ molecule was studied in the afterglow of a pulsed low pressure argon-N_2 ($1-10^{-3}$) discharge[1]. To determine the specific contribution of each argon metastable species for the production of the $N_2(C^3\Pi_u, v', N')$ a cw tunable dye laser was used to selectively depopulate one of the metastable levels by optical pumping technique[1]. Analysis of the nitrogen $2^+(C^3\Pi_u - B^3\Pi_g)$ emission spectrums resulting from the excitation by either metastable atoms show that the initial population of the rotational and vibrational levels of the $N_2(C^3\Pi_u)$ state depends on the argon metastable species. The high resolution (R = 300000) spectrum of the $2^+(0-0)$ band shows a diminution of the emission line width with increasing rotational quantum number. By simultaneous measurement of the argon metastables density we have also determined the relative reaction rates in rotational and vibrational excitation of $N_2(C^3\Pi_u)$ by both argon metastable atoms.

1. N. SADEGHI and T.D. NGUYEN, J. Phys. Lett. (Paris) 38 L 283 (1977).

INDEX TO ABSTRACTS

Albritton, D.L. GA3, GA6, GA7, LB2

Alge, E. GA1

Alger, S.R. FB2

Allan, M. MA2

Allison, J. JA9, KB4

Anderson, J.A. LB8

Bacal, M. MA1

Bailey, W.F. FB5

Baille, P. HB7

Bardsley, J.N. HA4, I, MA3

Bearman, G.H. NB4

Beaton, M.S. AB1

Benedict, R.P. AA6

Benenson, D.M. CB7, DB2, FA2

Bergman, R.C. MB7

Bergman, R.S. BB6

Betts, J.A. JB3, JB4

Bhansali, C.K. CB7

Biondi, M.A. GA5, HA2, HA3, I

Bischel, W.K. E3

Bjurstrom, R.J. KA3

Bletzinger, P. MA3

Bohme, D.K. GA8

Bokor, J. E3

Boness, M.J.W. JB2

Bonifield, T.D. JB1

Boody, F.P. BA7, BA8

Borst, W.L. NB5

Bose, N. JA3

Boulmer, J. HB8

Brau, C.A. MA8

Braglia, G.L. LA1

Brooks, H. MA6, MA7

Brown, T.J. GA3

Bruneteau, A.M. MA1

Bullis, R.H. CA2

Burrow, P.D. NA2, NA4

Butcher, R.R. KA2

Carnahan, B.L. JA7

Carter, J.G. MA11

Center, R.E. AA9, CA6

Chandra, R. HB3

Chang, J.S. HB7, I-1

Champagne, L.F. BA3, BA4

Chantry, P.J. DA8, MA5

Chellehmalzadeh, M.A. LB7

Chen, A.K. GA5

Chen, C.H. CA8

Chien, Y.K. DB2

Christensen, C.P. MB5

Christiansen, W.H. LA6

Christodoulides, A.A. MA10

Christophorou, L.G. MA10, MA11

Clark, K.E. HB6

Cohen, J.S. HA4, NB6

Collier, F. NB3

Collins, C.B. LB7, LB8, NB1

Cosby, P.C. LB2

Cottin, P. NB3

Cox, D.M. KA1

Crane, J.K. KB1

Crompton, W. FA2

Cunningham, A.J. NB2, I

Davis, H.T. FB4

DeJoseph, C.A. MB3

Delpech, J.F. HB8

Denes, L.J. DA8, DA9, DA10

deRuyter, J. HB1

Dicks, J.B. AB1

Dollinger, R.E. FA1, FA2, FA3, FA6

Dotan, I. GA7

Doucet, H.J. MA1

Drouet, M.G. DB5, FA4, FA5

Drullinger, R.E. LB1

Drummond, D.L. AA6, AA7

Dunn, G.H. I

Duzy, C. CA7, DA1, JB2

Dvore, D.S. AB2

Eckhardt, G. FA7

Eckstrom, D.J. JB3, JB4

Eddy, T.L. BB5

Eden, J.G. AA2

Elford, M.T. FB3

Elgin, J.B. AB2

Elliott, C.J. KA3

Faist, M.B. AB2

Fang, T.-M. AB4

Feeney, R.K. JA1

Fehsenfeld, F.C. GA3, GA6, GA7

Feld, M.S. DA2

Feldman, R.B. MB6

Fentress, M.L. BB5

Finn, T.G. BA4

Fisher, C.H. CA6

Fitzsimmons, W.A. MB2

Foltyn, S.R. MA6

Fontaine, B. CA4

Forestier, B. CA4

Fournier, G. MB1

Franklin, R.D. JB7

Fricke, J. NB5

Frind, G. CB4

Frost, L.S. CB2

Fulghum, S.F. DA2

Gallagher, A. AA8, JA2

Gallimberti, B. KA4

Gallimberti, I. KA4

Garscadden, A. FB5

Gauyacq, J.P. NB3

Gillmour, A.S. FA3, FA6

Gist, T.E. FB8

Goldman, M. FA4

Gorman, M.R. JA6

Gousset, G. MB1

Greene, A.E. MA8

Grossl, M. GA2

Gurbaxani, S.H. KA2

Gutcheck, R.A. JB1

Haas, R.A. JB7

Hamil, R.A. AA6, AA7

Harris, L.P. FA8

Hatziprokopiou, M. HB4

Haug, R. FA4

Hay, P.J. NB6

Helm, H. GA2, JA4

Herman, I.P. DA2

Hilhorst, D. KA4

Hill, R.M. AA3

Hobbs, R.H. CA3

Hobson, R.M. HB7, I-1

Hodges, R.V. LB6

Hopper, D.G. HA5

Howorka, F. GA4, LA2

Hoye, J.B. I-1

Hron, F. BB4

Hsia, J.C. DA4, DA5, DA6

Huestis, D.L. DA3, E2

Hui, A.K. HB2

Hunter, R.O., Jr. DA3

Hunter, S.R. MA6, MA7

Hutchison, S.B. LA4

Ingold, J.H. BB6

Jacob, J.H. CA5, DA4, DA5, DA6, FB6, MA9

Jahn, R.G. HB6

Javan, A. DA2

Johnsen, R. GA5, HA2, HA3

Johnson, P.D. BB1

Johnston, A.R. NA2

Jones, G.R. CB1

Jones, P.L. LB3

Judish, J.P. CA8

Jusinski, L.E. AA7

Kadlecek, J.A. HA8

Kakishima, T. GB5

Kando, M. GB5

Karny, Z. KB4

Keijser, R.A.J. GB6

Keskinen, K. HB7

Kiefl, H.K. NB5

Kinsinger, R.E. CB5

Kligler, D.J. E 3

Kleban, P. FB4

Kline, L.E. DA9, DA10

Kolb, C.E. AB2, AB7

Komine, H. AA5

Kovitya, P. DB1

Krebes, E.S. BB4

Kuen, I. GA4, LA2

Lakdawala, V.K. MA4

Lam, L.K. HB5

Langenwalter, M. GA2

Laudenslager, J.B. BA1

Lauer, E.J. KA1

Lecuiller, M. MA1

Lee, A. CB2

Lee, C.H. HB3

Lee, C.M. MB4, I

Lee, F.W. NB1

Lee, J.L. FA2

Lee, L.C. LB4, LB5

Leslie, S.G. DA10

Levatter, J.I. DA11, KA5

Leventhal, J.J. HA1, NB4

Levron, D. JA5

Ligthart, F.A.S. GB3, GB6

Lin, S.C. DA11, KA5

Lin, S.L. FB1, FB7

Lindinger, W. GA1, GA6

Lineberger, W.C. LB3

Long, W.H., Jr. LA5

Lorents, D.C. AA3, JB1, JB3, JB4

Lowke, J.J. AB3, DB1, DB4, LA1

MacKay, G.I. GA8

Malone, D.P. FA2, FA3, FA6

Mandl, A. AA1

Mangano, J.A. CA5, DA4, DA5, DA6, FB6, MA9

Manikopoulos, C.N. FA1, HB3, HB4

Marechal, A.M. MA1

Margalith, E. LA6

Mark, T.D. GA2, JA4

Marode, E. KA4

Mason, E.A. FB1, FB7

Martinez-Sanchez, M. AB2

Mazeau, J. NA1

McCorkle, D.L. MA10

McCusker, M.V. AA3, JB1

McGeoch, M.W. AA4

McGowan, W.A. I

McLain, D.K. DB3

McLaughlin, R.W. JA6

Mead, R.D. LB3

Meador, W.E. BA9

Melamed, N.T. DA8

Mercure, H. FA5

Messerle, H.K. AB3

Meyer, T.W. MB4

Michejda, J.A. NA4

Michels, H.H. CA3 , I

Miley, G.H. BA7, BA8

Mitchell, R.R. DA10

Mohnen, V.A. HA8

Moody, S.E. AA9

Morgan, W.L. JB7

Moruzzi, J.L. MA4

Moseley, J.T. LB2

Murphy, R. A. LA7

Myers, G.D. HA1

Naaman, R. KB4

Nadeau, F. DB5

Nagalingam, S.J.S. BA7

Nagamatsu, H.T. CB6

Nakano, H.H. JB3, JB4

Newman, L.A. DA7

Nguyen, T.D. NB7

Nielsen, P.E. FB8

Nighan, W.L. CA1

Nobata, K. GB5

Noeske, H.O. CB3

Novak, J.P. BB4

Nygaard, K.J. MA6, MA7

Ogram, G.L. HB7, I-1

Ozenne, J.B. LB2

Pacala, T.J. BA1

Pack, J.L. DA9

Palumbo, L.J. BA4

Parks, J.H. AA1

Paulson, J.F. HA6

Payne, M.G. CA8

Perry, B.E. AA3

Persson, K.B. LA3

Phelps, A.V. AA8, JA5

Pigache, D. MB1

Popescu, D. LB8

Popescu, I. LB8

Powell, H.T. JB6

Prelas, M.A. BA7, BA8

Prescott, L.E. CB4

Prosnitz, D. JB6

Radpour, F. HB4

Rambow, F.H.K. JB1

Rathge, R.D. AA7

Rautenberg, T.H., Jr. BB1

Rees, J.A. FB2

Rhodes, C.K. E3

Rich, J.W. MB7

Robson, R.E. FB7

Rockwood, S.D. MA8

Rogoff, G.L. GB1, GB4

Rokni, M. CA5, DA4, DA5, DA6, FB6, MA9

Rosenfeld, M. FA1

Rosocha, L.A. MB2

Rothe, D.E. BA2

Rothem, T. JB4

Sadeghi, N. NB7

Saporoschenko, M. GA9, GA10

Sauers, I. MA11

Sayle, W.E., II JA1

Schearer, L.D. HB5

Schiff, H.I. GA8

Schleicher, B.R. JB6

Schlie, L.A. AA6, AA7

Schneider, B.I. MA8

Schwartz, P.R. FA3

Scott, M.H. AB1

Scott, P.B. BA6

Seward, E.D. FB8

Shah, N. HB3

Shaw, D.T. HB3, HB4

Shaw, M.J. JB5

Shui, V.H. CA7, DA1

Shuker, R. AA8

Sierra, R.A. NB2

Silfvast, W.T. KB2, KB3

Simpson, T. B. HB6

Smith, D.L. MB4

Smith, G.C. BB3

Smith, G.P. FA6

Smith, G.P. LB4, LB5

Smits, R.M.M. GB2

Spreadbury, R.J. DA8

Srivastava, B.N. FB6

Srivastava, S.K. JA8

Stamm, M.R. FB5

Stappaerts, E.A. AA5

Stephan, K. JA4

Stokes, A.D. DB1

Stori, H. GA1

Svorec, R.V. BA1

Symolon, P.D. CB6

Sze, R.C. BA5, BA6

Szeto, L.H. KB2, KB3

Tam, W.C. NA3

Tang, K.Y. DA3

Tannen, P.D. MB4

Taylor, L.H. MB6

Taylor, T.S. BB3

Thiagarajan, V. AB5

Tiernan, T.O. HA7

Torr, D.G. I

Trainor, D. W. CA5

Trajmar, S. JA8

Trung, D. AB3

Turner, R. LA7

Vanderhoff, J.A. LB6

Van Noy, J.H. CB4

Varney, R.N. GA1, GA4, LA2

Verdeyen, J.T. KB1, LA4

Viehland, L.A. FB1

Viggiano, A.A. GA7

Vlachos, G. GA8

Von Jaskowsky, W.F. HB6

Vriens, L. HB1

Wadehra, J.M. HA4, MA3

Wadt, W.R. E1, NB6

Walls, F.L. LB1

Walters, G.K. JB1

Wang, S.Y. AB6

Warner, B.E. LA3

Waynant, R.W. AA2

Weaver, W.R. BA9

West, J.B. AA5, BA2

Wiegand, W.J. CA2

Wineland, D.J. LB1

Winter, N.W. JA8

Wong, S.F. MA2, NA3

Wood, O.R., II KB2, KB3

Wormhoudt, J.C. AB7

Wu, R.L.C. HA7

Yao, F.N. FA2

York, T.M. HB6

Yu, S.S. KA1

Zajonc, A. JA2

Zare, R.N. JA9, KB4

Zipf, E.C. IA, JA6, JA7

Zollweg, R.J. BB2, DB3

31st ANNUAL GASEOUS ELECTRONICS CONFERENCE
October 17-20, 1978
Buffalo, New York

PARTICIPANTS

Albritton, Dan, NOAA
Alcock, John, National Research Council of Canada
Allis, William, MIT
Allison, John, Stanford University
Anderson, Jay, University of Illinois
Anderson, John M., General Electric R&D Center
Armstrong, Russell A., AFOSR/NC

Bacal, Marthe, Ecole Polytechnique
Ballik, Edward A., McMaster University
Bardsley, J. Edward, University of Pittsburgh
Barreto, Ernesto, State University of New York at Albany
Beatty, Earl, C., JILA
Benedict, R.P., Air Force Weapons Lab/Ale
Benenson, David M., SUNYAB
Bergman, Richard, Calspan Corporation
Bergman, Rolf, Photolamp Engineering
Betts, Jeanette, TRW
Beverly, Robert E., III, Consulting Physicist
Beyerinck, H.C.W., Eindhoven University
Bhattacharya, Ashok, G.E. Lamp Group
Binns, Bob, McDonnell Douglas Research Laboratory
Biondi, M.A., University of Pittsburgh
Bleekrode, Richard, Philips Research Laboratories
Bletzinger, Peter, USAF/AR Aero
Bokor, Jeffrey, University of Illinois
Boness, John, Avco Everett Research Laboratory
Bonifield, Thomas D., Rice University
Boody, Frederick, P., University of Illinois
Brau, Charles A., Los Alamos Scientific Laboratory
Braverman, Leonard, GTE Sylvania
Brooks, Howard, University of Missouri-Rolla
Browne, T.E., Westinghouse Consultant
Bullis, Robert H., United Technologies Research Center
Burnham, Ralph, Naval Research Laboratory
Burrage, L.M., McGraw Edison Co.
Burrow, Paul, University of Nebraska
Butcher, Robert, Los Alamos Scientific Laboratory

Carnahan, Bryon, University of Pittsburgh
Carroll, James J., General Electric Company
Center, Robert, Mathematical Sciences, N.M.
Champagne, Louis F., Naval Research Laboratory
Chang, Jen-Shih, York University
Chang, Robert S.F., Naval Research Laboratory
Chanin, L.M., University of Minnesota
Chantry, P.J., Westinghouse R&D Center
Chellehmalzadeh, Mohammadali, University of Texas at Dallas
Chen, Aikwo, University of Pittsburgh
Chen, Chung-Hsuan, Oak Ridge National Lab
Cheung, Na-Ho, Cornell University
Chernin, David, Maxwell Laboratories, Inc.
Cherrington, Blake, University of Illinois
Chien, K.R., TRW
Chilukuri, Santaram, Union College
Chou, Mau-Song, Exxon Research and Engineering Co.
Christensen, Paul, University of Southern California
Christiansen, Walter, University of Washington
Cobine, James D., SUNY Albany
Cohen, James, Los Alamos Scientific Laboratory
Collier, F., Laboratories De Marcoussis (DLA), France
Collins, Carl, University of Texas-Dallas
Cool, Terrill, Cornell University
Cosby, Philip C., Molecular Physics Lab
Crane, John K., Lawrence Livermore Laboratory
Cunningham, Austin, University of Texas-Dallas
Czuchlewski, Steve, Los Alamos Scientific Laboratory

De Joseph, Charles A., Jr., University Energy System, Inc.
Delpech, Jean F., University of Paris at ORSAY
Denes, Louis J., Westinghouse R&D Center
De Paola, Brett, Miami University
De Youns, Russell, NASA
Dollinger, Richard E., SUNYAB
Dowell, Jerry T., IRT
Downes, Lawrence W., Miami University
Drullinger, R.D., Times & Frequency Division
Dunn, Gordon, JILA
Duzy, C.L., Avco Everett Research Laboratory
Dvore, David, Aerodyne Research

Eckhardt, Gisela, Hughes Research Laboratory
Eckstrom, D.J., Molecular Physics Laboratory
Eddy, T.L., West Virginia University
Edwards, Kent. R., Science Applications
Ehrlich, D., MIT
Elford, Malcolm T., Australian National University
Elrin, James B., Aerodyne Research
Eliasson, B., Brown Boveri Research Center
Ewing, J.J., University of California

Fang, Ta-Ming, Boston University
Farral, George, General Electric R&D Center
Feeney, Robert K., GA Institute of Technology
Fehsenfeld, Fred, NOAA
Fentress, Michael, West Virginia University
Filcoff, John, USAF Weapons Lab
Finn, Tom, Science Applications
Fisher, Charles, Mathematical Sciences NM
Fisher, Leon, California State University, Haywood
Fisher, Robert, Los Alamos Science Laboratory
Fitzsimmons, William, National Research Group, Inc.
Fontaine, Bernard, Marseille University, France
Fournier, Georges, D.R.E.V.
Franklin, Richard D., A.F. Aero Propulsion Lab
Freund, Robert, S., Bell Labs
Früchtenicht, Joseph, TRW
Frind, Gerhard, General Electric Research & Development Center
Fulghum, Stephen F., MIT

Gallagher, Alan, JILA
Gerardo, James B., Sandia Laboratories
Gerber, R.A., Sandia Laboratories
Goldhar, Julius, Lawrence Livermore Lab
Gorman, Michael R., University of Pittsburgh
Greene, Arthur, Los Alamos Scientific Laboratory

Haas, Roger, Lawrence Livermore Laboratory
Hamil, Roy, Air Force Weapons Lab
Hammond, John, W.J. Schafer Assoc.
Harris, L.P., General Electric R&D Center
Harsahy, Alexandru, Central Institute of Physics, Bucharest/Romania
Harvey, James, Lawrence Livermore Laboratory
Haugsjaa, Paul O., GTE Laboratories, Inc.
Heberlein, Joachim, Westinghouse R&D Center
Helm, Hanspeter, Institute Für Atomphysik, Innsbruck, Austria
Hernquist, Karl, RCA Labs
Herzenberg, Arvid, Yale University
Hill, Robert M., SRI International
Hodges, Ronald V., Ballistic Research Lab
Hoffmann, Peter, DFVLR, FR Germany
Hopper, Darrel, Science Applications Inc.
Hsia, J., Avco Everett Research Laboratory, Inc.
Hudson, David F., NSWC
Huestis, D.L., SRI International
Hughes, David W., Georgia Institute of Technology
Hughes, William, LASL
Hui, Amit K., Vanderbilt University
Hunter, Scott, University of Missouri-Rolla
Hutchison, Sheldon, Gaseous Electronics Lab, University of Illinois
Hyman, Howard, Avco Everett Research Laboratory

Jacob, Jonah H., Avco Everett Research Laboratory, Inc.
Jacobs, Ralph, Lawrence Livermore Laboratory
Janiak, Daniel, Bell Aerospace
Johnsen, Rainer, University of Pittsburgh
Johnston, Alan R., University of Nebraska
Johnson, Peter, General Electric Co. Corp., R & D Center
Johnson, Stephen G., GTE Sylvania
Jones, G. R., University of Liverpool, England
Jones, Patrick L., JILA, University of Colorado
Judd, O., Los Alamos Scientific Laboratory
Junker, Bob R., Office of Naval Research Code 421
Jurenka, Henry, SUNYA
Jusinski, Leonard, Air Force Weapons Laboratory

Kadlecek, John, SUNYA
Karras, Thomas W., General Electric Company
Keeffe, William M., GTE Sylvania
King, Terence, Manchester University
Kinsinger, Richard E., General Electric Company
Kleban, P., University of Maine
Kline, L. E., Westinghouse R & D Center
Kolb, Charles E., Aerodyne Research Inc.
Kovacs, Mark, Avco-Everett Research Laboratory
Krauss, Morris, National Bureau of Standards

Lacour, B., Laboratories De Marcoussis (DLA) France
Lam, Leo, University of Missouri-Rolla
Laudenslager, James, Jet Propulsion Laboratory
Lauer, Eugene J., Lawrence Livermore Laboratory
Lawton, S. A., McDonnell Douglas Corp.
Lee, A., Westinghouse R & D Center
Lee, John, McMaster University
Lee, L. C. Molecular Physics Laboratory
Leslie, Scott G., Westinghouse Research
Levatter, Jeff, University of California
Leventhal, Jacob, University of Missouri - St. Louis
Ligthart, Franciscus, Philips Research Laboratory
Lin, Chun C., University of Wisconsin
Liu, Chi-Sheng, Westinghouse Research Laboratory
Long, William, Northrop Research and Technology Center
Lorents, Donald C., Molecular Physics Laboratory
Lowke, J. J., University of Sydney, Australia

MacKay, Gervase, York University, Canada
Malone, Dennis, SUNYAB
Mandl, A., Avco Everett Research Laboratory
Mani, Siva, W. J. Schafer Assoc., Inc.
Manikopoulos, C. N., SUNYAB
Marcum, Doug, Miami University
Marode, Emmannel, Laboratory Physics Déch. CNRS-ESE, France
Mason, E. A. Brown University

Mason, E.A., Brown University
Mastroianni, Martin, Allied Chemical Corp.
Maya, Jakob, GTE Sylvania
Mazeau, Jean, Universite' Pierriet Marie Curie, France
Meador, Willard E., NASA
Mercure, Hubert, I.R.E.Q.
Michels, Harvey H., United Technologies Research Center
Miley, George H., University of Illinois
Miller, John L., Lawrence Livermore Laboratory
Mitchell, Robert R., Westinghouse R&D Center
Moeny, William M., Tetra Corp.
Moody, Steven, Mathematical Sciences NM
Morton, Richard G., Richland, Washington
Mosburg, Earl R., JILA
Myers, Gary, University of Missouri-St. Louis

McAllister, G.L., Exxon Nuclear R&T Center
McClure, G.W., Sandia Laboratories
McGarvey, John, Cornell University
McGeoch, M. Rutherford Lab
McKee, Terry, Lumonics Research Ltd.
McRae, Tom, Lawrence Livermore Lab

Nagalingam, Samuel, University of Illinois
Nagamatsu, Henry T., General Electric
Newman, Leon, United Technology Research
Nielsen, Philip E., Wright-Patterson AFB
Nighan, William L., United Technologies Research Center
Noeske, Heinz, General Electric
Novak, Jaroslav, IREQ

Ogram, G.L., York University
Olivier, Marc, McMaster University
Opran, Marius, Bucharest-Romania
Oskam, H.J., University of Minnesota
Ottinger, Cathy, University of Illinois

Pack, John L., Westinghouse R&D Center
Palumbo, Louis J., Naval Research Lab
Parsons, Mark, Los Alamos Scientific Laboratory
Perry, Bryce, SRI International
Peterson, J.R., SRI International
Phelps, A.V., University of Colorado
Pigache, Daniel, ONERA, France
Pilloff, H.S., ONR
Pitchford, Leanne, JILA
Pleasance, Lyn D., Lawrence Livermore Laboratory
Pointu, Anne Marie, Universite Paris
Popescu, Niculae , Bucharest-Romania
Powell, Howard, Lawrence Livermore Laboratory
Prelas, Mark, University of Illinois
Prosnutz, Darold, Lawrence Livermore Laboratory

Redmon, Michael J., Battelle Columbus Laboratories
Rees, J.A., University of Liverpool
Rhodes, Charles, University of Illinois
Ricard, Andre, Universite Paris-Sud
Rice, J.K., Sandia Laboratories
Rich, William, Calspan Corporation
Roberts, Victor, General Electric R&D Center
Rogoff, G.L., Westinghouse R&D Center
Rosocha, Louis, National Research Group
Rostenbach, Royal E., National Science Foundation
Rothe, Dietmar, E., Northrup Research & Technology Center
Rothwell, Harold, Jr., GTE Sylvania
Rowe, Irving, Office of Naval Research
Rumble, John, JILA

Sadeghi, Nader, Grenoble, France
Saporoschenko, M., Southern Illinois University
Sauers, Isidor, Oak Ridge Nat'l Lab
Schall, Wolfgang, DFVLP, Fr Germany
Schearer, Laird D., University of Missouri-Rolla
Scheps, Richard, Maxwell Laboratories, Inc.
Schlie, LaVerne A., AFWL
Schuebel, W.K., Avionics Lab
Schumann, Lee, JILA
Scott, Mary, University of Tenn.
Scott, Peter, Los Alamos Scientific Laboratory
Searles, Stu, NRL
Shaw, Michael, Rutherford Laboratory
Shepherd,William B., The Boeing Aerospace Co.
Shortridge, Robert G., Bell Aerospace Textron
Schui, Ven., Avco Everett Research Laboratory
Silfvast, William, Bell Labs
Sirchis, Michael, W.J. Schafer Assoc.
Smith, David L., Kirtland AFB
Smith, Gregory C., Ohio State University
Smits, Robertus M.M., Royal Dutch/Shell Research
Springer, Robert, GE Lamp Group
Srivastava, B.N., Avco Everett Research Laboratory
Srivastava, Santosh K., Jet Propulsion Lab
St. John,Robert, University of Oklahoma
Sze, Robert, Los Alamos Scientific Laboratory

Tachibana, Kunihide, University of Colorado
Tai, Chen-Yu, University of B.C.
Tam, W-C, National Research Council, Canada
Tang, Ken, Maxwell Laboratories, Inc.
Taylor, R.L., Physical Sciences Inc.
Taylor, Tony, Ohio State University
Theuws, P.G.A.,University of Technology, Eindhoven
Thiess, Paul E., The Catholic University of America

Tiernan, Thomas O., Wright State University
Tisone, G.C., Sandia Laboratories
Touzeau, Michel, Miami University
Treanor, Charles, Calspan Corporation
Tregay, G.W., Bell Aerospace Textron
Turner, Charles E., Jr., Lawrence Livermore Laboratory
Turner, Robert, Johns Hopkins University

Varney, Robert, University of Innsbruck
Viehland, Larry, Parks College of St. Louis University
Vlachos, George, York University
Vriens, L., Philips Research, Eindhoven

Wadehra, Jogindra, University of Pittsburgh
Wadt, Williard, Los Alamos Scientific Laboratory
Wang, Shih-Ying, DOE/PETC
Walters, G.K., Rice University
Warner, Bruce E., National Bureau of Standards
Waynant, Ron, Naval Research Laboratory
Weaver, L.A., Westinghouse R&D Center
Weinert, Ulrich, Brown University
Wells, William, Miami University
West, John, Northrop Research & Technology Center
Whitten, Barbara, Miami University
Wiegand, Walter, United Technologies Research Center
Wildman, David, JILA
Winans, J.G., SUNYAB
Witting, H.L., General Electric R&D Center
Wong, Shek-Fu, Yale University
Wormhoudt, J., Aerodyne Research
Wu, Richard L.C., Brehm Lab., Wright State University

Yu, Simon, Lawrence Livermore Laboratory

Zediker, Mark, University of Illinois
Zipf, Edward, University of Pittsburgh
Zollweg, Robert J., Westinghouse R&D Center

Allan, Michael, Yale University
Anderson, Jon, University of Texas at Dallas

Bhansali, C.K., SUNYAB
Bortner, M., General Electric/SSL
Böse, Norbert, University of Toronto
Borst, Walter, Southern Illinois University
Bjurstrom, Richard, Los Alamos Scientific Laboratory

Claeys, Wilfrid, Universite' Louvain-Lu-Neuve
Curns, Paul, Cornell University
Davis, D.K., Westinghouse R&D Center

Falk, Theodore, Calspan Corporation

Gurbaxani, Shyam, University of New Mexico

Kanehiro, Nobata, Shezuoka University
Ku, Robert, Lincoln Laboratory

Lin, S.L., Brown University

Morgan, Lowell, University of California/LLL
McCorkle, Dennis, University of Tennessee
McGowan, J. William, University of Western Ontario

Paulson, John, AFGL
Porter, Richard, Cornell University

Rosenfeld, Mark, SUNYAB
Rothe, Erhard, Wayne State University

Schwabs, William E., UHP International
Shaw, David, SUNYAB
Stamm, Michael, Wright-Patterson AFB
Suhre, Dennis, Westinghouse R&D Center

Taylor, Lyle, Westinghouse R&D Center
Trainor, W. Avco Everett Research Laboratory
Torr, Douglas, G., University of Michigan

Van Brunt, Richard, National Bureau of Standards
Verdeyen, Joseph T., University of Illinois

Wildman, David, JILA
Williams, Frazer, Texas Tech University
Wobschall, Darold, SUNYAB
Wood II, Obert, R., Bell Telephone Laboratory

York, Thomas, Penn State University